



CCAMLR

Commission for the Conservation of Antarctic Marine Living Resources
Commission pour la conservation de la faune et la flore marines de l'Antarctique
Комиссия по сохранению морских живых ресурсов Антарктики
Comisión para la Conservación de los Recursos Vivos Marinos Antárticos

WG-EMM-16/03

18 June 2016

Original: English

WG-EMM

**Scientific background document in support of the development of a
CCAMLR MPA in the Weddell Sea (Antarctica) – Version 2016 – Part
C: Data analysis and MPA scenario development**

K. Teschke, H. Pehlke, M. Deininger and T. Brey on behalf of the German Weddell Sea
MPA project team



This paper is presented for consideration by CCAMLR and may contain unpublished data, analyses, and/or conclusions subject to change. Data in this paper shall not be cited or used for purposes other than the work of the CAMLR Commission, Scientific Committee or their subsidiary bodies without the permission of the originators and/or owners of the data.

Scientific background document in support of the development of a CCAMLR MPA in the Weddell Sea (Antarctica) – Version 2016

- Part C: Data analysis and MPA scenario development –

K. Teschke¹, H. Pehlke¹, M. Deininger², Kerstin Jerosch¹ & T. Brey¹

On behalf of the German Weddell Sea MPA project team

¹ Alfred Wegener Institute, Helmholtz Centre for Polar and Marine Research, Bremerhaven, Germany

² University of Bayreuth, Germany

Contents

- Introduction 2
- 1. Data analysis 2
 - 1.1 Environmental parameters 3
 - 1.1.1 Benthic regionalisation..... 3
 - 1.1.2 Sedimentology..... 4
 - 1.1.3 Oceanography..... 7
 - 1.1.4 Sea ice 8
 - 1.1.5 Pelagic regionalisation 9
 - 1.2 Ecological parameters..... 11
 - 1.2.1 Chlorophyll-a concentration..... 11
 - 1.2.2 Pelagic ecosystem 13
 - 1.2.3 Benthic ecosystem..... 22
 - 1.2.4 Birds 30
 - 1.2.5 Marine Mammals 39
- 2. MPA scenario development 42
 - 2.1 Conservation objectives & parameters 42
 - 2.2 Marxan scenario – recursive approach 55
 - 2.3 Developing the borders of the WSMPA 59
- References 67
- Annex 1: Calculation of weighting factors for Marxan analysis 75

Introduction

Part C of the scientific background document informs on the data analysis and the MPA scenario development that were carried out within the framework of the Weddell Sea MPA (WSMPA) project.

Chapter 1 contains the data analyses of environmental and ecological parameters, and was prepared by members of the German WSMPA project team. Chapter 2 provides a systematic overview of the MPA scenario development. First, we present the defined general and specific conservation objectives for the WSMPA planning area. Then, we provide a systematic overview of the parameters and their specific regional objective for the Marxan analysis (see Tab. 2-1), and present the cost layer analysis. Subsequently, we set out the Marxan approach, and finally substantiate the Marxan analysis for the MPA proposal.

The authors thank Lucinda Douglass (Centre for Conservation Geography, Australia) for advice and comment on the data analysis and MPA scenario development.

Major parts of the data analysis and the MPA scenario development were already reported in the background document 'Part C: Data analysis and MPA scenario development' for the meeting of the CAMLR Scientific Committee in 2015 (see SC-CAMLR-XXXIV/BG/17). That version of Part C already reflected a number of the recommendations made by WG-EMM-15 (see report SC-CAMLR-XXXIV, Annex 6), i.e. visualizing the spatial inter-correlation conservation objectives and development of an initial cost layer for upcoming Marxan analyses. Further improvements and extensions that were proposed by WG-EMM-15 (e.g., adding data layers on seabirds and Adélie penguin movements as well as a complete re-analysis regarding the boundary region between Domains 1 and 3) were achieved in the 2015/16 intersessional period. Furthermore, the cost layer analysis was improved and the Marxan analysis was updated.

Please note that this document constitutes the final version of Part C of the WSMPA background document to be submitted to SC-CAMLR in 2016 for approval.

1. Data analysis

Katharina Teschke¹, Hendrik Pehlke¹, Michaela Deininger², Kerstin Jerosch¹ & Thomas Brey¹

¹ Alfred Wegener Institute, Helmholtz Centre for Polar and Marine Research, 27570 Bremerhaven, Germany; katharina.teschke@awi.de, hendrik.pehlke@awi.de, kerstin.jerosch@awi.de, thomas.brey@awi.de

² University of Bayreuth, Germany; michaela.deininger@gmx.de

For all environmental and ecological data layers South Pole (EPSG-Code: 102021; http://nsidc.org/data/polar_stereo/ps_grids.html) are used. Where data layers included missing data, “empty” pixels were flagged in using the abbreviation NA (not available) and were not used for the subsequent calculations. Data processing, such as transformation of data formats, statistical analysis and figure compilation was mainly performed using the R software (Version 3.1.2; R Core Team 2014), QGIS (Version 2.1.0) and the ESRI's GIS desktop software suite (ESRI 2011).

1.1 Environmental parameters

1.1.1 Benthic regionalisation

Based on the digital bathymetric model, i.e. on the depth or bathymetric raster (Arndt et al. 2013), (i) the slope, or the measure of steepness, (ii) the hillshade, (iii) the aspect, (iv) the terrain ruggedness, the variation on three-dimensional orientation of grid cells within a neighbourhood, and (v) the bathymetric position index (BPI) at broad and fine scale were calculated. The slope values (degree units) describe the gradient or the maximum change from each cell to its neighbour cell. The BPI compares the elevation of each cell to the mean elevation of the neighbourhood cells, and thus is a measure of relative elevation in the overall “seascape”. The broad and fine scale BPI were standardised to avoid spatial auto-correlation. The BPI at broad and fine scale was calculated with the Benthic Terrain Modeler (BTM) Version 3.0 extension for ArcGIS™ (Wright et al. 2005). To define a classification scheme in terms of the bathymetric derivatives the BTM requires a classification table. A modified version of the classification table of Erdey-Heydorn (2008) and Wienberg et al. (2013) appeared to be most appropriate, by using a fine scale radius of 0 - 5 km and a broad scale radius of 0 - 125 km (Jerosch et al. 2015).

The continental shelf break was defined as the 1000 m isobath. This was the best suited definition to distinguish between continental shelf to slope and deep sea regions although the slope in some areas starts at a slightly shallower depth. According to natural breaks in the data set, the slope was divided into three classes of different slope angles (in °) for the continental slope and abyssal plain areas (<0.4°, 0.4-1.2°, >1.2°) and the shelf areas (<0.15°, 0.15-1.2°, >1.2°). The spatial resolution of the bathymetric derivatives corresponds to the bathymetric data resolution.

The following data layers were generated:

- (1) Depth (IBCSO 2013)
- (2) Hillshade (ArcGIS 10.2.2, Spatial Analyst tools)
- (3) Aspect (ArcGIS 10.2.2, Spatial Analyst tools)
- (4) Slope (ArcGIS 10.2.2, Spatial Analyst tools)
- (5) Rugosity (ArcGIS 10.2.2, DEM surface tools)
- (6) Broad scale bathymetric position index (BTM, Version 3.0 extension for ArcGIS™)
- (7) Fine scale bathymetric position index (BTM, Version 3.0 extension for ArcGIS™)
- (8) Geomorphology derived from data layer (1), (4) and (6)-(7) is shown in Fig. 1-1.

In total 17 geomorphic classes were used to describe the structures at the sea floor of the WSMMPA planning area (see Fig. 1-1) (Jerosch et al. 2015). For more details on the diversity of ‘landscape’ see Teschke et al. (2016; WG-EMM-16/01).

This benthic regionalisation approach confirms in general the geomorphology of the Weddell Sea described by O’Brien et al. (2009; WS-VME-09/10) and published by Post (2012). Applying the BPI approach to the new IBCSO data (Arndt et al. 2013) resulted in a much more detailed mapping of the geomorphic features. Comparably small features (troughs and ridges) indicate a very diverse environment and facilitate our understanding of a wide range of processes, i.e., deposition of reworked sediment, deformation and melt-out, subaqueous mass-movements, fluvial processes, and settling through the water column.

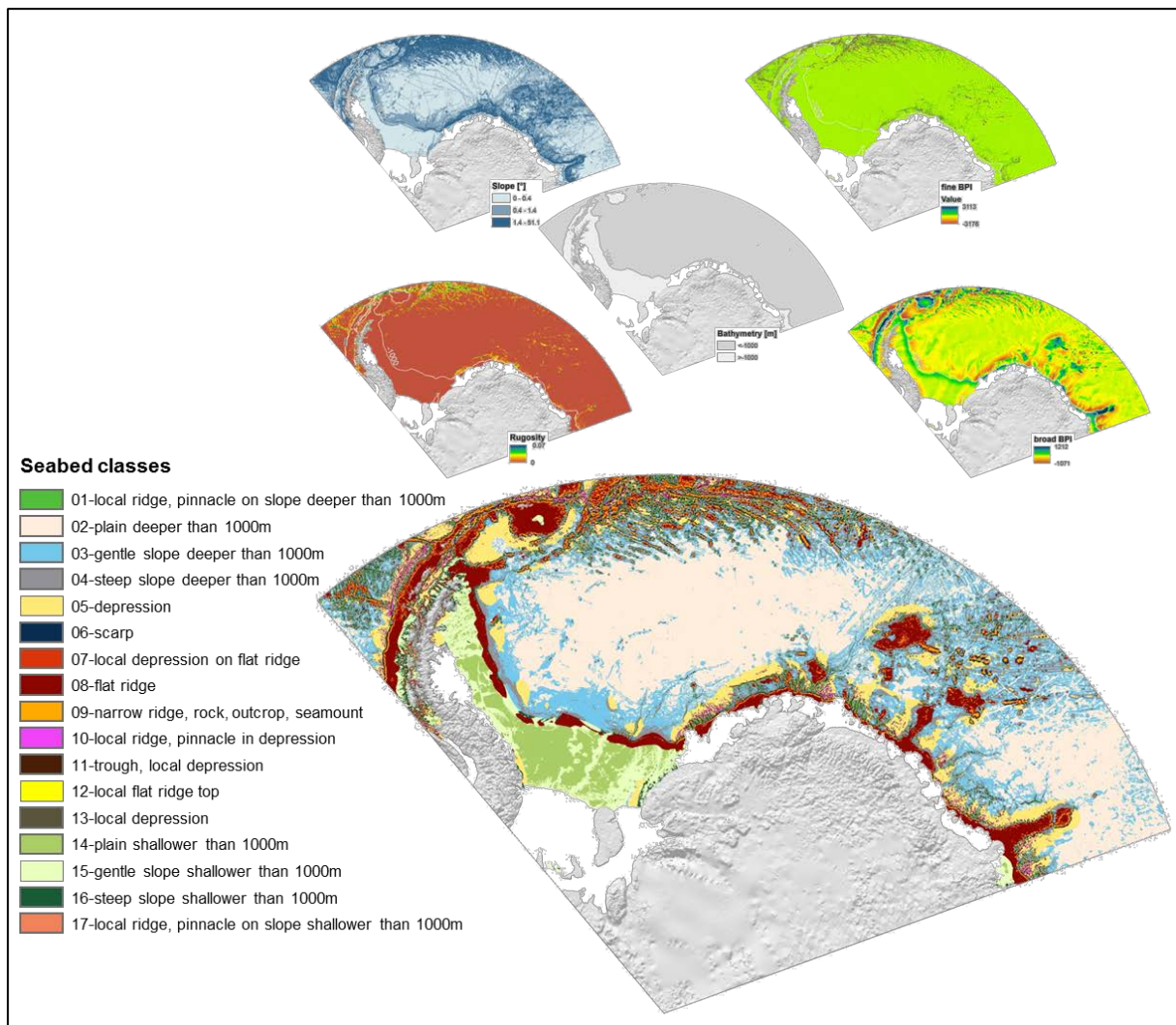


Figure 1-1 The following parameters were derived from bathymetry (IBCSO, Arndt et al. 2013): slope (ArcGIS 10.2.2 Spatial Analyst tool), rugosity (ArcGIS 10.2.2 DEM surface tool), broad and fine scale BPI (Benthic Terrain Modeler, Wright et al. 2005) as well as the seabed classes derived from bathymetry, slope, broad and fine scale BPI. Note that areas appearing as lines are artefacts from ship tracks.

1.1.2 Sedimentology

In total more than 400 grain size samples were standardised from absolute content values of gravel, sand, silt and clay to percentages. The data density of the grain size data restricted the ground truthing to six parcelled-out areas (see Fig. 1-2): (1) South Orkney Plateau, (2) Central Weddell Sea, (3) Ronne Basin, (4) Filchner Trough, (5) Explora Escarpment, (6) Lazarev Sea, according to IBCSO (Arndt et al. 2013).

Primarily, the potential link between geomorphology and sediment distributions was approved, since e.g. steep slopes do not provide the environment for accumulation. Furthermore, the shelf is a region influenced by ice keel scouring and strong currents with geological evidence for erosion of the sea floor. In contrast, the abyssal plain with its lower slope supplies areas of depositional sediment accumulation. For the analysis of this correlation, the mean grain size of all samples falling into one geomorphic feature was calculated and assigned to a sediment texture class according to Folk (1954). Note that not all

geomorphic features were covered with samples significantly also due to their differences in area size and number of samples (Jerosch et al. 2015). However, the analysis shows the relation between grain size distributions and geomorphic features although the values display high standard deviations (see Table 1-1). Exemplarily, the Maude Rise area (Area 6, Lazarev Sea) shows evidently that coarser grain sizes appear on more exposed geomorphic features like flat ridges (ID 08) and narrow ridges, outcrops and seamounts (ID 09) (see Fig. 1-3).

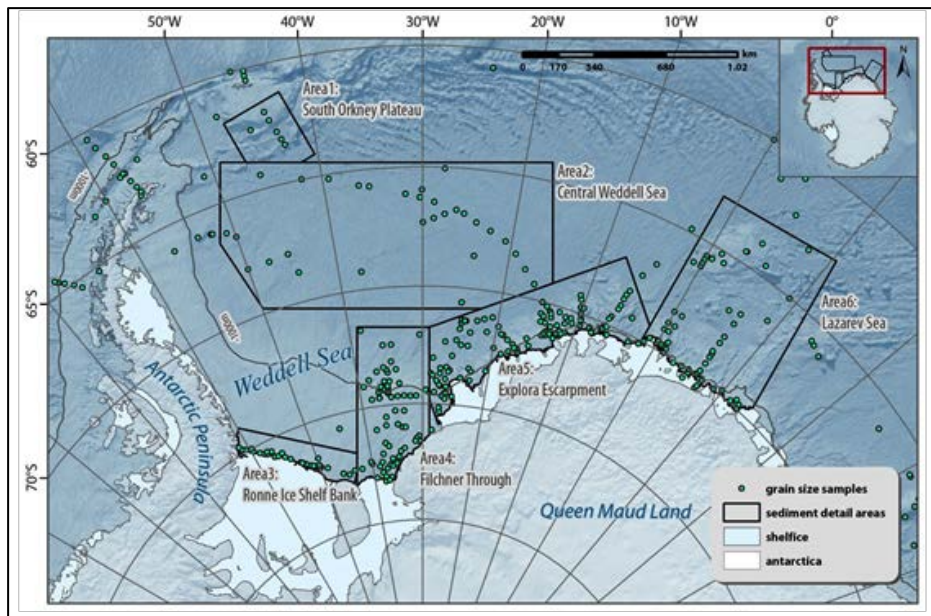


Figure 1-2 Data density of the grain size data restricted the ground truthing to six parcelled-out areas: (1) South Orkney Plateau, (2) Central Weddell Sea, (3) Ronne Basin, (4) Filchner Trough, (5) Explora Escarpment, (6) Lazarev Sea according to IBCSO (Arndt et al. 2013). Sediment grain size data are shown as green dots. Data were downloaded from PANGAEA and are published in Petschick et al. (1996) and Diekmann and Kuhn (1999), and were completed by unpublished data held by G. Kuhn, AWI.

The second approach in mapping the sediment texture was based on the geostatistical analysis of the sediment samples in areas of satisfying sampling densities, i.e. areas 4, 5 and 6 (see Fig. 1-2) (Jerosch et al. in prep.). Sediment texture maps were interpolated from the grain size data relying on other variables more densely available: bathymetry, geomorphology, distance to shelf ice and speed. Three different interpolation methods were applied in ArcGISTM geostatistical analyst extension and were evaluated: Ordinary Kriging, collocated Cokriging and Empirical Bayesian Kriging. The statistical mean values of the errors, such as mean, mean standardized, average standard error, of the three different interpolation methods have been calculated and analysed extensively for each area and each sediment grain size class (i.e. clay, silt, mud, sand and gravel). The results were consolidated and compared in a table of 45 best-fit-analyses. The collocated Cokriging was mainly adapted to small grain sizes such as clay and silt, while Ordinary Kriging and Empirical Bayesian Kriging were best suited for coarser grain sizes (i.e. sand, gravel). According to Jerosch (2013) the single grain size grids were combined to sediment texture maps applying different sediment texture classification schemes published by Folk (1954), Shepard (1954) and Flemming (2000) (see Fig. 1-4). Please note

that areas potentially characterised by hard substrate are not represented, they only can be indicated by high slope values resulting in geomorphic features.

Table 1-1: Grain size distribution (mean in %) and standard deviation (σ) per geomorphic feature.

ID Geomorphic feature	gravel		sand		silt		clay		Folk class (1954)
	mean	σ	mean	σ	mean	σ	mean	σ	
<i>Abyssal</i>									
1 Plain	5.59	17.43	7.60	22.13	37.59	28.64	49.22	31.80	gravelly mud
<i>Continental Slope</i>									
2 Lower Slope	3.95	12.62	10.48	32.14	42.57	24.87	43.00	30.36	slightly gravelly mud
3 Steep Slope	8.05	13.89	33.81	35.00	34.01	27.42	24.12	23.69	gravelly mud
4 Depression	6.32	16.49	16.35	34.65	41.59	24.12	35.75	24.73	gravelly mud
5 Scarp	3.56	9.94	51.84	40.91	29.61	26.92	14.99	22.23	slightly gravelly muddy sand
6 Trough, Local Depression	3.98	9.68	20.58	41.00	45.69	29.23	29.76	20.09	slightly gravelly sandy mud
7 Local Depression on Flat Ridge	4.33	17.45	51.20	37.78	30.17	27.03	14.30	17.74	slightly gravelly muddy sand
8 Flat Ridge	6.44	13.90	56.48	39.64	24.08	23.49	13.00	22.96	gravelly muddy sand
9 Narrow Ridge, Rock Outcrop, Seamount	10.51	16.42	57.41	38.77	21.10	24.87	10.98	19.94	gravelly muddy sand
10 Local Ridge, Pinnacle in Depression	2.30	2.69	34.68	47.12	32.15	23.72	30.87	26.47	slightly gravelly sandy mud
12 Local Ridge, Pinnacle on Slope	7.42	14.84	27.86	37.37	35.81	19.52	28.91	28.27	gravelly mud
<i>Continental Shelf</i>									
14 Plain	0.50	1.67	47.61	40.02	17.88	18.92	34.01	39.39	slightly gravelly sandy mud
15 Lower Slope	3.26	9.79	51.81	36.08	16.10	14.72	28.83	39.42	slightly gravelly muddy sand
16 Steep Slope	0.65	2.32	56.80	59.10	30.47	36.25	12.09	2.33	slightly gravelly muddy sand
17 Local Ridge, Pinnacle on Slopes	7.00	47.16	41.58	2.84	33.09	41.02	18.33	8.98	gravelly mud

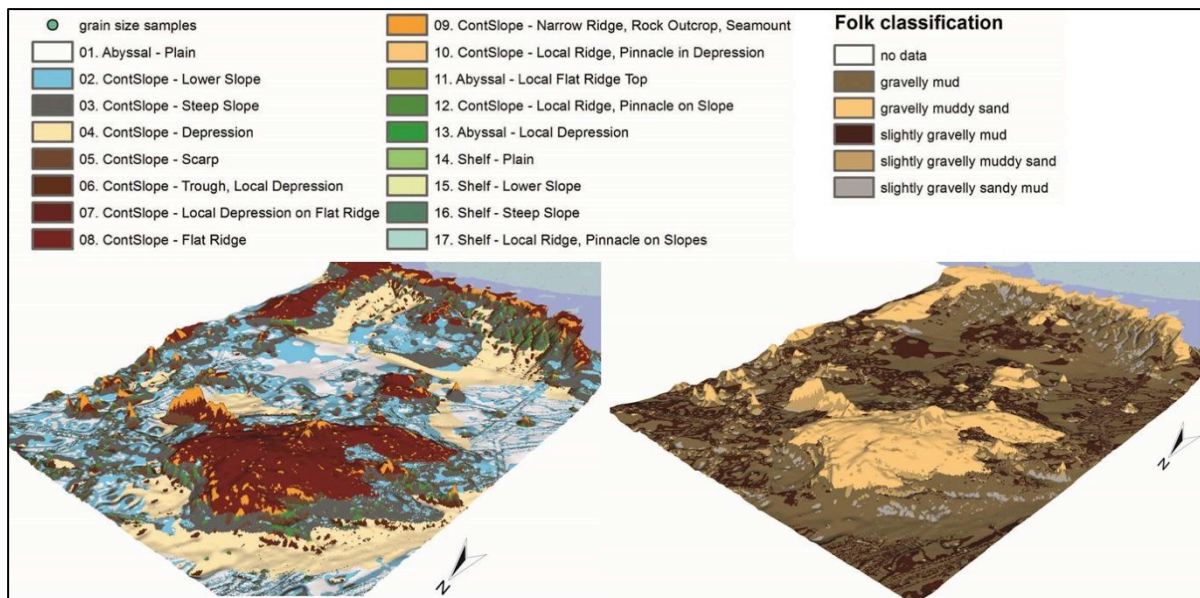


Figure 1-3 Display of the Folk (1954) classified mean grain sizes adapted to the geomorphic features of Maud Rise area.

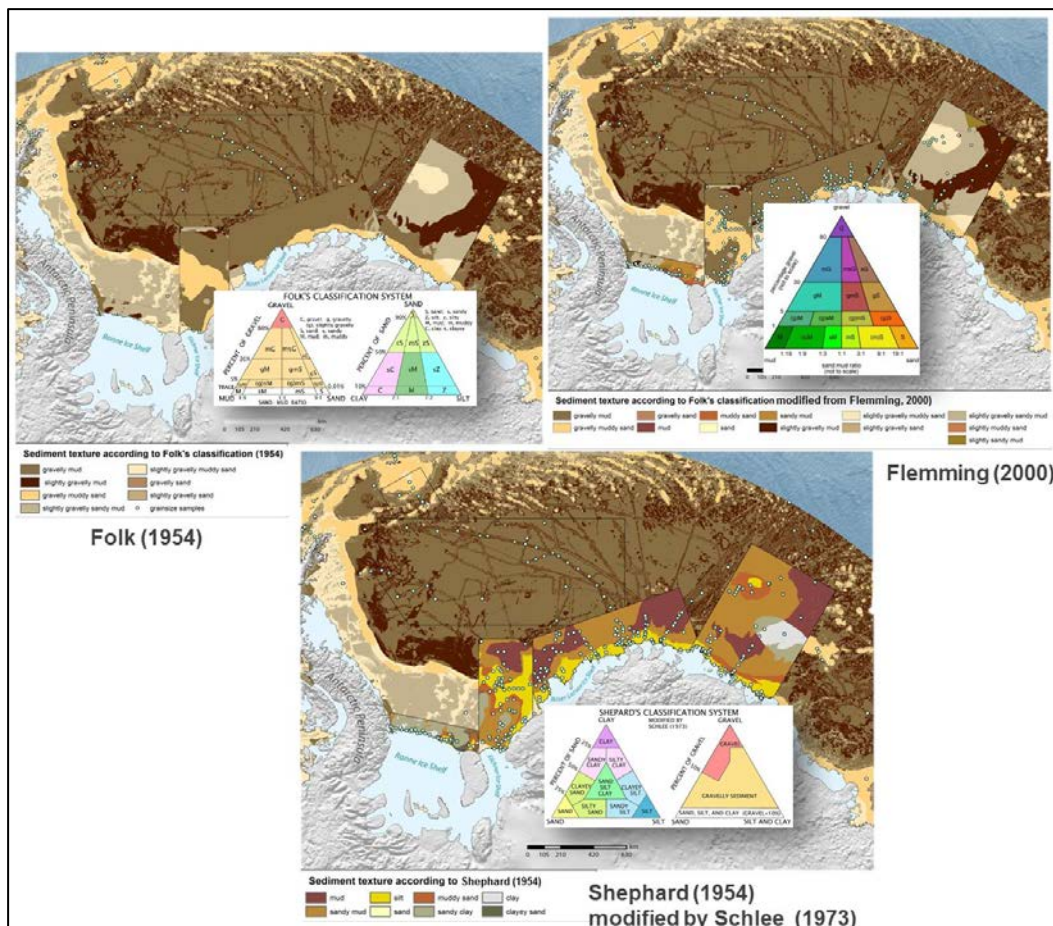


Figure 1-4 Application of sediment classification schemes according to Folk's (1954), Flemming's (2000) and Shepard's classification (1954) to the interpolated grain size maps. Interpolation methods were successfully applied for area 4, 5 and 6 due to data density (Jerosch et al. in prep.).

Please note that both the geomorphological and the sedimentological study were not directly incorporated into our subsequent spatial planning analyses, but served as supporting background information for the WSMMPA development. We used the benthic environmental analysis published by Douglass et al. (2014) which is designed specifically for general use in spatial planning and management, and is already being used in the Domain 1 MPA planning process. This benthic environmental analysis was also used to assist e.g. MPA planning at the Del Cano-Crozet MPA workshop in 2012 and the circumpolar workshop in Brussels in 2012.

1.1.3 Oceanography

Haid (2013) showed that the Finite Element Sea Ice Ocean Model (FESOM; Timmermann et al. 2009) is able to predict Weddell Sea hydrodynamics with high accuracy. For sea water temperature, salinity and currents, data layers for the sea surface and the sea bottom were established. For further details of the model see Haid (2013) and Haid & Timmermann (2013). Speed was calculated by $\sqrt{u^2 + v^2}$ where u is the zonal current with current values from west to east being positive and those from east to west being negative, and v is the meridional current with currents from south to north (positive values) or those from north to south (negative values). Direction (absolute value abs in degree deg from 0° to 360°) was

calculated by $\arcsin [u/(\sqrt{u^2 + v^2})]$ where u is the zonal current and v is the meridional current.

Here, data layers for sea water temperature, salinity and currents are not shown separately, but are included in the pelagic regionalisation analysis (chapter 1.1.5) and the habitat suitability models of Antarctic krill (chapter 1.2.2) and demersal fish fauna (chapter 1.2.3).

1.1.4 Sea ice

Two large data sets were used to describe the overall picture of sea ice dynamics in the Weddell Sea and to detect areas with high sea ice dynamic at different temporal scales. To this end, approximately 100 data layers in terms of dynamic sea ice behaviour were generated. For example, almost 30 data layers were generated to evaluate the inter- and intra-annual variation in open water areas (here: ≤ 15 % ice cover).

Satellite data of daily sea ice concentration

Areas of above-average number of days with sea ice cover ≤ 70 % were used as an indication for polynya formation or sea ice edge retreat. Those open water areas have an important ecological role during particular times of year. For example, the lack of sea ice cover in early summer promotes an earlier onset of the phytoplankton bloom, which in turn pushes secondary production (e.g. Arrigo & van Dijken 2003).

The relative number of days, for which a given pixel had ice cover ≤ 70 %, was calculated for the austral summer (Dec - Mar) from 2002 to 2011. Data on daily sea ice concentration were reclassified, i.e. a value of 1 was assigned to each pixel with ice cover less than 70 %, whereas pixels with ice cover > 70 % were set to N/A (not available). The data layer regarding relative number of days with sea ice cover ≤ 70 % was incorporated into the pelagic regionalisation analysis, and the results are described in paragraph 1.1.5.

Moreover, polynyas - here defined as ice free areas - constitute major access points to open water for emperor penguins (Zimmer et al. 2008) and are crucial for marine mammals for breathing (e.g. Gill & Thiele 1997), in particular during winter where almost the whole WSMMPA planning area is covered by ice. Thus, the mean sea ice concentration was calculated for the breeding period of emperor penguins (Jun to Jan) from 2002 to 2011 and was incorporated into a probability model of penguin occurrence. The results are described in paragraph 1.2.4.

FESOM data

FESOM have been shown to be able to reproduce real polynya dynamics very well in space and time. For example, Haid & Timmermann (2013) showed that a certain polynya exhibited similar size and ice concentration values in the FESOM simulation and in satellite observations derived from the Special Sensor Microwave / Imager (SSM/I). For more details of the model see Haid (2013) and Haid & Timmermann (2013).

The data on sea ice thickness, derived from the FESOM model, are not directly incorporated into further scientific analysis, but were used as additional background information to support the distribution pattern of polynyas in the Weddell Sea. The relative number of days with sea

ice thickness ≤ 20 cm per month (Jan – Dec) out of 20 years (1990-2009) was calculated. Data on monthly sea ice thickness were reclassified, i.e. a value of 1 was assigned to each pixel with ice thickness ≤ 20 cm, whereas pixels with ice thickness ≥ 20 cm were set to N/A (not available). We followed this procedure so that those data are comparably with ordinal data on coastal winter polynyas from the ICDC (University Hamburg), and we refrained from calculating means from categorical data on winter polynya distribution.

1.1.5 Pelagic regionalisation

Each data layer, which was incorporated into the pelagic regionalisation analysis, was generated with a raster of 6.25 km x 6.25 km. That raster size forms the basis of the AMSR-E 89 GHz sea ice concentration maps. The pelagic regionalisation analysis focuses on the austral summer (Dec – Mar), and used the following parameters:

(1) Sea ice concentration

1. AMSR-E 89 GHz sea ice concentration maps were used (see chapter 1.4 in Teschke et al. 2016, WG-EMM-16/02).
2. Data on sea ice concentration were log-transformed.
3. The relative number of days for which a given grid cell had ice cover ≤ 70 % was calculated from 2002 to 2011.
4. Weighting factor: 1.

(2) Bathymetry

1. Bathymetric data by IBSCO were used (see chapter 1.1 in Teschke et al. 2016, WG-EMM-16/02).
2. For each grid cell mean and standard deviation (SD) of depth and 'depth range' - expressed as the difference between maximum and minimum depth in each grid - was calculated.
3. Data on depth and depth range were log-transformed.
4. Each parameter, i.e. depth and depth range, was weighted with 0.5.

(3) Sea water temperature and salinity

1. FESOM model data were used (see chapter 1.3 in Teschke et al. 2016, WG-EMM-16/02).
2. Data on temperature and salinity were log-transformed.
3. For each grid cell mean and SD of temperature and salinity at the sea surface and the sea bottom was calculated from a 20 year time period (1990-2009).
4. Each parameter, i.e. (i) temperature at the sea surface, (ii) temperature at the sea bottom, (iii) salinity at the sea surface and (iv) salinity at the sea bottom was weighted with 0.25.

The parameters chosen for the pelagic regionalisation analysis are major structuring components of the pelagic Weddell Sea ecosystem. Furthermore, these parameters coincide to some extent with the variables which were incorporated in a circumpolar pelagic regionalisation of the Southern Ocean by Raymond (2011; WG-MPA-11/6). The highest

weighting factor was assigned to sea ice concentration, as the main aim of our analysis was to detect high productive areas (polynyas) in the WSMPA planning area.

For clustering we applied the K-means clustering algorithm of Hartigan & Wong (1979). In general, the goal of K-means algorithm is to find the best division of n entities in k groups, so that the total distance between the group's members and its corresponding centroid, representative of the group, is minimized. To determine the optimal number of clusters we used the 'clusGap' function from the R-package 'cluster' (Maechler et al. 2014). The first local maximum in the gap statistic was used to define the optimal number of cluster 'firstSEmax'. Due to the large amount of data, the 'clusGap' analysis could not be applied to the complete data matrix (119,862 samples times 7 variables). Therefore, the matrix was reduced to 4,000 samples x 7 variables by a permutation approach (number of permutations: 150). Finally, the median of the 150 values for optimal number of clusters were used for the K-means cluster analysis.

The result of the pelagic regionalisation approach is shown in Fig. 1-5. 'Coastal polynyas I' (blue-shaded area) denominates areas with a very high probability of ice-free days and high variation in sea surface temperature. Those areas occur along the south-eastern and eastern edge of the ice shelf (from Brunt Ice Shelf to eastern part of Fimbul Ice Shelf) and at the northern border of the Weddell Sea planning area near Larsen C Ice Shelf. Sea ice thickness data (FESOM model) support those results as they show relatively low sea ice thickness (< 20-30 cm) in about the same areas (i.e. from Riiser-Larsen Ice Shelf to Jelbart Ice Shelf and near Larsen C Ice Shelf; results not shown). 'Coastal polynyas II' (red-shaded area) show a high probability of occurrence of polynyas along the edge of the ice shelf. 'Coastal polynyas III' (green-shaded area) denominates areas with an above-average proportion of ice-free days, but significantly less compared to 'Coastal polynyas I and II'. Those areas occur along the south-eastern and eastern edge of the ice shelf (from Filchner Ice Shelf to eastern part of Fimbul Ice Shelf), at the northern border of the planning area near Larsen C Ice Shelf, and near Ronne Ice Shelf. The 'transition zone' (olive-shaded area) is characterised by an average probability of ice-free days and moderate depths (approx. 2000 - 3500 m). 'Deepwater I, II and III' (pink-, orange- and light green-shaded area) are all characterised by above-average water depth. While 'Deepwater I and II' exhibit depths between approx. 3500 m and 5000 m, 'Deepwater III' covers the areas below 4000 m. 'Deepwater I and III' differ in their depth range with 'Deepwater II' covering significantly smaller depth ranges. This coincides well with the benthic regionalisation approach (see paragraph 1.1.1.; Fig. 1-1) that shows distinct canyon structures (alternation of crests, slopes and troughs) at the south-eastern and eastern continental slope. The 'Ice-covered area' (yellow-shaded) on the continental shelf and in deep waters in the south-western Weddell Sea is characterised by the occurrence of perennial sea ice.

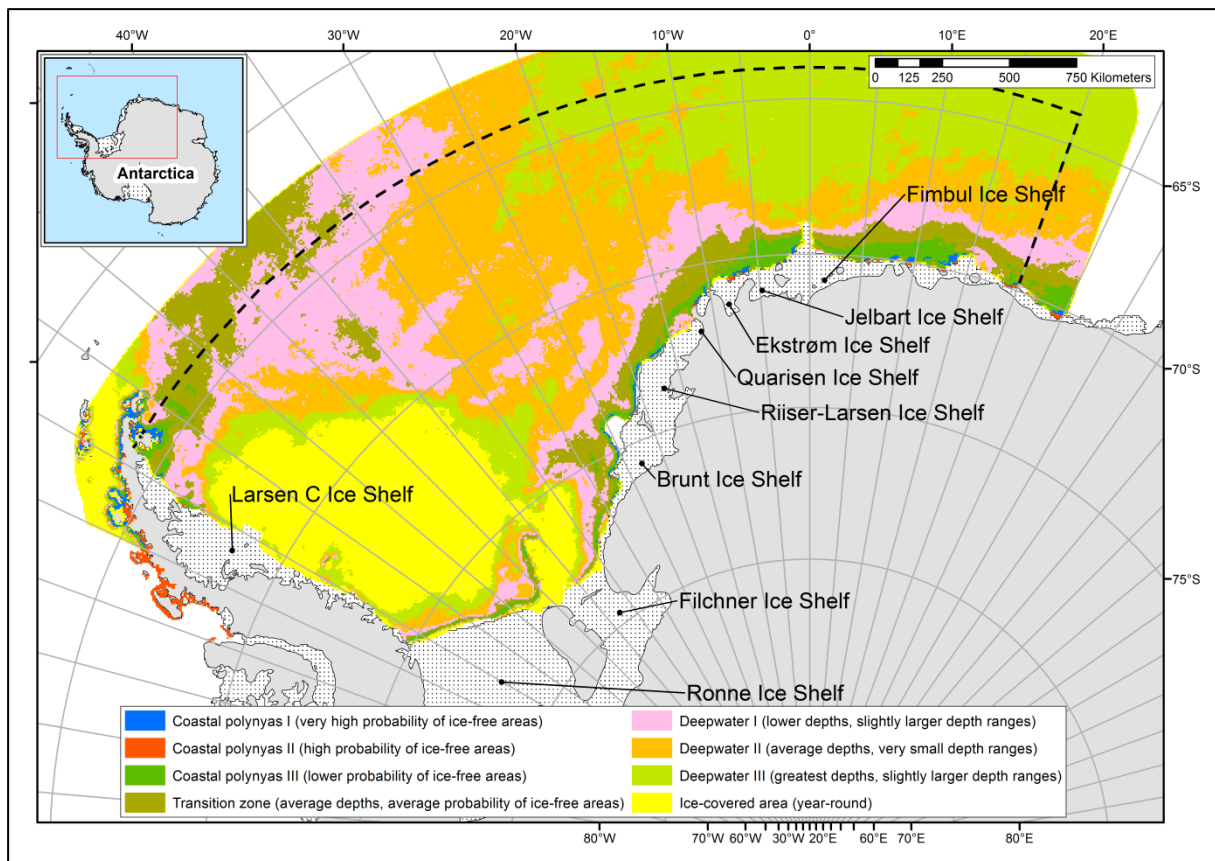


Figure 1-5 Pelagic regionalisation analysis based on (i) AMSR-E 89 GHz sea ice concentration data (Spreen et al. 2008), (ii) bathymetric data (i.e. depth and 'depth range') by IBSCO (Arndt et al. 2013), and (iii) FESOM model data on sea water temperature and salinity at the sea surface and the sea bottom (Timmermann et al. 2009). For more details on the pelagic regionalisation analysis see paragraph 3.2. Black dashed box: WSMPA planning area; boundaries of the planning area do not resemble the boundaries of any proposed WSMPA.

1.2 Ecological parameters

1.2.1 Chlorophyll-a concentration

In the monthly data set on chlorophyll-a (chl-a) data gaps naturally occur caused by clouds, ice and low incident light. There are little or no SeaWiFS data in our planning area (south of 64°S) during austral winter owing to the short day length and the inability of SeaWiFS to produce accurate chl-a estimates at very high solar angles (Moore & Abbott 2000). The high sea ice concentration in most parts of the Weddell Sea hampers the measurement of surface chl-a concentration data, too. Thus, only austral summer (Nov - Mar) chl-a data were considered. Mean and standard deviation were calculated for each grid cell of both raw and log-transformed chl-a concentration data of 14 austral summers (Nov 1997 - Mar 2010).

Here, chl-a is used as a proxy measure of phytoplankton biomass (e.g. Moore & Abbott 2000). Furthermore, several studies showed a positive relationship between chl-a concentration and the occurrence of zooplankton species (e.g. Atkinson et al. 2004) or mammals (e.g. Thiele et al. 2000, Širović & Hildebrand 2011) in the Southern Ocean.

Overall, raw and log-transformed data produced the same basic picture in terms of chl-a concentration, and thus the raw data are mapped (Fig. 1-6A, B). Mean chl-a concentration is low in most parts of the planning area despite the available nitrate and phosphate in surface waters (typically < 0.5 mg/m³). Phytoplankton blooms with chl-a concentration values exceeding 1-3 mg/m³ particularly occur in three areas:

- (i) near Larsen C Ice Shelf,
- (ii) offshore Ronne Ice Shelf,
- (iii) east of Filchner Trough.

Our findings reflect well the chl-a distribution published in Moore & Abbott (2000). High standard deviations are seen near Larsen C Ice Shelf and in the western part offshore Ronne Ice Shelf reflecting considerable intra- and inter-annual variation and/or outliers, e.g. due to measurement errors.

Please note that the chlorophyll-a concentration map was not directly incorporated into our subsequent spatial analyses, but indirectly through the pelagic regionalisation which had one focus on the identification of highly productive areas.

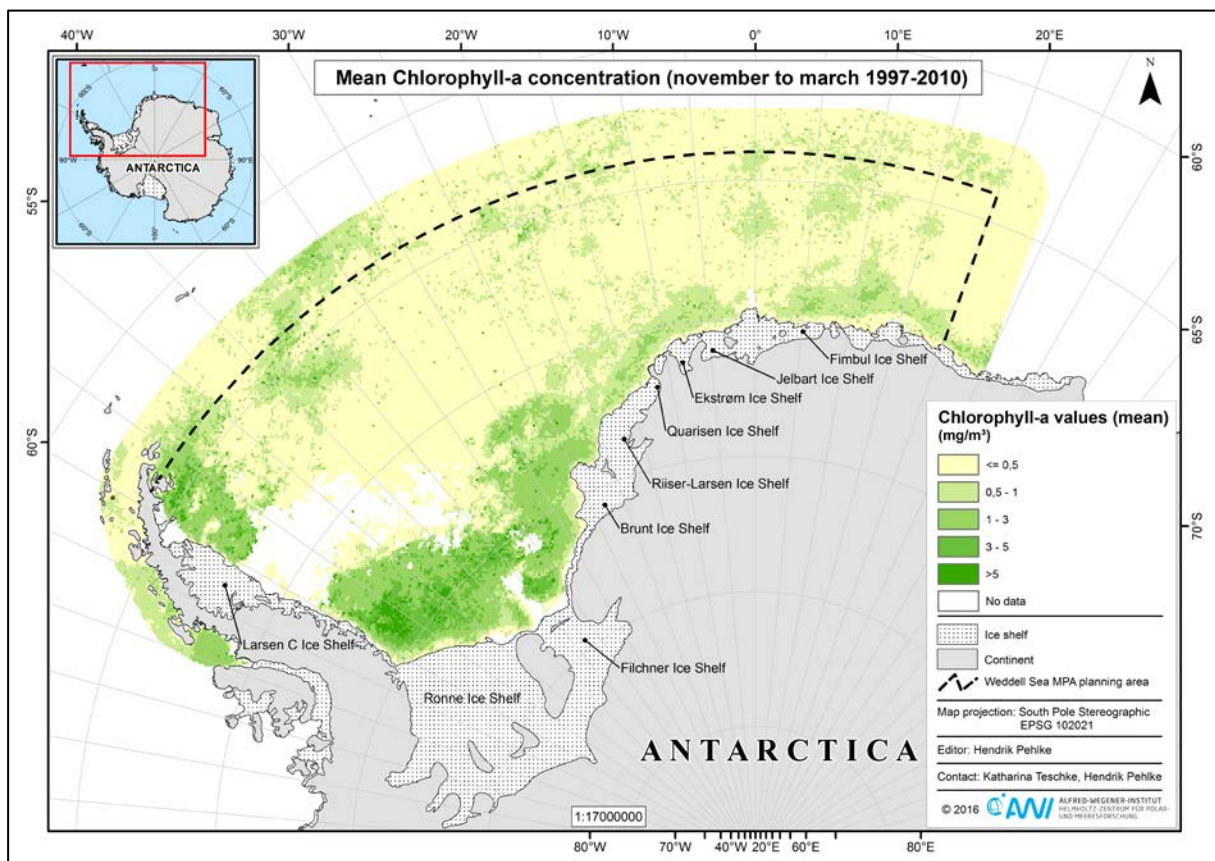


Figure 1-6A Mean value of data on chlorophyll-a concentration (in mg/m³) out of 14 austral spring and summer (Nov-Mar), 1997-2010. Areas in white had no valid chlorophyll data because of heavy sea ice or persistent cloud cover. Monthly data were downloaded via the NASA's OceanColor website. Black dashed box: WSMMPA planning area; boundaries of the planning area do not resemble the boundaries of any proposed WSMMPA.

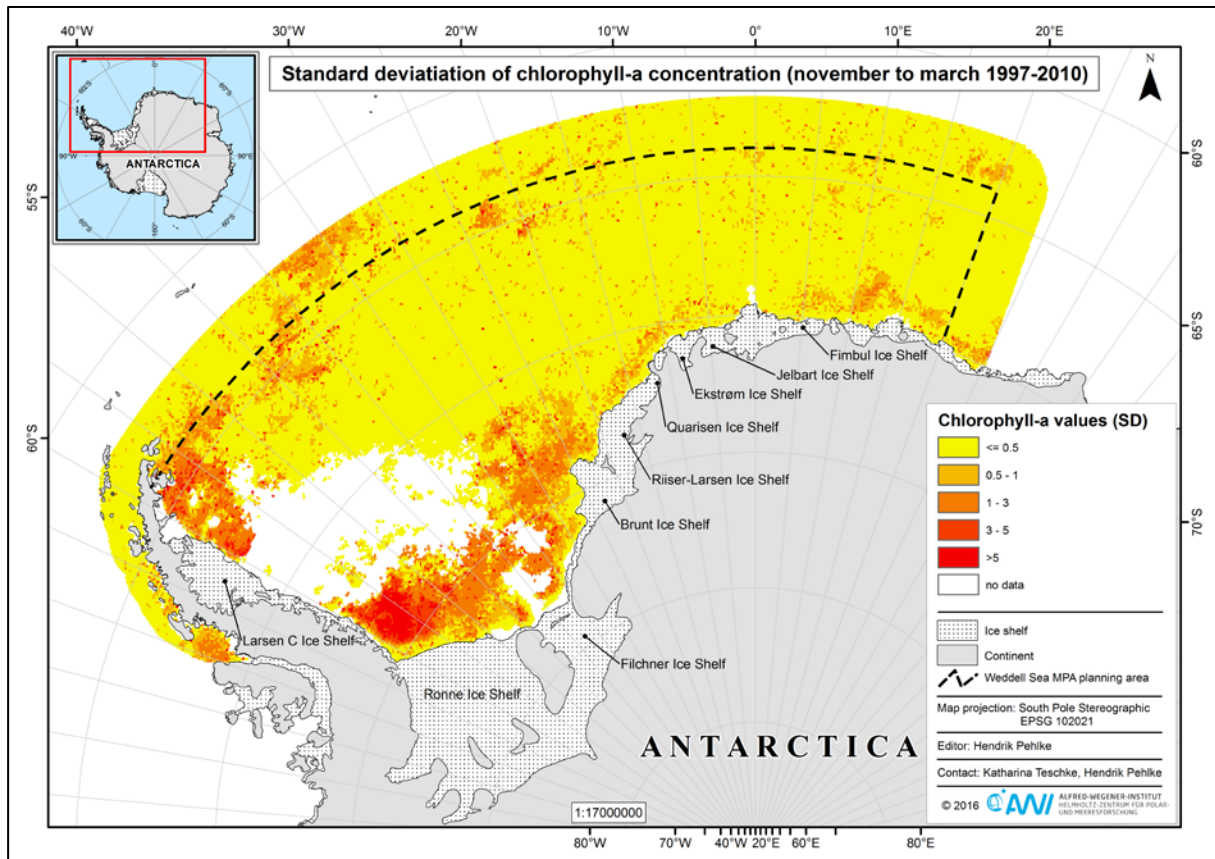


Figure 1-6B Standard deviation of data on chlorophyll-a concentration (in mg/m^3) out of 14 austral spring and summer (Nov-Mar), 1997-2010. Areas in white had no valid chlorophyll data because of heavy sea ice or persistent cloud cover. Monthly data were downloaded via the NASA's OceanColor website. Black dashed box: WSMPA planning area; boundaries of the planning area do not resemble the boundaries of any proposed WSMPA.

1.2.2 Pelagic ecosystem

Antarctic krill (Euphausia superba)

The habitat suitability model of the Antarctic krill was developed by means of the biodiversity modelling package "biomod2" (version 3.1-64; Thuiller et al. 2009, 2014). This freeware package is implemented in the R statistics environment (Version 3.1.2; R Core Team 2014). The "biomod" manual (Thuiller et al. 2010) provides detailed information on how to run the suite of models. "Biomod2" includes ten different state-of-the-art modelling techniques, such as generalized linear models (GLMs; McCullagh & Nelder 1989), generalized additive models (GAMs; Hastie & Tibshirani 1990) or random forest (RF; Breiman 2001), to describe the relationships between a given species and its environment (see e.g., Thuiller et al. 2014, Elith & Graham 2009 for further information). Furthermore, "biomod2" allows the application of ten different measures of model performance (e.g., relative operating characteristic (ROC), true skill statistic (TSS), fraction correct (ACCURACY)) by evaluating the agreement between observation and prediction (true positive (sensitivity), true negative (specificity), false positive, false negative). For information on the different evaluation methods see for example Allouche et al. (2006), Liu et al. (2009) and Pearce & Ferrier (2000).

To predict the potential distribution of adult Antarctic krill (*Euphasia superba*) in the WSMMPA planning area we fed "biomod2" with presence/absence data from KRILLBASE (Atkinson et al. 2004, 2008, 2009; Siegel 1982), from published data (Fevolden 1979; Makarov & Sysoeva 1985; Siegel 2012; Siegel et al. 2013) as well as from unpublished data (Volker Siegel, Thünen Institute, Hamburg).

The predictor variables used in our final predictive model were defined in a stepwise procedure. First, we fed "biomod2" with more than 20 environmental predictor variables and the model was run. The relative importance of each variable was evaluated by the following permutation procedure: Once the model is calibrated, a standard prediction is generated. Then, one of the predictor variables is randomised and a new prediction is made. The Pearson's correlation coefficient (r) between that new prediction and the standard prediction is used to measure this variable's relative importance in the model ($= 1 - r$; for more details on the permutation procedure see Thuiller et al. 2012). Variables with low importance were then excluded from the subsequent permutation, and the relative importance in the model of each remaining variable was measured again. Based on this procedure we reduced the number of variables to the most important predictors (in total five variables) without negatively influencing the model performance. Thus, for our final predictive model we used the following five environmental variables (ranked by decreasing mean importance value calculated by "biomod2"): (i) dissolved oxygen (WOA 2013; Garcia et al. 2014a), (ii) ice coverage (AMSR-E sea ice maps, Spreen et al. 2008), (iii) temperature (FESOM data; Timmermann et al. 2009), (iv) bathymetry (IBCSO; Arndt et al. 2013) and (v) chlorophyll-a concentration (SeaWiFS data). Except bathymetry all variables are based on data sampled in water column close to the sea surface and during austral summer (Jan - Mar). The data sets for each exploratory variable are described in detail in Teschke et al. (2016; WG-EMM-16/02).

In our model we focused on nine different modelling techniques and three different evaluation methods (see Fig. 1-7). Each modelling technique was calibrated with 70 % of the data and the remaining 30 % of the data were used to evaluate their performances. Each modelling algorithm was computed ten times evaluated with three evaluation methods and ten permutations to test the variable importance; hence, the total number of models was 270.

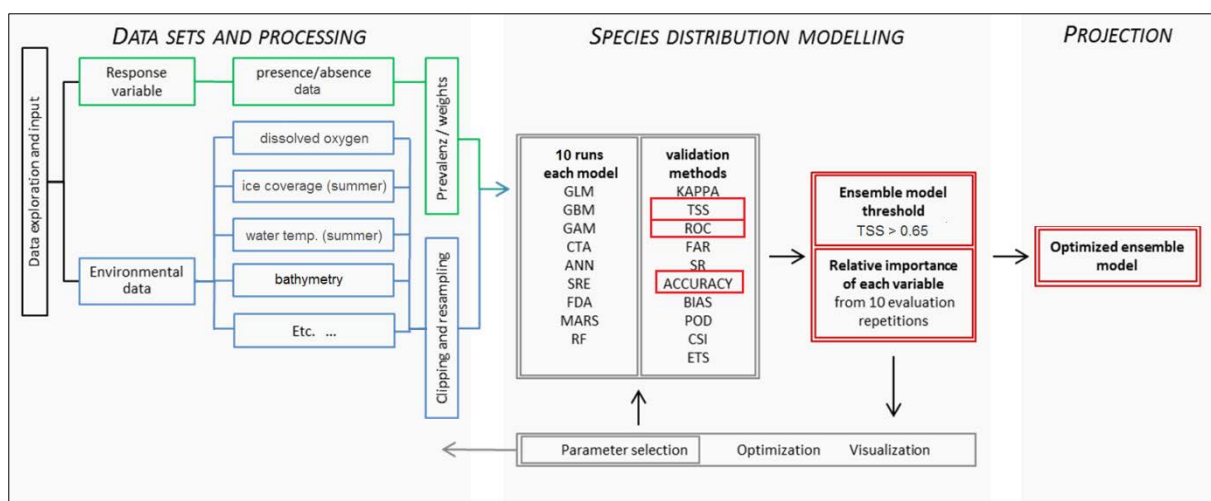


Figure 1-7 Workflow of "biomod2" approach (according to Jerosch et al. submitted).

Subsequent to the different model runs we applied a model synthesis where the different analytical models were combined into a single ensemble model (EM) to improve the stability and accuracy of the predictive models. Ensemble modelling is a procedure of Monte Carlo analysis: multiple predictions are conducted using slightly different initial conditions providing a set of current observations, or measurements (Kroese et al. 2014). For the model synthesis into a single EM we scaled all models applying a binomial GLM as implemented in "biomod2" to ensure comparable model results. Out of the 270 individual models we selected those models for our EM with a TSS threshold higher than 0.65 (i.e., good prediction accuracy according to Thuiller et al. 2010). Ten models in total exceeded the TSS quality threshold of 0.65. The two other measures of model performance, ROC and ACCURACY, showed also values higher than 0.65 in all ten models ($ROC \geq 0.85$, $ACCURACY \geq 0.80$). Finally, our EM combined two generalised additive models (GAM), two generalised boosted models (GBM), two multiple adaptive regression splines (MARS), two random forest (RF), one classification tree analysis (CTA) and one artificial neural networks (ANN). The EM performed quite well ($ROC: 0.94$, $TSS: 0.73$ and $ACCURACY: 0.86$). The evaluation showed that almost 94 % of the real presence data (sensitivity) and more than 78 % of the real absence data (specificity) were correctly classified by the EM, respectively.

The habitat suitability model predictions for adult Antarctic krill are mapped in Figure 1-8A. Most suitable habitat conditions for the Antarctic krill occur (*i*) in the border area between Planning Domain 1 and Planning Domain 3 near the tip of the Antarctic Peninsula, (*ii*) at the continental slope between 15°W and 15°E and (*iii*) at the Maud Rise plateau.

Our findings coincide quite well with the distribution pattern of Antarctic krill reported by e.g., Atkinson et al. (2008) and Siegel (2012). For example, at the Maud Rise plateau Atkinson et al. (2008) show Antarctic krill densities of 256 - 512 individuals/m² (see Fig. 1-8B). Our krill model predicts for the largest proportion of this area suitable habitat conditions ($\geq 70\%$), although parts of this area are characterised by unsuitable to less suitable habitats (Fig. 1-8A), too. Moreover, Atkinson et al. (2008) mention densities of 64 - 128 individuals/m² at the tip of the Antarctic Peninsula. In our model, this area shows again all values from $\leq 25\%$ up to 100 % habitat suitability; more than half of the area, however, is characterised as more suitable habitats (i.e. values $\geq 60\%$).

Furthermore, we checked our Antarctic krill model against the historical krill catch data from the CCALMR database. In total 60 historical krill catches (Jan 1974 - Mar 2009) in the WSMMPA planning area were compared with our habitat suitability model predictions. This "ground truthing" shows that catch data and model predictions match rather well: more than 55 % of the historical krill catches are situated in areas with highly suitable habitat conditions for krill ($\geq 70\%$), 30 % of the data refer to less suitable habitats (25 - 50 %) and no catches refer to unsuitable habitats ($< 25\%$).

Finally, it is important to note that the WSMMPA planning area constitutes a relatively negligible krill habitat compared to other regions of the Southern Ocean, such as the region to the north of our planning area (i.e., approx. between 50°S and 60°S; Fig. 1-8B).

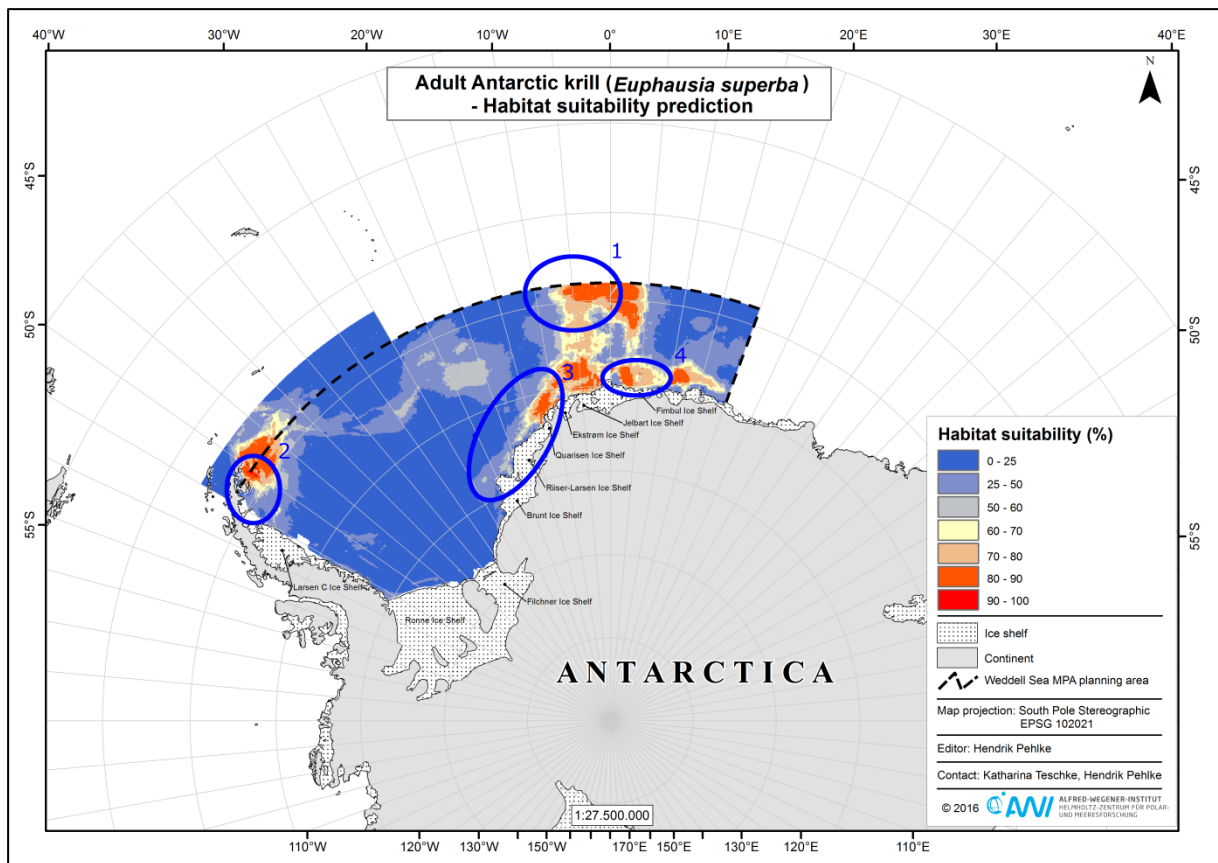


Figure 1-8A Habitat suitability model predictions of adult Antarctic krill (*Euphausia superba*). Model predictions based on data from KRILLBASE (Atkinson et al. 2004, 2008, 2009; Siegel 1982) and (un-) published data held by Volker Siegel, Thünen Institute, Hamburg (e.g., Siegel 2012; Siegel et al. 2013). Habitat suitability is colour-coded with yellow and grey colours indicating less suitable to unsuitable habitat and red colours indicating more suitable habitat conditions. Blue circles (1-4) cover exactly the same areas as in Fig. 1-8B for comparison between both maps. Black dashed box: WSMMPA planning area; boundaries of the planning area do not resemble the boundaries of any proposed WSMMPA.

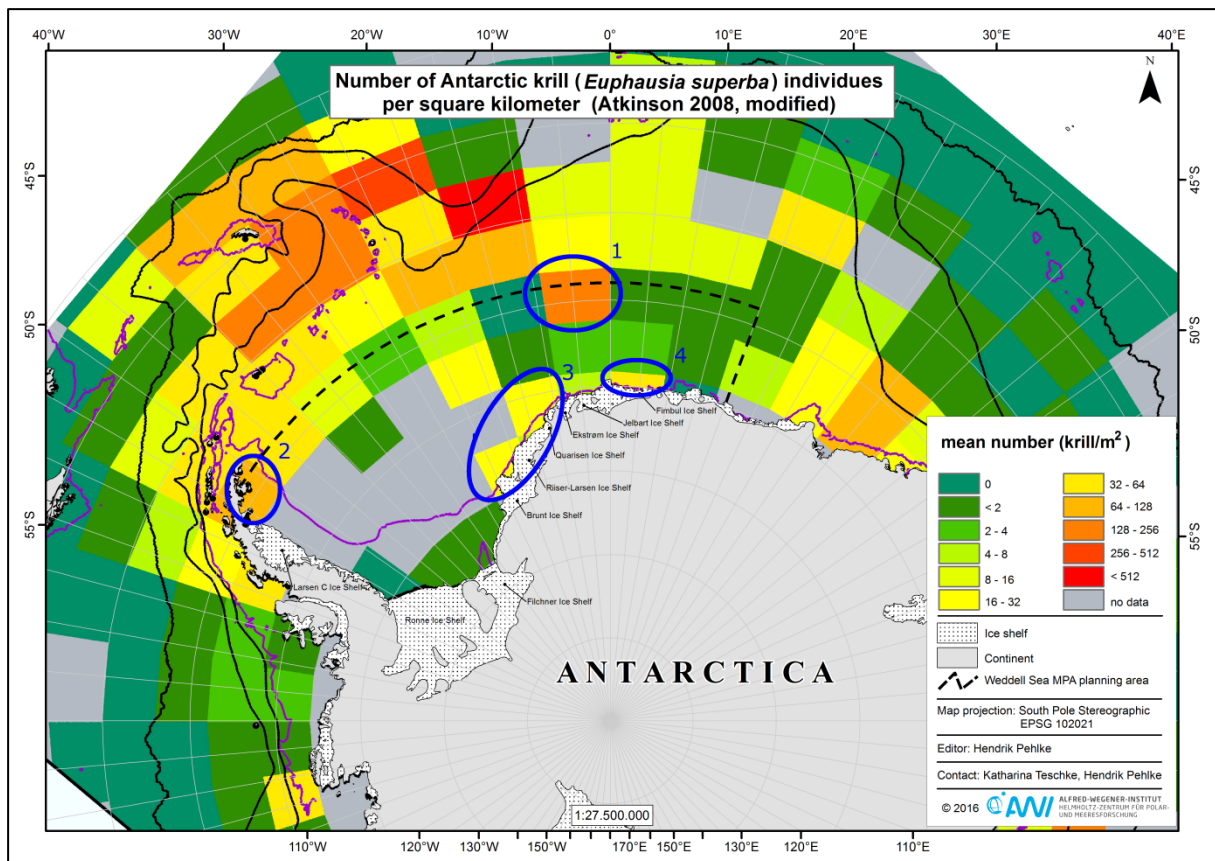


Figure 1-8B Distribution of Antarctic krill (*Euphausia superba*) based on standardised abundance data from KRILLBASE (map modified after Atkinson et al. 2008). The data are plotted as arithmetic mean krill densities (individuals/m²) of all stations within each 3° latitude by 9° longitude grid cell. Fronts shown in black lines (north to south) are the Antarctic Polar Front (Moore et al. 1999) and the Southern Boundary of the Antarctic Circumpolar Current (Orsi et al. 1995). Blue circles (1-4) cover exactly the same areas as in Fig. 1-8A for comparison between both maps. Black dashed box: WSMMPA planning area; boundaries of the planning area do not resemble the boundaries of any proposed WSMMPA.

Antarctic krill larvae

The distribution pattern of *E. superba* larvae was calculated based on published data from Fevolden (1979, 1980), Hempel and Hempel (1982), Menshenina (1992) and Siegel (2005, 2012) and complemented by unpublished data held by V. Siegel, Thünen Institute, Hamburg. An Inverse distance weighted (IDW) interpolation was used in the ArcGIS™ spatial analyst tool; see Burrough & McDonnell (1988) and Lu & Wong (2008) for more details. The IDW interpolation was performed using log-transformed data. The interpolated data were finally expressed as densities of *E. superba* larvae (individuals/m²) for a 30 km radius around each record. The IDW settings were chosen as follows: output cell size (x, y): 1000 m, and distance coefficient power P: 2.

A hotspot of *E. superba* larvae (> 1000 individuals/m²) occur west of the Prime Meridian from approximately 65°S to the ice shelf (see Fig. 1-9).

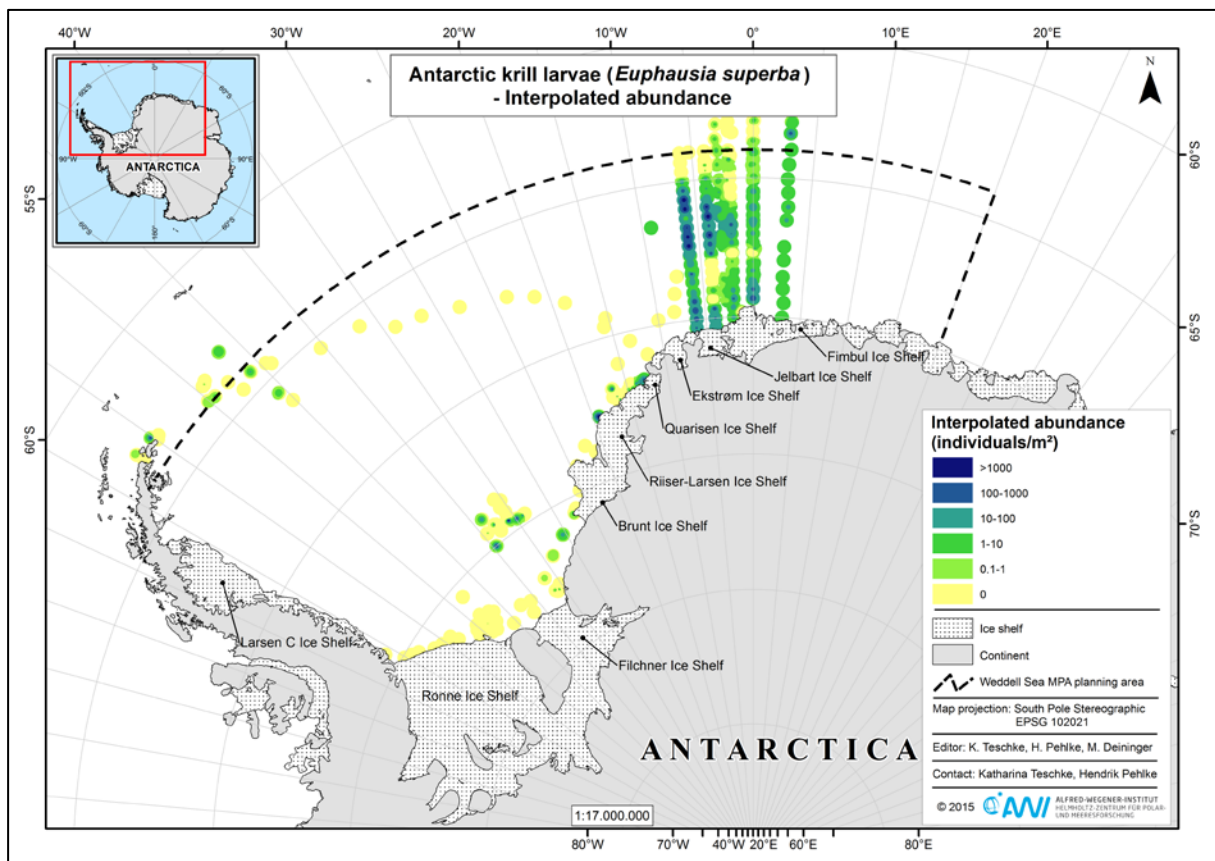


Figure 1-9 Distribution patterns of *Euphausia superba* larvae in the Weddell Sea. Abundance data on *E. superba* larvae were derived from Fevolden (1979, 1980), Hempel and Hempel (1982), Menshenina (1992) and Siegel (2005, 2012 and unpublished data). The data are plotted as densities (individuals/m²) for a 30 km radius around each record. Black dashed box: WSMMPA planning area; boundaries of the planning area do not resemble the boundaries of any proposed WSMMPA.

Ice krill (Euphausia crystallorophias)

Efforts to detect hotspots for other pelagic key species, such as ice krill, were discussed at the 1st International Expert Workshop (see WG-EMM-14/19, supplementary material).

In a first step potential ice krill habitats were generated from bathymetric data by IBSCO (Arndt et al. 2013) and temperature data by the FESOM model (Timmermann et al. 2009). We used two parameters, water depth from 0 m to 550 m and mean SST $\leq 0^{\circ}\text{C}$, as proxies of ice krill occurrence. The biological characteristics of ice krill were taken from the Biogeographic Atlas of the Southern Ocean (Cuzin-Roudy et al. 2014).

In a second step we compiled a data layer of the distribution pattern of adult ice krill from the acquired data. Studies between 1976 and 1989 (Siegel 1982 and unpublished data from V. Siegel, Thünen Institute, Hamburg) are complemented by more recent data collected between 2004 and 2013 (Siegel 2012). Ice krill data (non-standardised, log-transformed abundance) were interpolated using the inverse distance weighted (IDW) method (see e.g. Burrough & McDonnell (1988), Lu & Wong (2008) for more details). The interpolated data were finally expressed as densities of adult ice krill (individuals/m³) for a 30 km radius around each

record. The IDW settings were chosen as follows: output cell size (x, y): 1000 m and the distance coefficient power (P) was set at 2.

The pink coloured area in Figure 1-10 indicates potential ice krill habitats to the north and to the east of the Filchner Trough. The distribution pattern of adult ice krill based on interpolated *in situ* data support these potential ice krill habitats. High ice krill densities have been reported from within the potential habitat mainly, i.e. abundance categories "10-100", "100-1000" and "more than 1000" individuals/m³ match the potential habitat by 95 %, 97 % and 100 %, respectively. Furthermore, misclassification of absence data is low with approx. 12 % of absence data located inside the potential ice krill habitat.

High densities, with hotspots of *Euphausia crystallorophias* (> 1000 individuals/m³), are shown near the tip of Antarctic Peninsula, near Brunt Ice Shelf and next to Quarisen Ice Shelf.

For our final Marxan scenario we only used the potential ice krill habitat (proxies: bathymetry and temperature) as this data layer covers a broader area than the data layer based on interpolated *in situ* data. Areas, which were not sampled but may be considered as a potential suitable ice krill habitat, are included in the data layer.

Pelagic fish

Here, we focused on Antarctic silverfish, *Pleuragramma antarctica*, a pelagic key species of the Weddell Sea ecosystem that plays a similar role as clupeids do in temperate ecosystems. The distribution pattern of *P. antarctica* in the WSMFA planning area was evaluated from several data sets. Abundance data on adult *P. antarctica* were derived from Boysen-Ennen & Piatkowski (1988), Flores et al. (2014), extracted from PANGAEA (Drescher et al. (2012), Ekau et al. (2012a, b), Hureau et al. (2012), Kock et al. (2012), Wöhrmann et al. (2012)) and obtained from R. Knust (AWI, unpublished data). Abundance data on *P. antarctica* larvae were derived from Boysen-Ennen & Piatkowski (1988) and Hubold et al. (1988).

For data on adult *P. antarctica* inverse distance weighted (IDW) interpolation was used in the ArcGIS™ spatial analyst tool; see Burrough & McDonnell (1988) and Lu & Wong (2008) for more details. IDW was performed using log-transformed data, and the interpolated data were finally expressed as densities of adult *Pleuragramma antarctica* (individuals/1000 m²) for a 30 km radius around each record. The IDW settings were chosen as follows:

- Z value: The calculated log₁₀-transformed *P. antarctica* density per 1000 m²
- Output cell size (x, y): 1000 m
- Distance coefficient power P: 2
- Search radius setting, number of points: 10

Figure 1-11 shows in general quite low densities of adult Antarctic silverfish in the WSMFA planning area. Highest *Pleuragramma* densities (100 to 650 individuals/1000 m²) occur near Brunt Ice Shelf on the continental shelf at 75°S, and east and west of the prime meridian near Fimbul and Jelbart Ice Shelf.

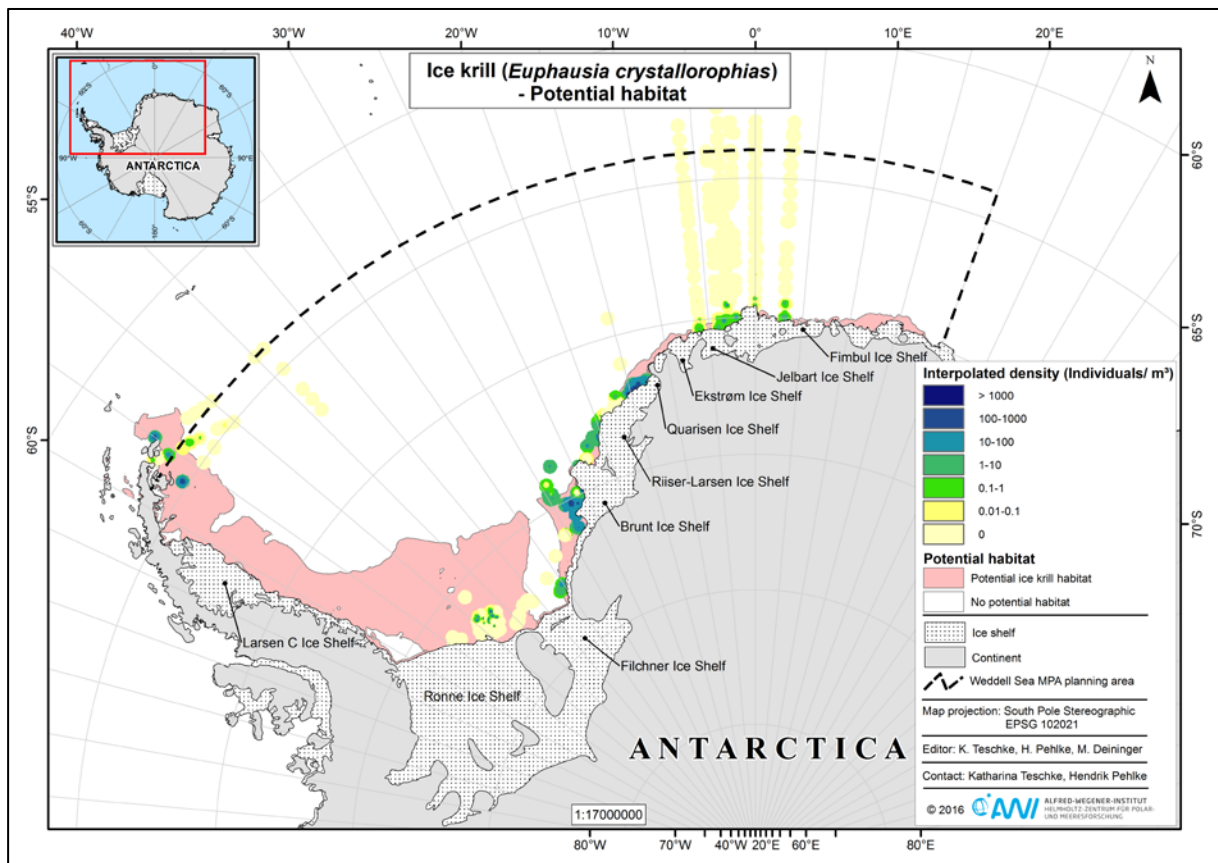


Figure 1-10 Distribution patterns of adult ice krill, *Euphausia crystallophias*, in the Weddell Sea (WS). Abundance data on adult *E. crystallophias* were derived from Siegel (1982, 2012 and unpublished data; Thünen Institute, Hamburg). Pink coloured area: Potential habitat of ice krill in the WS based on depth range and seawater temperature as proxies. Red dashed box: WSMMPA planning area; boundaries of the planning area do not resemble the boundaries of any proposed WSMMPA.

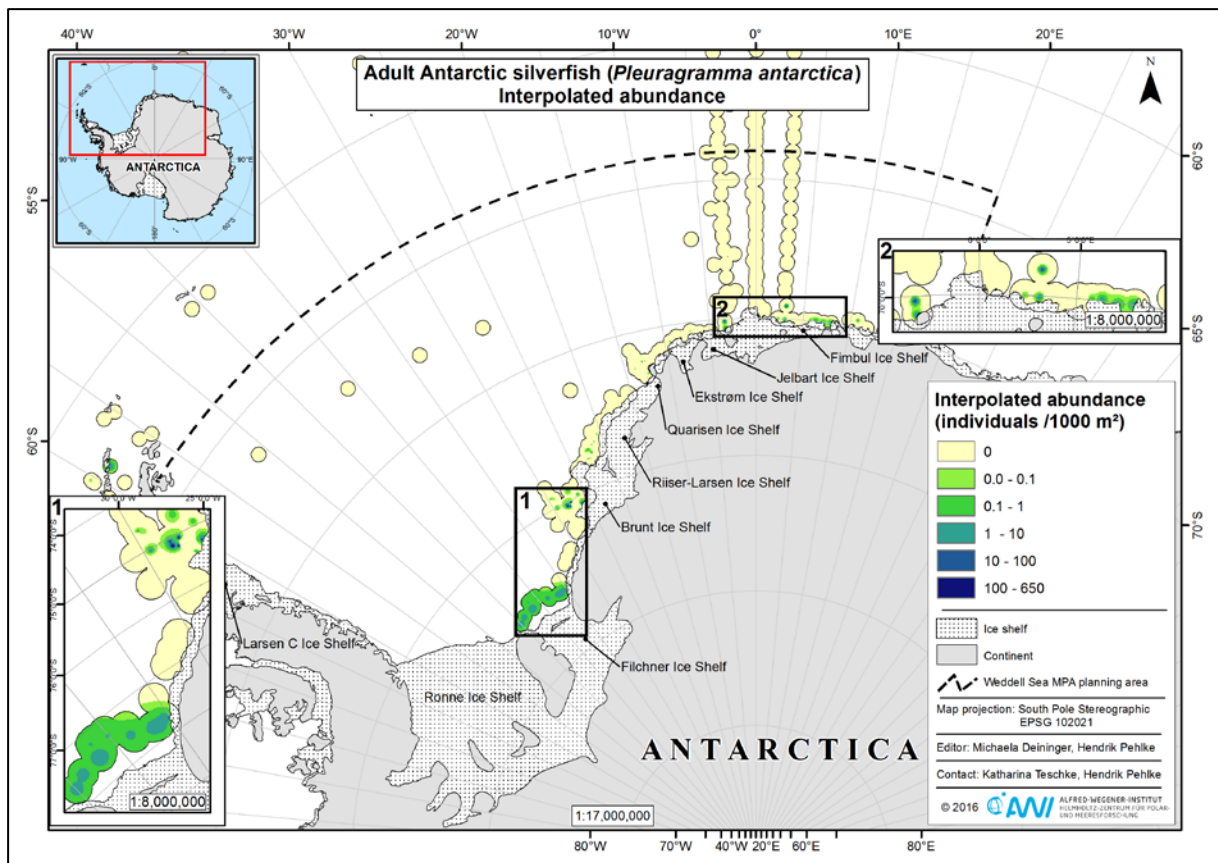


Figure 1-11 Distribution pattern of adult *Pleuragramma antarctica* in the Weddell Sea. Abundance data on adult *P. antarctica* were derived from Boysen-Ennen & Piatkowski (1988) and Flores et al. (2014), based on data from PANGAEA (Drescher et al. (2012), Ekau et al. (2012a, b), Hureau et al. (2012), Kock et al. (2012), Wöhrmann et al. (2012)) and unpublished data held by R. Knust, AWI. The data are plotted as densities (individuals/1000 m²) for a 30 km radius around each record. Black dashed box: WSMPA planning area; boundaries of the planning area do not resemble the boundaries of any proposed WSMPA.

Regarding *P. antarctica* larvae IDW interpolation was performed using log-transformed data. The result of the IDW was reclassified, and the interpolated data were finally expressed as $\log_{10}((\text{individuals}/1000 \text{ m}^3) + 1)$ for a 30 km radius around each record. The output cell size (x, y) was 1000 m; the distance coefficient power was set at 3.

A "hotspot" of *Pleuragramma* larvae (almost six individuals / m³) occurs on the southern continental Weddell Sea Shelf, i.e. south of 75°S near Filchner Ice Shelf (see Fig. 1-12).

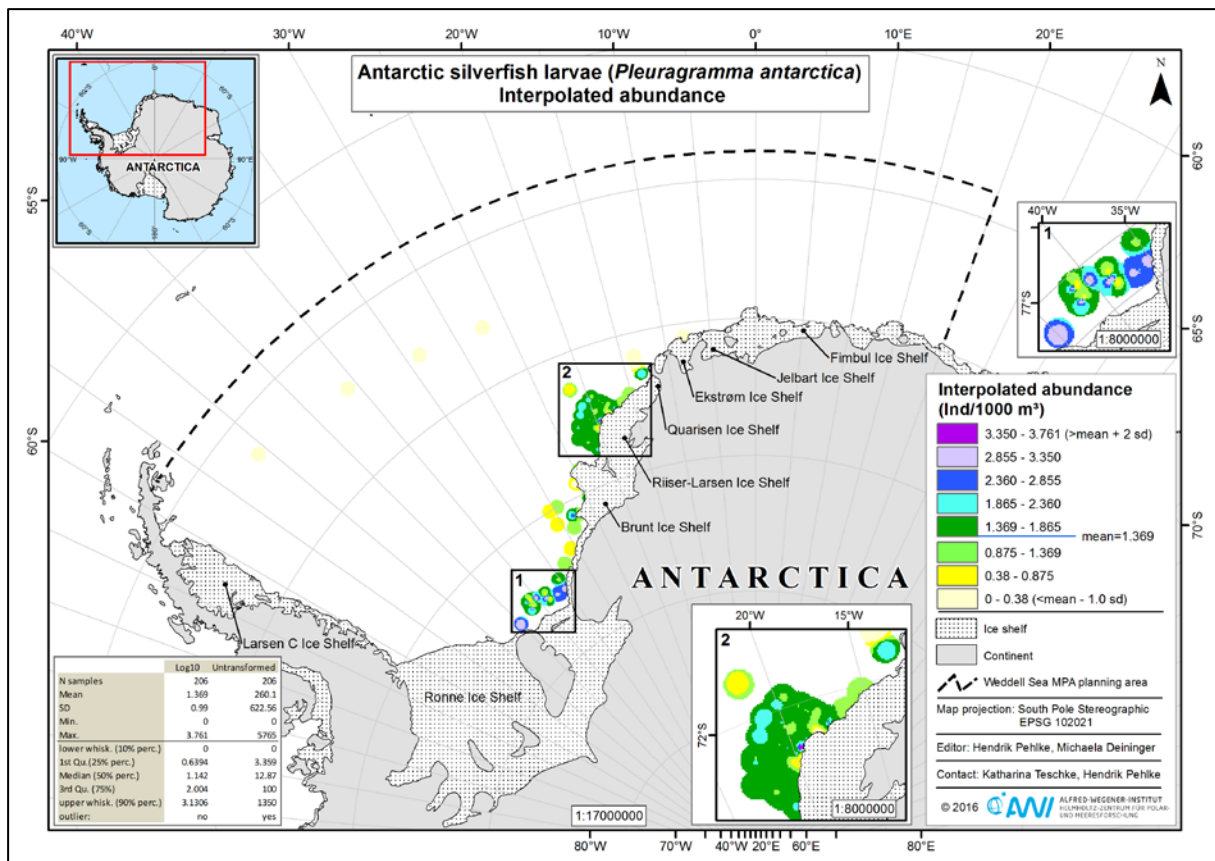


Figure 1-12 Distribution patterns of *Pleuragramma antarctica* larvae in the Weddell Sea planning area. Abundance data on *P. antarctica* larvae were derived from Boysen-Ennen & Piatkowski (1988) and Hubold et al. (1988). Log-transformed, interpolated data are plotted as mean densities +/- n-fold SD (individuals/1000 m³) for a 30 km radius around each record. Red dashed box: WSMPA planning area; boundaries of the planning area do not resemble the boundaries of any proposed WSMPA.

1.2.3 Benthic ecosystem

Zoobenthos – Shelf and slope

Sponge presence

Here, the main objective was to identify areas with important ecosystem functions, i.e. here supporting strongly structured habitats. The distribution pattern of sponges in the WSMPA planning area was calculated based on quantitative data held by D. Gerdes (AWI) and U. Mühlenhardt-Siegel (DZMB), and semi-quantitative data (four categories of relative abundance, i.e. absent, rare, common, very common) from W. Arntz (AWI, retired). The latter had to be digitised and consolidated into one data set.

We transformed the quantitative data into the same four-category system as the semi-quantitative data. First, a Monte Carlo sample was built using Sobol low-discrepancy sequences to generate a Weibull distribution (n = 10,000,000). Within the Weibull distribution following values were identified:

- (i) Class 0 = 0
- (ii) Class 1 = 0 to mean - standard deviation (SD)

- (iii) Class 2 = mean - SD to mean
- (iv) Class 3 = mean to mean + SD

Then, the classified quantitative data were merged with the semi-quantitative data, and inverse distance weighted (IDW) interpolation was performed. The interpolated data were finally expressed as sponge relative abundance classes (i.e. absent, rare, common, very common) for a 10 nm radius around each record. The IDW settings were chosen as follows: output cell size (x, y): 1000 m, and distance coefficient power P: 2.

Figure 1-13 shows sponge hotspots (i.e. very common occurrence of sponges) from Brunt Ice Shelf along Riiser-Larsen Ice Shelf to Ekstrøm Ice Shelf. This result coincides quite well with the distribution pattern of macrozoobenthic communities, classified by functional traits after Gutt (2007) and Turner et al. (2009). Along the shelf near Brunt and Ekstrøm Ice Shelf the dominant community types are mostly sessile suspension feeder communities dominated by sponges (see more details in Gutt et al. 2013).

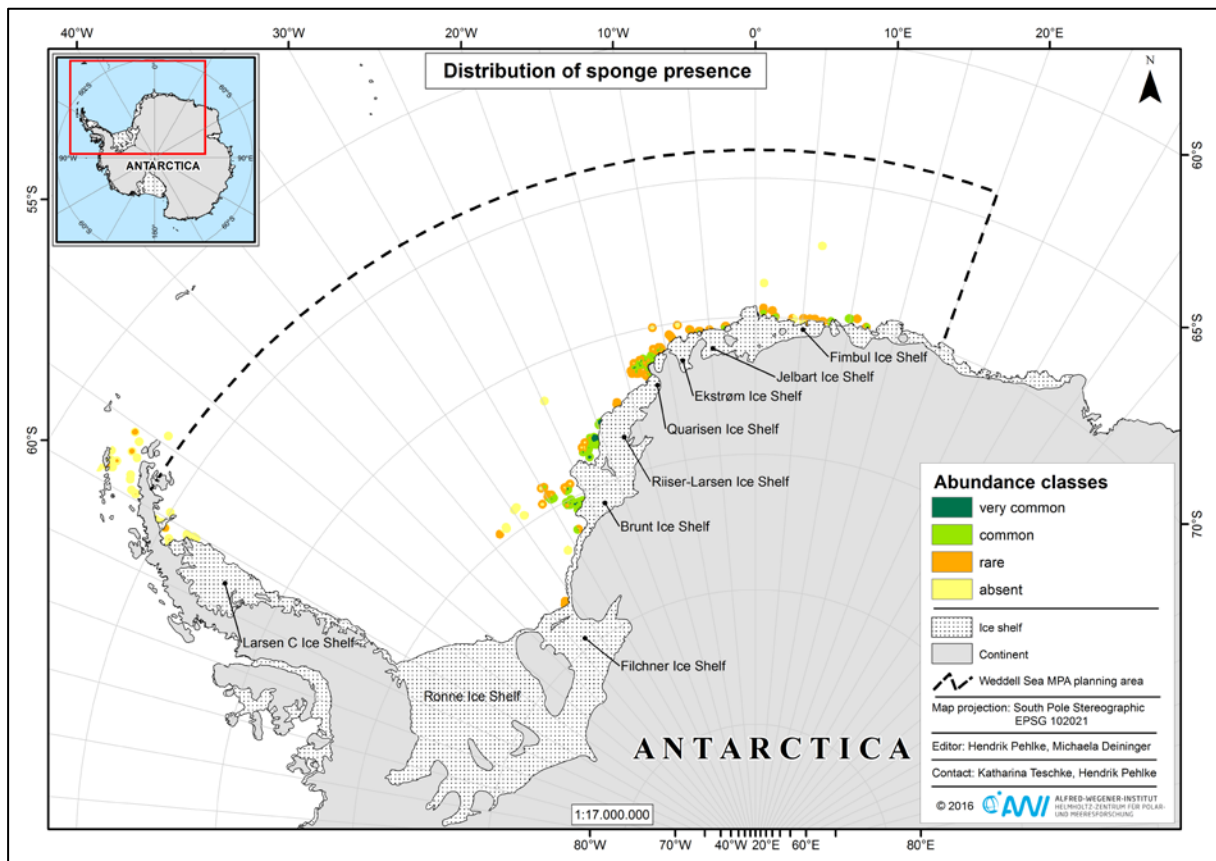


Figure 1-13 Distribution pattern of sponges based on a partly unpublished data set held by D. Gerdes (AWI) and U. Mühlenhardt-Siegel (DZMB), and unpublished data from Wolf Arntz (AWI, retired). The data are plotted as four abundance classes: absent, rare, common and very common. Black dashed box: WSMMA planning area; boundaries of the planning area do not resemble the boundaries of any proposed WSMMA.

Potential habitats for echinoderms

Cluster analysis with species x station data sets of Asteroidea, Ophiuroidea and Holothuroidea identified specific assemblages on the very cold Filchner shelf. This indicates a particular cold water shelf echinoderm fauna. We approximated this habitat by $SBT \leq -1^\circ$, based on seawater temperature data by the FESOM model (Timmermann et al. 2009), generated a corresponding data layer (see Fig. 1-14).

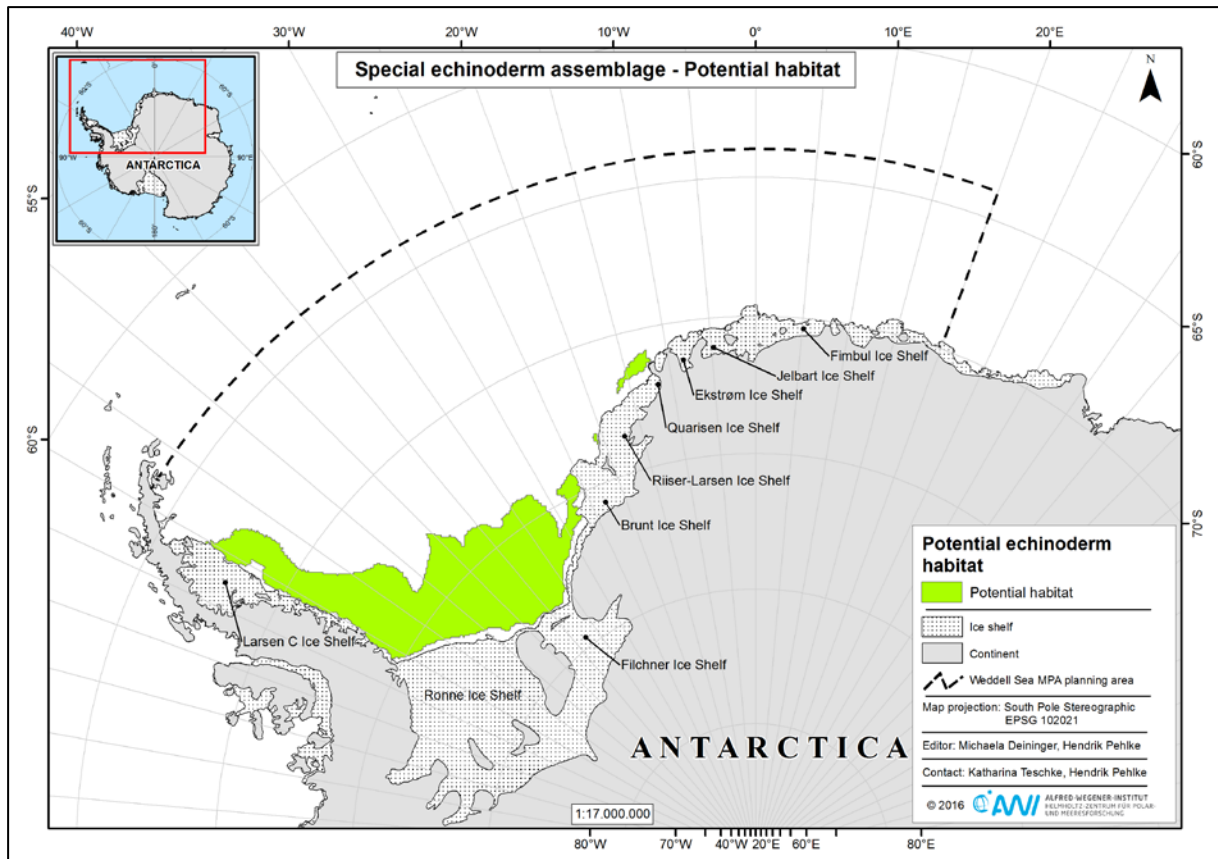


Figure 1-14 Potential habitat of the cold water shelf echinoderm fauna in the Weddell Sea (green coloured area) based on seawater temperature data by the FESOM model (Timmermann et al. 2009) as a proxy. Black dashed box: WSMPA planning area; boundaries of the planning area do not resemble the boundaries of any proposed WSMPA.

Zoobenthos – Deep Sea

The low sampling effort in the deep sea did not allow generating corresponding data layers, i.e. spatially interpolated data layers for the conservation planning software MARXAN. No scientific analyses were carried out within the framework of the WSMPA project. Data on deep-sea isopods (Brandt et al. 2007) were used as descriptive background information to support the identification of potential conservation areas.

Demersal fish

According to the recommendations of the 1st International Expert Workshop (see WG-EMM-14/19, workshop report) we focused on nest guarding fish species and their spawning areas. Furthermore, we concentrated on toothfish as marine living resource in the WSMMA planning area. As we mentioned at the SC-CAMLR-XXXIV meeting (see report, paragraph 5.10) we also concentrated on demersal fish analyses in the 2015/16 intersessional period.

Observation of nesting sites

Figure 1-15 displays information on nest-guarding behaviour of demersal fish. Within the WSMMA planning area, most nesting sites were observed to the west of 25°W (unpublished data held by D. Gerdes, AWI; T. Lundälv, Swedish Institute for the Marine Environment; and E. Riginella, University of Padova). Furthermore, a literature research showed several nesting site observations north of the tip of the Antarctic Peninsula (La Mesa et al. 2009) and along the Western Antarctic Peninsula (Daniels 1978 and 1979, Brodeur et al. 2003). So far, the following fish species have been reported from nesting sites: *Harpagifer bispinis*, *H. antarcticus*, *Chaenocephalus aceratus*, *Pogonophryne scotti*, *Chaenodraco wilsoni* and *Neopagetopsis ionah*. Nest-guarding behaviour seems to be more wide-spread among Antarctic fish species than previously assumed.

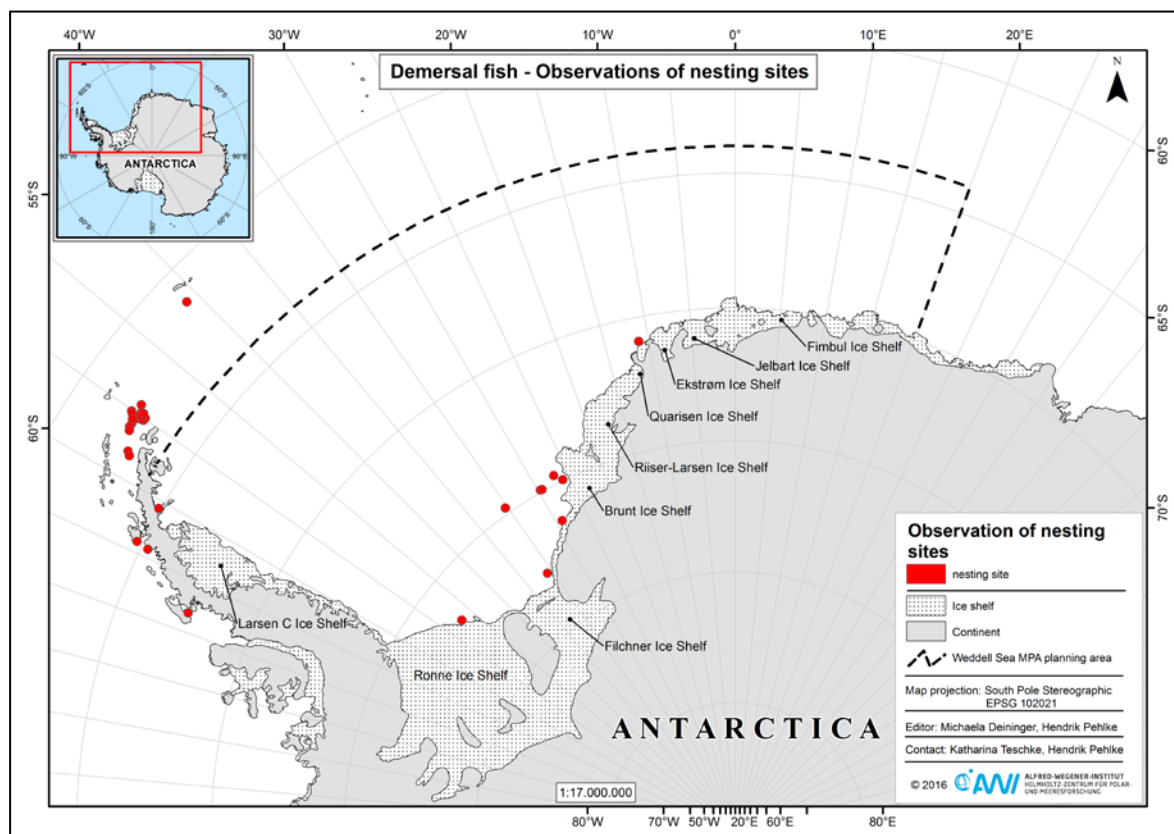


Figure 1-15 Observations of nesting sites in the Weddell Sea planning area, north of the tip of the Antarctic Peninsula and along the Western Antarctic Peninsula. Data were derived from unpublished data held by D. Gerdes (AWI), T. Lundälv (Swedish Institute for the Marine Environment), E. Riginella (University of Padova), and from literature (Daniels 1978 and 1979, Brodeur et al. 2003, La Mesa et al. 2009, Jones & Near 2012). Black dashed box: WSMMA planning area; boundaries of the planning area do not resemble the boundaries of any proposed WSMMA.

Probability of demersal fish occurrence

The habitat suitability model of demersal fish was developed by means of the biodiversity modelling package "biomod2" (version 3.1-64; Thuiller et al. 2009, 2014). For more information on the suite of models and on the measures of model performance please see chapter 1.2.2 (Antarctic krill) and references therein.

To analyse the habitat suitability for the demersal fish fauna in the WSMPA planning area we fed "biomod2" with presence/absence data from a substantial data set that was surveyed during various *Polarstern* cruises between 1996 and 2011 particularly along the Weddell Sea shelf, but also in deeper waters (unpublished data held by R. Knust, AWI).

The predictor variables that were used for our final predictive model were defined in the same iterative process as described in chapter 1.2.2 (Antarctic krill). The remaining environmental variables for the SDMs were: (i) distance to coast, (ii) bathymetry (IBCSO; Arndt et al. 2013), (iii) calcium carbonate (Seiter et al. 2004a), (iv) broad benthic positioning index (see chapter 1.1.1; Jerosch et al. 2015, Wright et al. 2005), (v) silica (Seiter et al. 2004a), (vi) dissolved oxygen (WOA 2013; Garcia et al. 2014a), (vii) biogenic silica (Geibert et al. 2005), (viii) total organic carbon (Seiter et al. 2004b), (ix) nitrate (WOA 2013; Garcia et al. 2014b), (x) salinity, (xi) temperature and (xii) speed (FESOM data; Timmermann et al. 2009), (xiii) slope (see chapter 1.1.1; Jerosch et al. 2015) and (xiv) phosphate (WOA 2013; Garcia et al. 2014b) (list ranked by mean variable importance value). While the first three variables showed mean importance values of more than 0.15, the other predictor variables had values of < 0.05. The variables are described by data that were sampled in the water column close to the sea bottom or directly in surface sediments and during austral summer (Jan - Mar). More information on these data, their spatial and temporal resolution and their original sources is given in Teschke et al. (2016; WG-EMM-16/02).

Distance to coast, i.e. distance to the nearest land from each pixel in the WSMPA planning area, was calculated by the Euclidean distance using the GRASS GIS package 'v.distance' (Soimasuo et al. 1994). The coast line derived from the IBCSO data set (Arndt et al. 2013), and the raster distance to coast line has a spatial resolution of 8.02 x 8.02 km.

For data on calcium carbonate (CaCO₃), silica (SiO₂) and biogenic silica (bSi) the statistical errors of several interpolation methods were evaluated. Ordinary kriging, empirical bayesian kriging and simple kriging featured the best error values for CaCO₃, SiO₂ and bSi, respectively (see Tab. 1-2).

Table 1-2: Calculated statistical errors of the interpolation methods used for data on calcium carbonate (CaCO₃), silica (SiO₂) and biogenic silica (bSi).

Class	Interpolation method	Mean	Root mean square (RMS)	Mean standardised	RMS standardised	Average standard error
CaCO ₃	Ordinary kriging	-0.0219	21.1302	0.0007	0.9475	22.2204
SiO ₂	Empirical bayesian kriging	-0.1090	11.5283	-0.0171	0.9802	10.3391
bSi	Simple kriging	-0.0093	9.8973	-0.0077	0.9431	9.6767

In our model we focused on nine different modelling techniques (see Fig. 1-7). Each modelling technique was calibrated with 70 % of the data and the remaining 30 % of the data were used to evaluate their performances. Each modelling algorithm was computed five times evaluated with two evaluation methods (TSS and ROC) and ten permutations to test the variable importance; hence, the total number of models was 135.

Subsequent to the different model runs we applied a model synthesis where the different analytical models were combined into a single ensemble model (EM) to improve the stability and accuracy of the predictive models. For the model synthesis into a single EM we scaled all models applying a binomial GLM as implemented in "biomod2" to ensure comparable model results. Out of the 135 individual models we selected those models for our EM with a TSS threshold higher than 0.9 (i.e., high or excellent prediction accuracy according to Thuiller et al. 2010). 66 calculated models in total (out of 135 models) exceeded the TSS quality threshold of 0.9. ROC as the other measure of model performance showed also values higher than 0.93 in all 66 models. Finally, our EM combined six generalised linear models (GLM), three generalised additive models (GAM), twelve generalised boosted models (GBM), nine flexible discriminant analysis (FDA), ten multiple adaptive regression splines (MARS), 14 random forest (RF), five classification tree analysis (CTA) and seven artificial neural networks (ANN). The EM performed quite well (ROC: 0.99, TSS: 0.97 and ACCURACY: 0.98). The evaluation showed that both the real presence data (sensitivity) and the real absence data (specificity) were correctly classified by the EM with 98 %.

The habitat suitability model predictions for demersal fish are shown in Figure 1-17. Most suitable habitat conditions for demersal fish in the WSMMPA planning area occur (*i*) between approx. 5° and 15°W on the continental shelf, (*ii*) between 20° and 30°W on the continental shelf and slope and (*iii*) in the areas of the disintegrating Larsen A & B Ice Shelves east of the tip of the Antarctic Peninsula in the Western Weddell Sea. It is important to note here that our model predictions are less significant for deeper parts of the WSMMPA planning area (0-5 % probability of demersal fish occurrence) as data from areas deeper than 2500 m water depth are rare.

Furthermore, we checked our demersal fish model against catch abundance data from Drescher et al. 2012, Ekau et al. 2012 a, b, Hureau et al. 2012, Kock et al. 2012 and Wöhrmann et al. 2012. All these data sets are published in PANGAEA (www.pangaea.de; see also Tab. 2-1 in Teschke et al. 2016, WG-EMM-16/02). In total more than 100 fish catches in the WSMMPA planning area between 1983 and 2007 were compared with our habitat suitability model predictions. This "ground truthing" shows that "true" catch data and model predictions match rather well: lowest total abundance of fish (0 - 0.001 individuals/m²) was caught in areas with lowest mean habitat suitability of 64 % ± 25 % standard deviation (SD), whereas catches with highest total abundance (0.1 - 1.0 individuals/m²) refer to areas with model predictions of high mean habitat suitability (86 % ± 10 % SD). Zero catches, however, are also situated in areas with high mean habitat suitability (i.e. 90 % ± 5 %). It is important to note here that such a mismatch between the "true" catch data and the model predictions must not necessarily mean that the model does not work well. A mismatch may also be caused by the fact that each station in the "true" data set was sampled once in the period between 1983 and 2007, and thus the data cannot reflect the spatio-temporal variability in abundance of demersal fish.

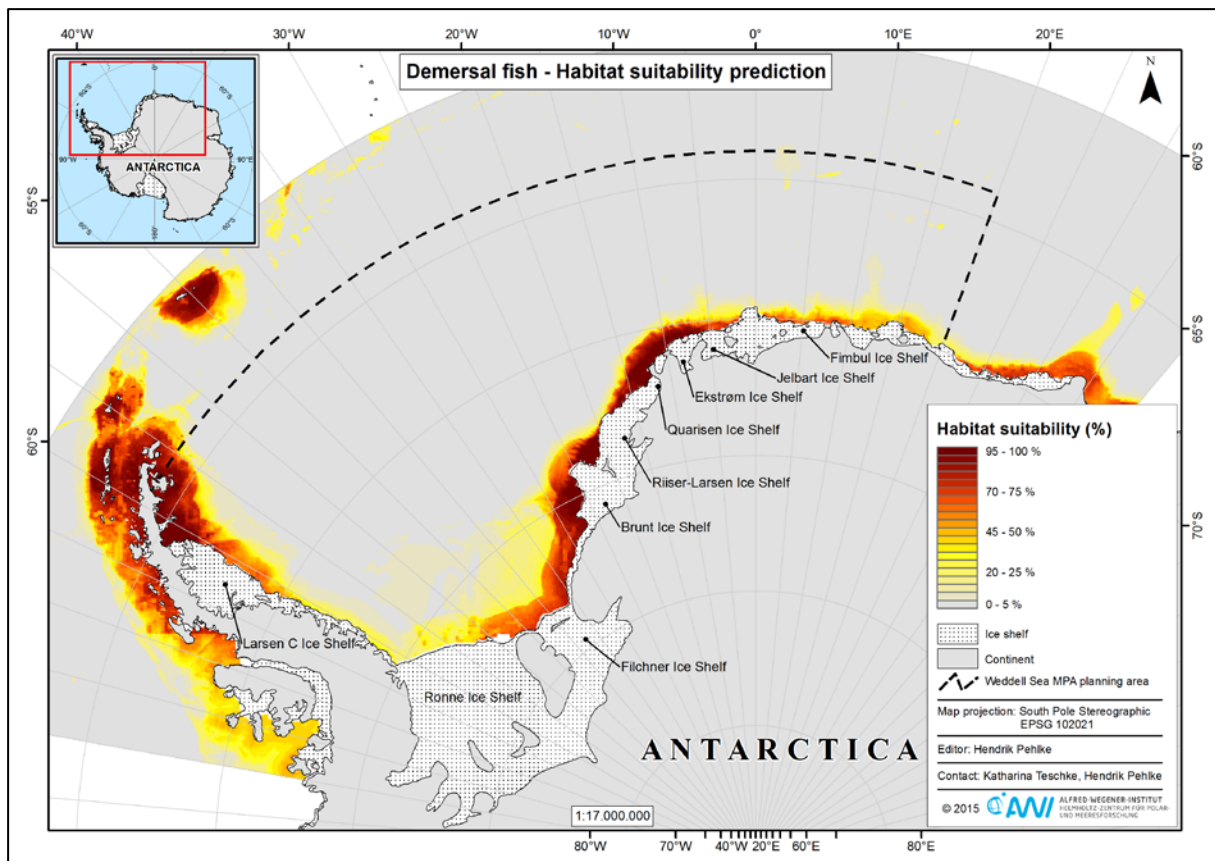


Figure 1-17 Habitat suitability model predictions for demersal fish fauna. Habitat suitability is colour-coded with yellow and grey colours indicating less suitable to unsuitable habitat and red colours indicating more suitable habitat conditions. Black dashed box: WSMMPA planning area; boundaries of the planning area do not resemble the boundaries of any proposed WSMMPA.

Potential toothfish habitat

In a first step we generated a data layer on the potential habitat of adult toothfish (*Dissostichus* spp.) from bathymetric data by IBSCO (Arndt et al. 2013). We used a vertical depth range from 550 m to 2500 m, according to CCAMLR research and exploratory fishery and CM 22-08, as a proxy of toothfish occurrence.

In a second step our original depth range (550 m - 2500 m) was modified to 400 m - 3100 m according to habitat suitability model predictions for the Antarctic toothfish (*Dissostichus mawsoni*) compiled by the CCAMLR Secretariat. For information on the model approach and the model performance please see WG-FSA-15/64.

Finally, the current depth range (400 m - 3100 m) includes most areas with favourable habitat conditions for toothfish as predicted by the model published in WG-FSA-15/64 (see Figure 1-16A). Furthermore, Figure 1-16B shows that our current data layer also includes areas where no model predictions exist, but where habitat suitability for toothfish can be assumed to a certain degree. Thus, we refrain from using the CCAMLR habitat model and used the data layer on our potential habitat of adult toothfish for the subsequent Marxan scenario.

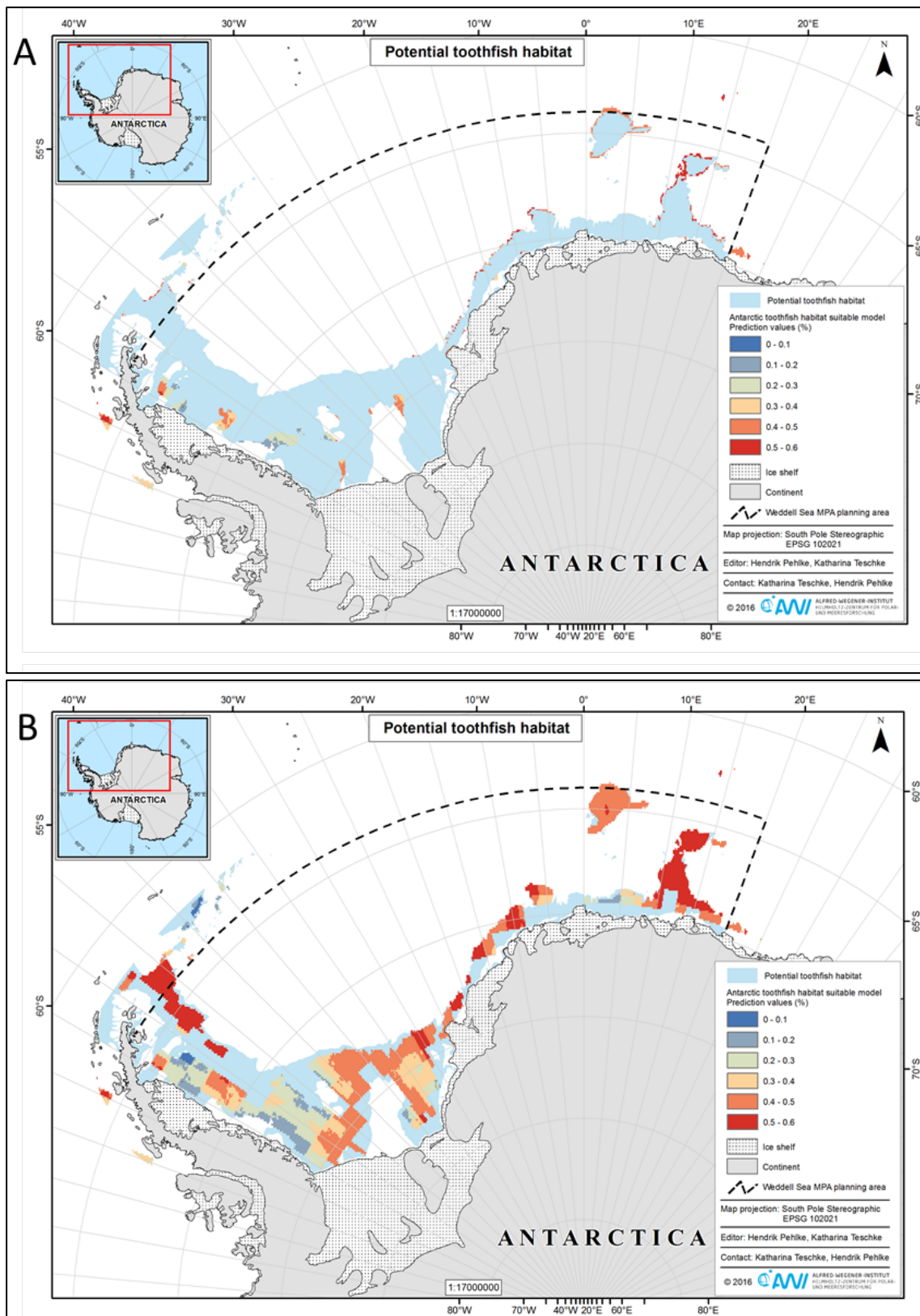


Figure 1-16 (A) Potential habitat of adult toothfish in the Weddell Sea (light blue coloured area) based on depth range (400 m - 3100 m) as proxy and is in accordance to (B) habitat suitability model predictions for the Antarctic toothfish compiled by the CCAMLR Secretariat (WG-FSA-15/64). Habitat suitability is colour-coded with green and blue colours indicating less suitable to unsuitable habitat and red colours indicating more suitable habitat conditions. Black dashed box: WSMPA planning area; boundaries of the planning area do not resemble the boundaries of any proposed WSMPA.

1.2.4 Birds

Seabirds

Data on birds are very sparse. Although there are shipboard observations of seabirds, there are few tracking data available. At sea observation are difficult to interpret due to methodological caveats (e.g. ship following). Nevertheless, we developed a relative simple model of Antarctic Petrel (*Thalassoica antarctica*) and its potential foraging habitat, as the largest colony of this species in the Antarctic is located in the WSMPA planning area. We focus on potential foraging habitats during the crucial breeding period, i.e. from January to March. The model is based on relevant environmental proxies characterising potential foraging habitats of Antarctic Petrel, i.e. the model based on (i) sea ice concentration, (ii) bathymetry and (iii) sea water temperature.

Sea ice concentration

Daily sea ice concentration data were derived from the Advanced Microwave Scanning Radiometer - Earth Observing System instrument (for more details see chapter 1.4 in Teschke et al. 2016, WG-EMM-16/02). We focus on the marginal ice zone, i.e. 15 % - 80 % ice coverage, according to van Franeker (1996) and Ainley et al. (1984, 1994). Data on daily sea ice concentration were reclassified as first step, i.e. a value of 1 was assigned to each cell with ice cover 15 % - 80 %, whereas cells with ice cover less than 15 % and more than 80 % were set to 0. Then, for each raster cell the relative number of days (in %), for which a given raster cell had an ice cover between 15 % and 80 %, was calculated for the bird's breeding period (Jan - Mar) from 2002 to 2011. Subsequently, eight classes regarding the frequency of occurrence of the marginal ice zone were defined and scaled between 0 and 1.

Bathymetry

We used abundance data from Ainley & Jacobs (1981) and calculated mean Antarctic Petrel densities for three depth classes over all sampled transects, i.e. deep ocean: > 2600 m, continental slope: 2600 to 600 m, shelf break: < 600 m (but within 50 km landward of the shelf break) and continental shelf: the remainder of the continental shelf. Then, the mean values were scaled between 0 and 1. Finally, bathymetric data by IBSCO (Arndt et al. 2013) were used to identify the three different depth zones in the Weddell Sea planning area.

Sea water temperature

Monthly sea water temperature data were derived from the FESOM model (Timmermann et al. 2009, Haid & Timmermann 2013; for more details see also Teschke et al. 2016, WG-EMM-16/02; chapter 1.3). According to Ainley et al. (1984) Antarctic Petrel seems to prefer water temperatures colder than 0.5°C. Thus, SST data were reclassified for each raster cell as follows:

- Value 3 = SST \leq 0.5°C in all three months (Jan-Mar).
- Value 2 = SST \leq 0.5°C in only two months between Jan and Mar.
- Value 1 = SST \leq 0.5°C in only one month between Jan and Mar.
- Value 0 = SST > 0.5°C in all three months (Jan-Mar).

Subsequently, the values were scaled between 0 and 1.

Finally, we approximated a potential foraging habitat of Antarctic Petrel by stacking the three environmental proxies and corresponding data layers, respectively, and by assigning different weighting factors to the proxies. The highest weighting factor was assigned to sea ice concentration (weighting factor: 1) as we assume sea ice as the major structuring component of the Antarctic Petrel foraging habitat. Bathymetry and sea water temperature, in contrast, got lower weighting factors of 0.75 and 0.25, respectively.

Favourable habitat conditions for Antarctic Petrel are predicted for an area between 50°W and 60°W at the northern fringe of the Weddell Sea planning area, along the eastern and south-eastern coast of the Weddell Sea between approx. 5° to 35°W within a depth range from approx. 600 m to 2600 m as well as around Astrid Ridge (see Fig. 1-18).

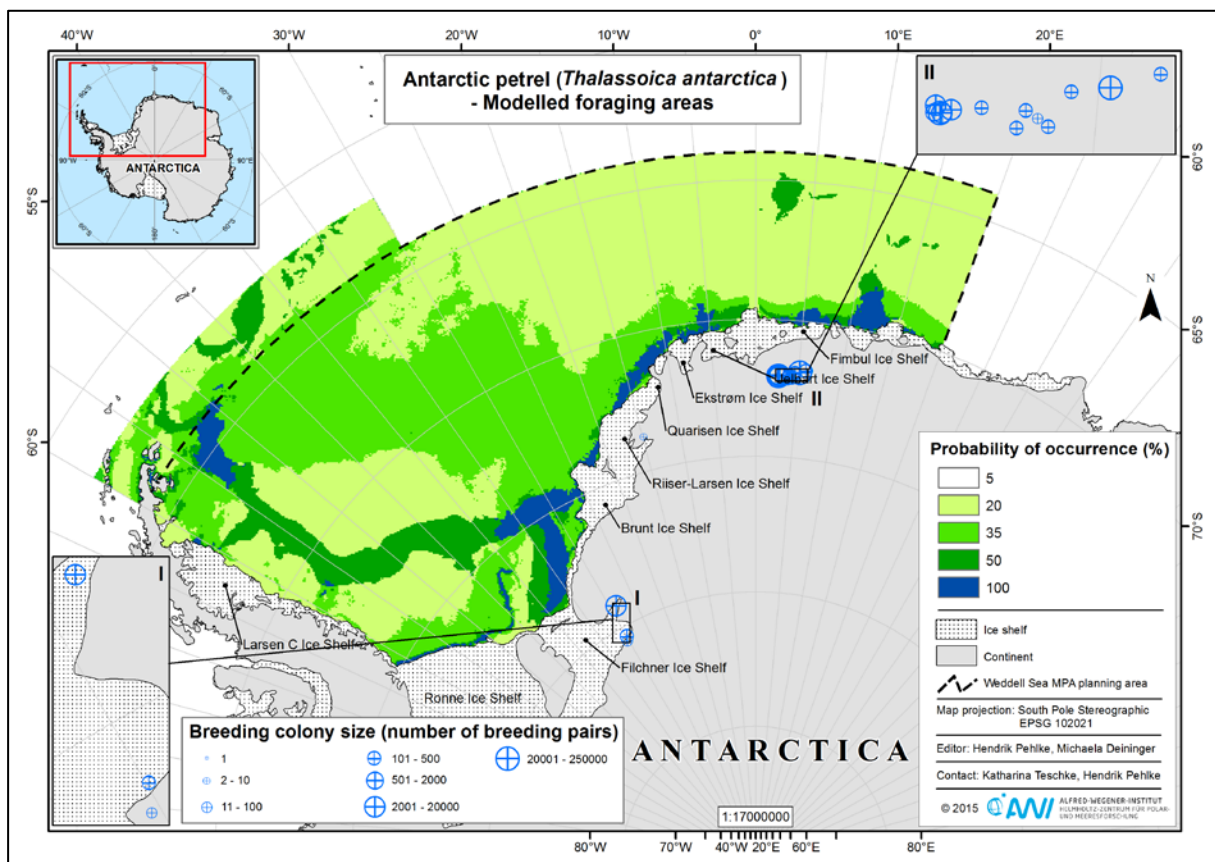


Figure 1-18 Spatial prediction map for Antarctic Petrel (*Thalassoica antarctica*) in the Weddell Sea. Foraging habitat probability is colour-coded with green and yellow colours indicating less suitable to unsuitable habitat and blue colours indicating more suitable habitat conditions. Breeding locations and estimated number of breeding pairs based on van Franeker et al. (1999). Black dashed box: WSMPA planning area; boundaries of the planning area do not resemble the boundaries of any proposed WSMPA.

Adélie penguin

In the Weddell Sea planning area there are two Adélie colonies situated near the tip of the Antarctic Peninsula with a total estimated abundance of 31,736 breeding pairs, and a 95th percentile confidence interval (CI) from 24,703 to 42,803 breeding pairs (Lynch & LaRue 2014). In the border area between Planning Domain 1 and Planning Domain 3 some Adélie

colonies occur e.g. at King Georg Island and at Joinville Island. The largest Adélie penguin population in this region is situated at Joinville Island with an estimated abundance of 29,170 breeding pairs (CI: 17,817 to 47,445 breeding pairs).

For analysing the spatial distribution pattern of breeding and non-breeding Adélie penguins in the border area between Planning Domain 1 and Planning Domain 3 we used six tracking data sets - stored in the seabird tracking database (www.seabirdtracking.org) and based on BAS Inventory and US AMLR Program. Tracking data are available for Adélie populations at South Orkney Islands and in Graham Land.

ARGOS position data were processed with a state-space model described by Johnson et al. (2008) and implemented in the R package *crawl* (Johnson 2011). We used the model to generate predictions of the location of each tracked individual on an hourly time scale. Raw ARGOS data were first processed by assigning error values to the different ARGOS location quality codes, i.e. location code 3 (= highest accuracy of ARGOS position estimate) was set off against the lowest error value, the highest error was assigned to location code B (= lowest accuracy of ARGOS position estimate). We used the fitted continuous-time correlated random walk model to generate 250 simulated track-lines between the temporally sequenced ARGOS positions respectively of each tracked individual. The simulated track-lines were binned onto a spatial grid (cell size: 6.25 km x 6.25 km) and were pooled per grid cell so that the final data layer identifies the areas that were used most often by tracked Adélies.

Areas that were used most often for foraging by tracked breeders are predicted particularly for areas not more than approx. 50 km away from the colonies at King Georg Island and the colony at Hope Bay (Graham Land) as well as from the colonies at South Orkney Islands (see Fig. 1-19A, B).

To estimate suitable feeding habitats for breeding Adélies in others colonies in the border area between Planning Domain 1 and Planning Domain 3, too, we used a 50 km buffer and a 50-100 km ring buffer around each colony according to the recommendations of the 2nd International Workshop for identifying CCAMLR-MPAs in Planning Domain 1 (see WG-EMM-15/42 and references therein). A "ground truthing" by means of the *crawl* model shows that 100 % of highest habitat utilisation is situated within the 50 km buffers (see Fig. 1-19B). Furthermore, the 50-100 km ring buffer includes relevant area proportions with high habitat suitability.

Regarding the non-breeders highest habitat utilisation is concentrated in relative small areas (e.g. close to King Georg Island); however, the non-breeding Adélies seem to roam through large parts of the Weddell Sea planning area (see Fig. 1-20).

Please note that we used the buffer areas around each Adélie colony in our final Marxan scenario as a proxy of the potential foraging habitats of breeding penguins. As described above the buffer areas reflect well the results of the *crawl* model. To represent potential foraging habitats of non-breeding Adélies we used the data layer based on the modelled foraging trips.

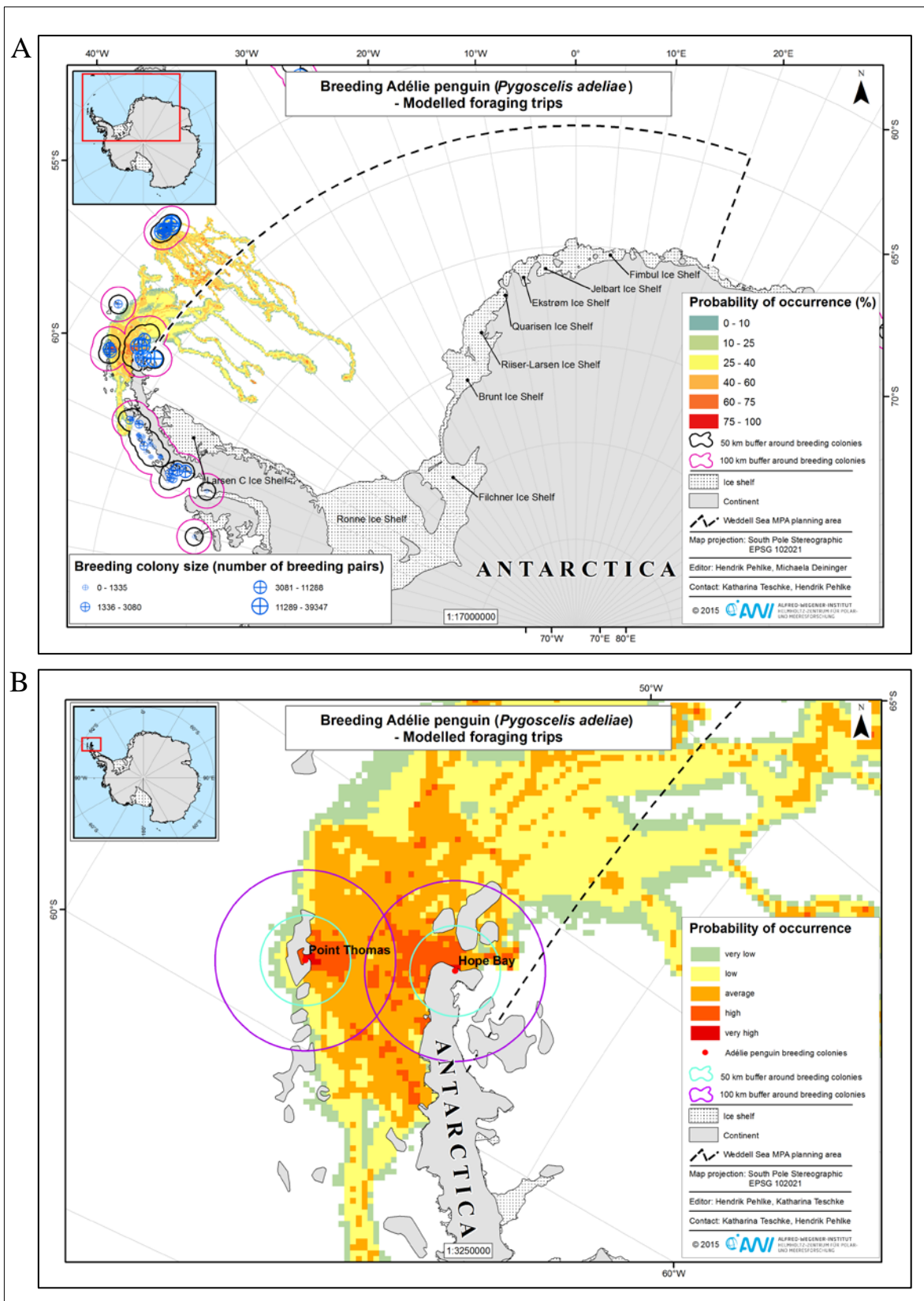


Figure 1-19 Prediction map for Adélie penguin (*Pygoscelis adeliae*) breeding distribution in the border area between Planning Domain 1 and Planning Domain 3. Areas that were used most often by tracked individuals is colour-coded with yellow and green colours indicating less suitable to unsuitable habitat and red colours indicating most often used areas. Black dashed box: WSMPA planning area; boundaries of the planning area do not resemble the boundaries of any proposed WSMPA.

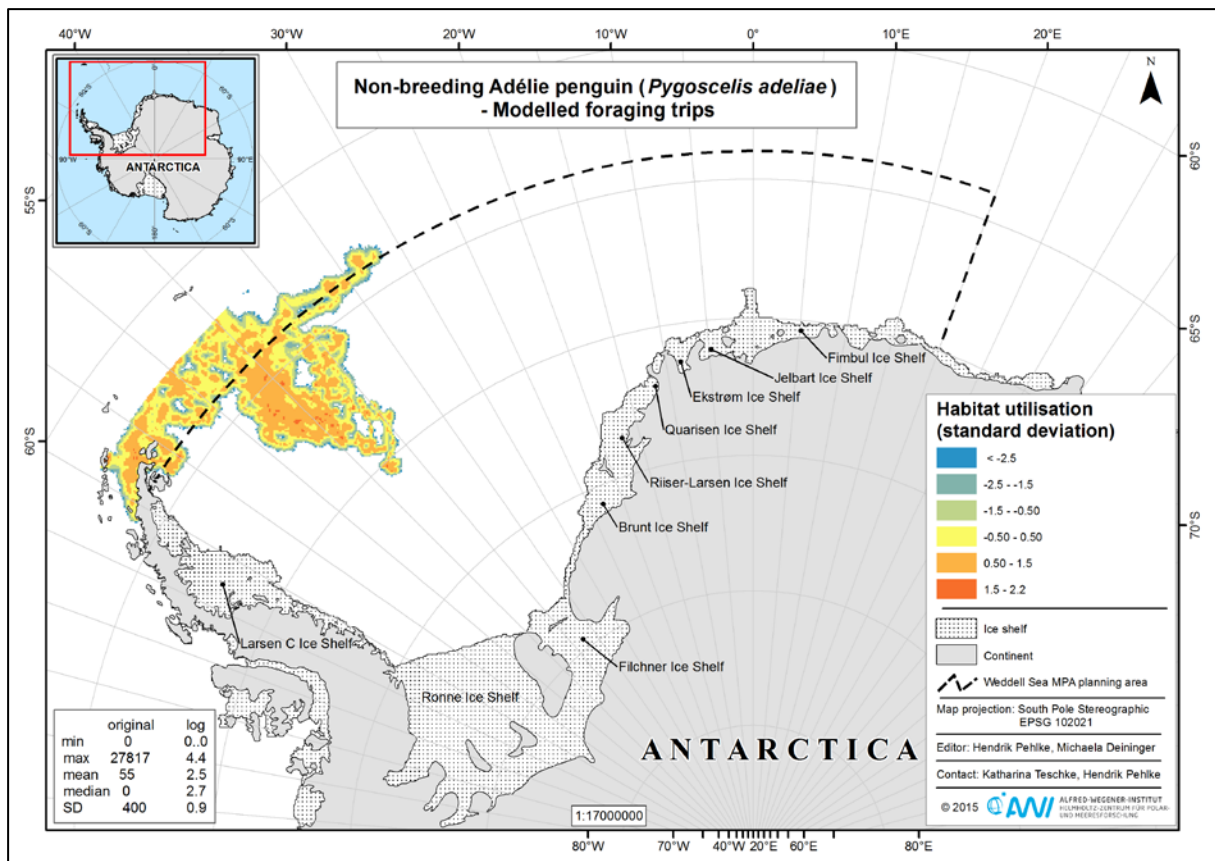


Figure 1-20 Prediction map for Adélie penguin (*Pygoscelis adeliae*) non-breeding distribution in the border area between Planning Domain 1 and Planning Domain 3. Modelled data are plotted as log-transformed standard deviation. Areas that were used most often by tracked individuals is colour-coded with yellow and blue colours indicating less suitable to unsuitable foraging habitat and orange/red colours indicating most often used areas. Black dashed box: WSMMPA planning area; boundaries of the planning area do not resemble the boundaries of any proposed WSMMPA.

Emperor penguin

Populations of emperor penguins play a prominent role in shaping biological diversity patterns and ecosystem processes in Antarctica on regional scales, i.e. in those areas where penguin foraging exerts a significant impact on their prey and penguin abundance attracts their principal predators. In the Weddell Sea 15 colonies with more than ~78,000 pairs breed which comprises ~33% of the global population. There is growing consensus that emperor penguin populations will be affected by predicted climate change and by subsequent changes in marine food webs (e.g., increased competition for marine living resources, increased predation). Therefore, solid knowledge of emperor penguin ecological requirements, particularly during sensitive periods such as breeding and chick rearing, is essential for successful Antarctic marine conservation/spatial planning. The spatial distribution of penguins while foraging is of specific interest, as it indicates the hinterland on which a colony depends for alimentation and thus the likely sphere of ecological influence of this colony. Hence, models that can predict emperor penguin distribution patterns would constitute a valuable tool in ecosystem analysis. We presume that the probability of an emperor penguin being present at a certain geographical locality depend on three major factors, the overall density of penguins in the wider area, the distance from the colony and the sea ice conditions,

i.e. to which extent entry into the water is possible. Polynyas (i.e. ice free areas) constitute major access points to open water for emperor penguins to forage (Zimmer et al. 2008) in particular during winter where broad areas are covered by ice. Local prey abundance may be of importance, too, but this information is not readily available. Accordingly, we propose a simple model of emperor penguin foraging occurrence and distribution during breeding season as a function of (i) colony size, (ii) distance from colony, and (iii) sea ice concentration.

We used data on emperor penguin colony locations and breeding population estimates from Fretwell et al. (2012, 2014). Moreover, daily sea ice concentration data were derived from the Advanced Microwave Scanning Radiometer - Earth Observing System instrument (for more details see Teschke et al. 2016, WG-EMM-16/02; chapter 1.4).

Analysis 1: Probability model of penguin occurrence as a function of distance from colony and of colony size

The following assumptions were made (see eq. 1):

1. Under spatially homogeneous ice conditions foraging emperor penguins of one colony show a standard normal distribution (ND) pattern with highest probability of occurrence close to the colony (defined as the centre of the distribution).
2. According to Zimmer et al. (2008) and reference therein mean maximum foraging distance to the colony of male penguins in winter is 106 km (standard deviation (SD) = 28 km). We assume that the maximum foraging distance to the colony (***dmax***) is equivalent to the mean maximum foraging distance of 106 km plus three SD, i.e. $106 \text{ km} + 3 \cdot 28 \text{ km} = 190 \text{ km}$. Foraging distribution patterns of emperor penguins beyond ***dmax*** were cut off.

Please note, that the maximum foraging distance to the colony ***dmax*** is not necessarily synonymous with the maximum length of the foraging trip. Although penguins generally forage with a directional axis, it seems that some foraging movements show more a zig-zag path parallel to the coast than a directional way (see Zimmer et al. 2008). Therefore, the length of the foraging trip may be greater than the maximum Euclidian distance to the colony ***dmax***. For example, winter-foraging females travelled on average a total distance of 1,050 km, but their travelled maximum distance to the colony is much lower (median: 104 km).

To calculate the foraging distances from colony, we used a raster grid with a spatial resolution of 6.25 km x 6.25 km (as for sea ice concentration). We calculated the Euclidian distance for each raster pixel centre (centroid) ***j*** (in total 119862 raster cells) to each emperor penguin breeding colony ***i*** (in total 15 colonies in the study area plus the Ragnhild colony at the eastern boundary outside the study area; this colony was included in the calculation as we assume a potential influence on the study area, and its breeding populations) (see eq. 1 - 3).

Thus, the probability of occurrence ***PI_{i,j}*** of one penguin from colony ***i*** in centroid ***j*** was calculated by the following approximation:

$$P1_{i,j} = \left(\frac{1}{\sqrt{\pi}}\right) * e^{\left(\frac{-\left(3*\frac{d_{i,j}}{d_{max}}\right)^2}{2}\right)} \quad (1)$$

where d_{max} is the maximum foraging distance to breeding colony, and $d_{i,j}$ is the Euclidean distance (in km) between colony i and centroid j , which was calculated by:

$$d_{i,j} = \left(\sqrt{(x_i - x_j)^2 + (y_i - y_j)^2}\right) - d_{ice_edge_i} \quad (2)$$

where $d_{ice_edge_i}$ is the distance of colony to the shelf ice edge (see Table 1-3). Distances $d_{i,j} \leq 0$ were set to 1. Subsequently, different boundaries of ice shelf edge were adjusted by a 10 km puffer, which was subtracted from the distances $d_{i,j}$, too, and a reclassification was performed again ($d_{i,j} \leq 0$ were set to 1).

Then, the probability of penguin occurrence $PI_{i,j}$ from colony i in centroid j was normalized to a range between 0 and 1 (i.e. $0 \leq PI_{i,j} \leq 1$). Finally, all $PI_{i,j}$ were added for each centroid j and normalized to a range between 0 and 1:

$$P1_j = \frac{\sum_{i=1}^n PI_{i,j}}{\max(\sum_{i=1}^n PI_{i,j})} \quad (3)$$

where n is the number of emperor penguin breeding colonies.

Table 2-3: Emperor penguin breeding colonies in the Weddell Sea and their distance to the shelf ice edge as potential access point to the sea.

Colony	Distance to ice shelf (km)
Astrid	0.00
Atka	2.90
Dawson	1.40
Dolleman	0.00
Drescher	0.00
Gould	0.00
Halley	0.00
Jason Peninsula	6.80
Lazarev	2.80
Luitpold	29.80
Ragnhild	0.00
Riiser	0.50
Sanae	6.20
Smith	2.90
Snowhill	1.60
Stancomb	0.00

To account for breeding colony size (number of animals), each probability of penguin occurrence $P1_{i,j}$ was weighted with the best population estimate (BE) for this emperor penguin colony according to Fretwell et al. (2012).

$$P1'_{i,j} = P1_{i,j} * BE_i \quad (4)$$

Subsequently, all $P1'_{i,j}$ were added for each centroid j and normalized to a range between 0 and 1 (i.e. $0 \leq P1'_j \leq 1$):

$$P1'_j = \frac{\sum_{i=1}^n P1'_{i,j}}{\max(\sum_{i=1}^n P1'_{i,j})} \quad (5)$$

where n is the number of emperor penguin breeding colonies.

Analysis 2: Probability model of penguin occurrence as a function of sea ice concentration

The probability model of penguin occurrence as a function of sea ice concentration was calculated in following steps: (1) A sigmoid transfer function was applied (eq. 6) to achieve an even distribution of the mean sea ice concentration data; (2) the ice index data (IC_j) were normalised to a range between 0 and 1 (eq. 7); and (3) the probability of penguin occurrence was calculated using the transformed data and a hyperbolic *tanh*-function (eq. 8).

The mean sea ice concentration was calculated for the breeding period of emperor penguins (Jun to Jan) from 2002 to 2011 (in total 2265 satellite images).

$$IC_j = \frac{1}{1+e^{(-\ln(x+10^{-5})*gain)}} \quad (6)$$

with x = mean sea ice concentration/100 and gain set to 6.23.

Subsequently, the ice index data (IC_j) were normalised to a range between 0 and 1:

$$IC_j = norm_{IC_j} = \frac{IC_j - \min(IC_{j_1}, IC_{j_2}, \dots, IC_{j_n})}{\max(IC_{j_1}, IC_{j_2}, \dots, IC_{j_n}) - \min(IC_{j_1}, IC_{j_2}, \dots, IC_{j_n})} \quad (7)$$

For the probability model of penguin occurrence we assume penguin preference does not relate linearly to sea ice conditions but with a sigmoid pattern, i.e. areas with medium sea ice concentration are suitable foraging grounds already. This sigmoid pattern was modelled by the following *tanh*-function:

$$P2_j = \frac{\tanh(\pi*(IC_j*2-1))+1}{2} \quad (8)$$

Analysis 3: Combining the distance/colony size model with the sea ice concentration model

An overall probability of penguin occurrence P_j , i.e. a combination of the distance/colony size model and the sea ice coverage model, was calculated by the following equation:

$$P_j = \frac{(P1_j * P2_j) - \min(P1_j * P2_{j_1}, P1_j * P2_{j_2} \dots P1_j * P2_{j_n})}{\max(P1_j * P2_{j_1}, P1_j * P2_{j_2} \dots P1_j * P2_{j_n}) - \min(P1_j * P2_{j_1}, P1_j * P2_{j_2} \dots P1_j * P2_{j_n})} \quad (9)$$

Please note that P_j was normalized to a range between 0 and 1 (i.e. $0 \leq P_j \leq 1$), and thus relative probability values that indicate differences between centroids, instead of absolute values, are mapped in Figure 1-21.

Our model of emperor penguin foraging distribution during breeding season shows that the probability of occurrence is highest at the Halley and Dawson colony near Brunt Ice Shelf and at the Atka colony near Ekström Ice Shelf.

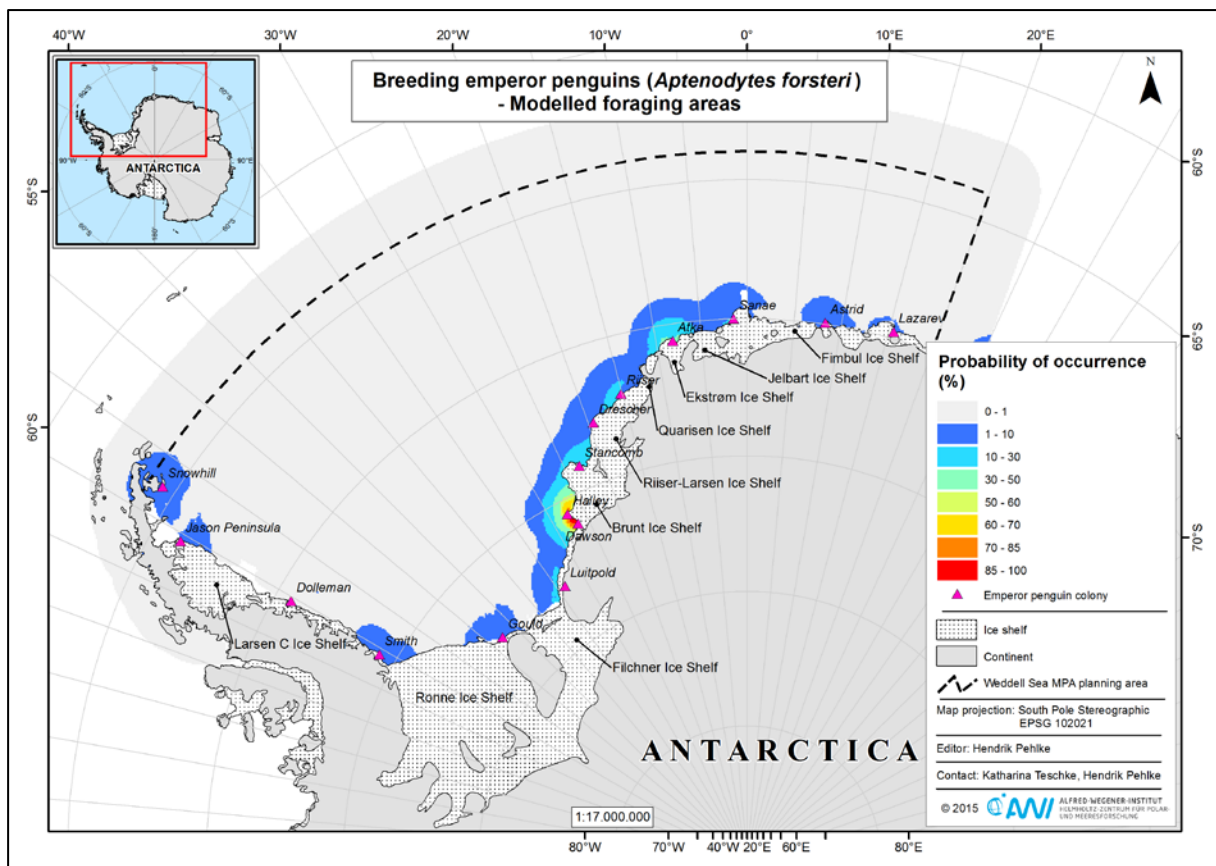


Figure 1-21 Probability of penguin occurrence P_j as a function of distance to colony, colony size and sea ice concentration (see eq. 9). Black dashed box: WSMMA planning area; boundaries of the planning area do not resemble the boundaries of any proposed WSMMA.

1.2.5 Marine Mammals

Pinnipeds

Data for the western part of the WSMPA planning area were derived from Flores et al. (2008) and Forcada et al. (2012). Flores et al. (2008) calculated the density of seals (non-standardised data) for each transect, and the average transect densities were calculated for each region. In contrast, Forcada et al. (2012) used standardised data for the density calculations. Several factors potentially influencing the probability of animal detection for their density estimations were considered (e.g. probability of detection for perpendicular sighting distances). To interpolate the seal densities, a more sophisticated approach, i.e. a combination of different generalized additive models, was used in Forcada et al. (2012). Calculated seal densities were pooled in case of areas where both studies collected data.

Data for the south-eastern and eastern part of the Weddell Sea were derived from Bester et al. (1995, 2002) and Plötz et al. (2011a-e). Seal densities (individuals/km²) were calculated for the data from PANGAEA (Plötz et al. 2011a-e) with the count method for line transect data (Bester et al. 1995, Bester & Odendaal 2000, Hedley & Buckland 2004). We used non-standardised data for the density calculations as the data set from Plötz et al. (2011a-e) is based on video material, and thus at least observer related factors potentially influencing the probability of animal detection are not relevant to consider. Regarding seal densities from Bester et al. (1995) we calculated the mean of up to three sampling seasons for each transect. Bester et al. (2002) assigned the transects to three different zones, and then the average transect densities were calculated for each zone.

To interpolate the seal density (point data) in the south-eastern and eastern part of the WSMPA planning area, we applied the inverse distance weighted interpolation method (IDW) in ArcGISTM spatial analyst tool to the data from PANGAEA (Plötz et al. 2011a-e) and Bester et al. (1995, 2002). Following settings for the IDW were chosen:

- Z value: The calculated seal density for a strip of 60 m width
- Output cell size: 2000 m
- Distance coefficient power P: 2
- Search radius setting, number of points: 10

The following map shows the result of the approaches from Flores et al. (2008) and Forcada et al. (2012) combined with the IDW that we applied. The classification concerning the number of individuals per km² was chosen from Forcada et al. (2012), and a new classification category (> 15 individuals per km²) was added.

Figure 1-22 indicates highest absolute seal density (i.e. > 15 individuals/km²) on the Riiser-Larsen Ice Shelf to Quarisen Ice Shelf. Seal densities of 2-15 individuals/km² occur more large-scale on the Riiser-Larsen Ice Shelf to Ekstrøm Ice Shelf, and offshore between 5-15°W and 0-5°E. The greater part of the western Weddell Sea is characterised by relatively low crabeater seal densities (1-2 individuals/km²). However, crabeater seals are the most abundant pinniped species in the western Weddell Sea compared to leopard seals and Weddell seals with highest estimated densities of ≤ 0.02 individuals/km² and ≤ 0.5 individuals/km², respectively (see Forcada et al. 2012).

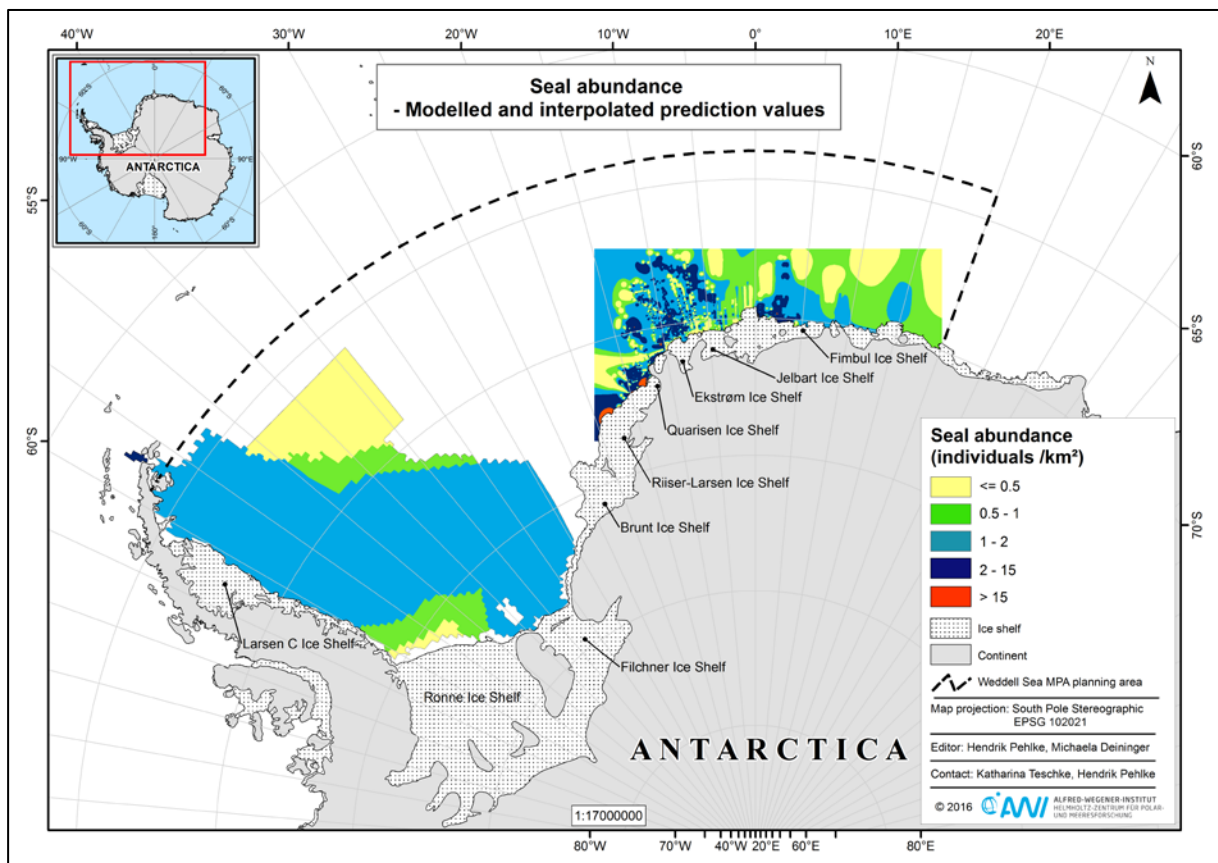


Figure 1-22 Distribution patterns of seals in the Weddell Sea. Abundance data on crabeater seals in the western part of the WSMMPA planning area were derived from Flores et al. (2008) and Forcada et al. (2012). Abundance data on seals in the south-eastern and eastern part of the Weddell Sea based on data from PANGAEA (Plötz et al. 2011a-e; unspecified taxa) and Bester et al. (1995, 2002; crabeater seals). The un-transformed, interpolated data are plotted as absolute seal densities (individuals/km²). Red dashed box: WSMMPA planning area; boundaries of the planning area do not resemble the boundaries of any proposed WSMMPA.

Whales

The Antarctic minke whale (*Balaenoptera bonaerensis*) is the most abundant cetacean in Antarctic waters. They are observed within dense sea ice regularly (e.g., Williams et al. 2014, Gutt et al. 2011, Scheidat et al. 2011). During austral summer their distribution concentrates between 62°S and the pack ice (Gill & Evans 2002), with highest encounter rates in late January/early February south of 66°S between 66°E-80°E (Kasamatsu et al. 1996).

There are no systematic surveys for the ice-covered regions of the Weddell Sea so far, but minke whale calls have been recorded regularly at the PALAOA observatory near *Neumayer Base* (Van Opzeeland pers. comm., Risch et al. 2014). During austral winter, most Antarctic minke whales leave for their breeding grounds (10°-30°S), but some have been reported to overwinter in Antarctic waters (Thiele & Gill, 1999). Minke whales in the Southern Ocean feed on the Antarctic krill *Euphausia superba* primarily but on smaller zooplankton, too (Ohsumi et al. 1970, Stewart & Leatherwood 1985). Abundance is estimated to 515.000 individuals (95 % CI 360.000 - 730.000) by IWC but may be higher as surveys do not include

ice-covered areas. Antarctic minke whales are listed as *data deficient* (IUCN Red List of Threatened Species; Version 2014.2). Observation maps (Ropert-Coudert et al. 2014) and habitat models (Bombosch et al. 2014, see Fig. 1-23) indicate that Minke whales occur in the WSMPA planning area. Highly favourable conditions for minke whales throughout the season are predicted for an area around 70°S and 40°W.

The high latitude feeding area of Humpback whales (*Megaptera novaeangliae*) ranges from the Antarctic Convergence to the pack ice region. Higher densities are found in the southern Indian Ocean, around the Antarctic Peninsula and in the northern Ross Sea and highest encounter rates are reported for December to January (see Branch 2011). So far seven distinct feeding grounds corresponding to six breeding stocks are suggested (International Whaling Commission 2011). Humpback breeding stocks A, B and C are of relevance for the WSMPA planning area, since these individuals migrate between the Weddell Sea and their breeding grounds further north. Some individuals may stay in the Antarctic year-round, presumably to avoid the energetic demands of migration (Van Opzeeland et al. 2013). Humpback whales in the Southern Ocean feed on pelagic crustaceans, mainly krill *Euphausia superba* (Clapham 2002). The 1997/96 IWC population estimate is 42,000 for the Southern Ocean, with approximately 26,630 individuals allocated to breeding stocks A, B and C (Branch 2011). Humpback whales are listed as *least concern* (IUCN Red List of Threatened Species; Version 2014.2). Habitat suitability models indicate that favourable habitat conditions for humpback whales exist in open waters near Larsen C Ice Shelf and in the eastern part of the planning area throughout January and February (Fig. 1-23, Bombosch et al. 2014).

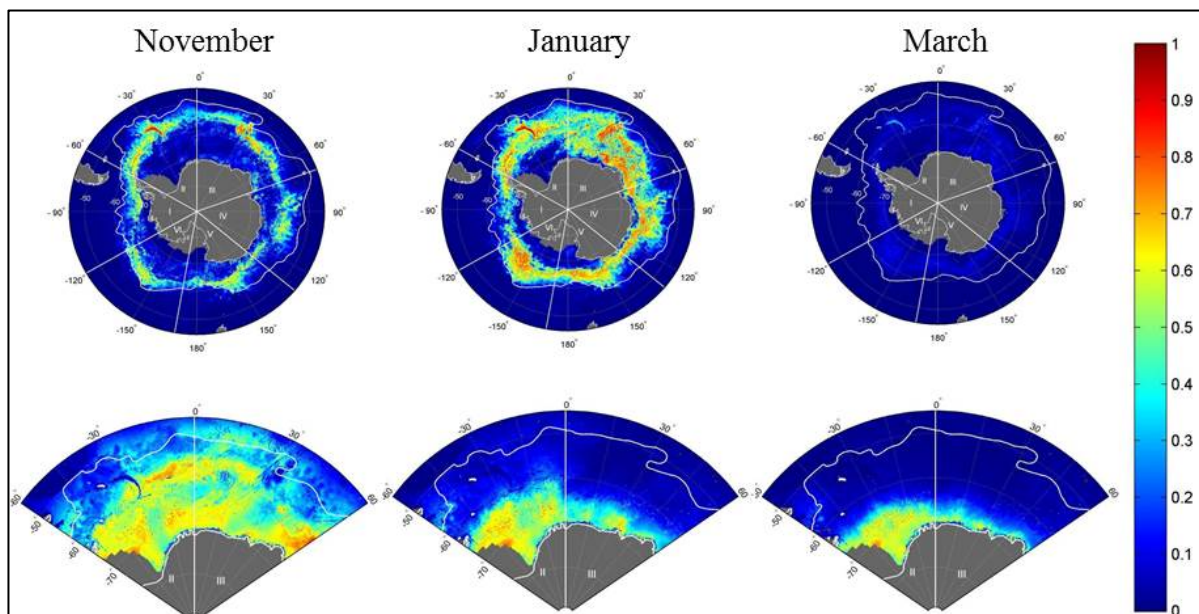


Figure 1-23 Maxent spatial prediction maps for humpback whales (upper row) and Antarctic minke whales from 60°W to 60°E (lower row) for the 15th of November, January and March 2006/2007. Habitat suitability is colour-coded with blue colours indicating less suitable to unsuitable habitat, greenish colours depicting ‘typical’ conditions for humpback whales and red colours indicating more suitable to highly suitable habitat conditions. The white line represents the Polar Front (Harris & Orsi 2001). Grey areas indicate land areas or regions for which values for one of the environmental variables are missing. The white lines extending from the South Pole indicate the 6 IWC management areas. Westerly and southerly coordinates are indicated as negative numbers (from Bombosch 2013).

2. MPA scenario development

Katharina Teschke, Hendrik Pehlke & Thomas Brey

Alfred Wegener Institute, Helmholtz Centre for Polar and Marine Research, 27570 Bremerhaven, Germany;
katharina.teschke@awi.de, hendrik.pehlke@awi.de, thomas.brey@awi.de

This chapter describes the MPA scenario development that is closely geared to the *Systematic Conservation Planning* approach (Margules & Pressey 2000) under CCAMLR. Firstly, we present the defined general and specific conservation objectives for the WSMMPA planning area. Then, we provide a systematic overview of the parameters and their specific regional objective for the Marxan analysis (see Tab. 2-1), and present the cost layer analysis. Subsequently, we set out the approach using the Marxan (version 2.43; see <http://www.uq.edu.au/marxan>; e.g. Ball et al. 2009), and finally substantiate the Marxan analysis for the MPA proposal.

2.1 Conservation objectives & parameters

The conservation objectives were developed by the German WSMMPA project team and further refined on the basis of the contributions by the participants of the 2nd International Expert Workshop on the Weddell Sea MPA that took place in Berlin (28-29 April 2015).

In accordance with Article II and IX of the Convention and Conservation Measure 91-04, paragraph 2, the following six general conservation objectives and, based on those, twelve specific objectives were defined for the WSMMPA. The general objectives classify the WSMMPA as a tool for the protection of special ecosystems, habitats, features and representative areas of the whole Weddell Sea planning area. The specific objectives focus on the protection of very concrete features within the WSMMPA.

The workshop agreed that consistency in wording and clarification of terms in a preamble for the objectives are necessary. A definition would subsequently allow the use of the wording protection within the overall conservation objective coherent with CM 91-04.

On this basis, the following conservation objectives for the WSMMPA were defined.

Objectives of the WSMMPA

In accordance with Article II and IX of the Convention and paragraph 2 of Conservation Measure 91-04, the WSMMPA will assist the conservation of Antarctic marine living resources while contributing to the following general and specific objectives in the long term:

General objectives

- G 1 Protection of representative examples of pelagic and benthic ecosystems, biodiversity and habitats (including the environmental and ecological conditions supporting them) of the Weddell Sea planning area.
- G 2 Protection of pelagic and benthic habitats and ecosystems which are rare, unique, vulnerable, diverse and/or endemic to the Weddell Sea planning area.

- G 3 Protection of areas, environmental features and species (incl. populations and life history stages) on various geographical scales which are key to the functional integrity and viability of local ecosystems and ecosystems processes in the Weddell Sea planning area.
- G 4 Establishment of scientific reference areas to study, in particular representative, rare, unique and/or endemic examples of marine ecosystems, as well as biodiversity and habitats, and to monitor the effects of climate change, fishing and other human activities in the Weddell Sea planning area.
- G 5 Protection of essential habitats for top predators such as marine mammals and seabirds in the Weddell Sea planning area.
- G 6 Protection of essential habitats in the Weddell Sea planning area as potential refugia for, inter alia, top predators, fish and other ice-dependent species, in order to maintain and /or enhance their resilience and ability to adapt to the effects of climate change.

Specific objectives

Pelagic conservation objectives

- S 1 Protection of representative examples of pelagic and sea ice ecosystems and habitats, such as the unique, persistent open ocean areas associated with the Maud Rise submarine plateau, or the areas along the shelf ice edge in the eastern and southern part of the WSMPA with no or very low sea ice cover throughout the austral summer;
- S 2 Protection of Antarctic krill, ice krill and Antarctic silverfish as key species in the Antarctic food web as well as of important areas / habitats for their life cycle, e.g. spawning areas;
- S 3 Protection of essential habitats for top predators such as flying seabirds, penguins and seals;

Benthic conservation objectives

- S 4 Protection of representative examples of benthic ecosystems and habitats, such as the ecologically important sponge associations on the shelf in the eastern and southern part of the WSMPA;
- S 5 Protection of Antarctic toothfish as a top predator incl. all life history stages and their habitats;
- S 6 Protection of the integrity and life cycles of unique and diverse suspension feeding assemblages, incl. benthic sponge associations and thereby maintaining the associated benthic communities as efficient sources for recolonization;
- S 7 Protection of rare and unique shallow (surface to –150 m water depth) sea floor areas with high habitat heterogeneity and species richness in order to preserve the ecologic function of these areas as “stepping stones” and sources for recolonization for associated communities and species;
- S 8 Protection of spawning areas and nesting sites of demersal fish species including those exhibiting parental care;

Pelagic and/or benthic conservation objectives

- S 9 Protection of higher productivity areas to support key ecosystem processes and functional integrity of the ecosystems;
- S 10 Protection of marine ecosystems and habitats vulnerable to effects of climate change, fishing and other human activities and critical to the function of local ecosystems, in order to maintain and/or enhance resilience and adaptive capacity, such as benthic three-dimensional suspension feeder communities in the eastern and southern part of the WSMPA or the marine areas important for the foraging and life cycle of top predators;

Research objectives

- S 11 Provision of scientific reference areas to monitor the natural variability and long-term changes on the Antarctic marine living resources and to study the effects of climate change and human activities on the Antarctic ecosystems;
- S 12 Provision of areas for fisheries research in form of a dedicated Fisheries Research Zone to enhance the understanding of the fish stocks and to study the effects of fishing activities.

Table 2-1 shows how the different parameters and data sets cover the general and specific conservation objectives. The data sets behind each parameter are described in detail in Teschke et al. (2016; WG-EMM-16/02), whereas the analyses of the different parameters are depicted in chapter 1 of this document. In addition, specific regional conservation objectives for each parameter, i.e. a target value as a proportion of the area of the total distribution of that parameter, i.e., $0 \leq \text{target value} \leq 100\%$, are listed. In general, for a common parameter lower values might be sufficient to ensure its conservation, whereas for a unique, rare or sensitive parameter higher target values might be used. For example, 20 % was used as the target value for most of the pelagic and benthic (bio) regions. To encompass larger areas for highly mobile species with less predictable distribution patterns values of 30 % to 40 % were used. Target values of 100 % were set for highly productive areas, important or unique geomorphic features and highly sensitive areas, such as spawning areas (see Tab. 2-1). For each parameter a range of proportional target values was compiled at the 2nd International Expert Workshop on the WSMPA project (28-29 April 2015; Berlin, Germany). For our final Marxan analysis we used for each parameter a medium target value, except for highly productive areas (e.g. coastal polynyas), unique geomorphic features (i.e. shallow water area on the Norsel Bank) and highly sensitive areas (e.g. sponge associations, nesting sites of demersal fish); here, we used target values of 100 %.

Table 2-1 Description of data sets and conservation objectives for the Marxan scenario.

Parameter	No. features	Description of features	Source (contact person, publication, web site)	Specific regional objective for MARXAN analysis	Relevant conservation objectives
Pelagic regionalisation (in situ data, satellite data, model data)	8	<p>8 pelagic regions:</p> <p><u>Coastal polynyas I</u> (very high probability of ice-free areas)</p> <p><u>Coastal polynyas II</u> (high probability of ice-free areas)</p> <p><u>Coastal polynyas III</u> (lower probability of ice-free areas)</p> <p><u>Transition zone</u> (average depths, average probability of ice-free areas)</p> <p><u>Deepwater I</u> (lower depths, slightly larger depth ranges)</p> <p><u>Deepwater II</u> (average depths, very small depth ranges)</p> <p><u>Deepwater III</u> (greatest depths, slightly larger depth ranges)</p> <p><u>Ice-covered area</u> (year-round)</p>	<p><u>Sea ice concentration:</u> Kaleschke et al. (2001), Spreen et al. (2008) Institute of Environmental Physics, University of Bremen: http://www.iup.uni-bremen.de/seaice/amr/</p> <p><u>Bathymetry:</u> Arndt et al. (2013); www.ibcso.org</p> <p><u>Seawater temperature and salinity:</u> FESOM model data; Timmermann et al. (2009)</p>	<p>100 % of each coastal polynya region</p> <p>20 % of each remaining pelagic region</p>	<p><u>General objectives:</u> G1 - G3, G5 & G6</p> <p><u>Specific objectives:</u> S1 - S3, S9 & S10</p>
Benthic bioregionalisation	50	<p>Depth classes nested in 18 geomorphic features resulted in 50 environmental types:</p> <p><u>Abyssal plain:</u></p> <ul style="list-style-type: none"> • > -3000m <p><u>Bank:</u></p> <ul style="list-style-type: none"> • 0m to -100m • -100m to -200m • -200m to -500m • -500m to -1000m <p><u>Canyon shelf commencing</u></p> <p><u>Canyon slope commencing</u></p> <p><u>Coastal Terrane</u></p> <p><u>Cross Shelf Valley:</u></p> <ul style="list-style-type: none"> • 0m to -100m • -100m to -200m • -200m to -500m • -500m to -1000m • -1000m to -1500m <p><u>Filchner Trough</u></p> <p><u>Lower slope:</u></p> <ul style="list-style-type: none"> • -2000m to -3000m 	Douglass et al. (2014)	<p>60 % of the following important or unique geomorphic types:</p> <ul style="list-style-type: none"> - Canyon Shelf Commencing - Canyon Slope Commencing - Filchner Trough (includes parts of Cross Shelf Valley) - Margin Ridge (= Astrid Ridge) & Marginal Plateau - Plateau & Plateau Slope (includes parts of Maud Rise) - Seamount & Seamount Ridge (includes parts of Maud Rise) - Shelf & Shelf Deep - Upper Slope <p>20 % of all other environmental types</p>	<p><u>General objectives:</u> G1 - G3</p> <p><u>Specific objectives:</u> S4 - S10</p>

Table 2-1 Description of data sets and conservation objectives for the Marxan scenario.

Parameter	No. features	Description of features	Source (contact person, publication, web site)	Specific regional objective for MARXAN analysis	Relevant conservation objectives
		<ul style="list-style-type: none"> • > -3000m <u>Margin Ridge:</u> • -500m to -1000m • -1000m to -1500m • -1500m to -2000m • -2000m to -3000m • -3000m to -4500m <u>Marginal Plateau:</u> • -2000m to -3000m • -3000m to -4500m <u>Plateau:</u> • -2000m to -3000m • -3000m to -4500m <u>Plateau Slope:</u> • -2000m to -3000m • -3000m to -4500m <u>Ridge:</u> • -1500m to -2000m • -2000m to -3000m • -3000m to -4500m <u>Rugose Ocean Floor:</u> • > -3000m <u>Seamount Ridge:</u> • -1000m to -1500m • -2000m to -3000m • -3000m to -4500m <u>Seamount:</u> • -1000m to -1500m • -1500m to -2000m • > -3000m <u>Shelf</u> <u>Shelf Deep:</u> • 0m to -100m • -200m to -500m • -500m to -1000m <u>Upper Slope:</u> • 0m to -100m • -100m to -200m 			

Table 2-1 Description of data sets and conservation objectives for the Marxan scenario.

Parameter	No. features	Description of features	Source (contact person, publication, web site)	Specific regional objective for MARXAN analysis	Relevant conservation objectives
		<ul style="list-style-type: none"> -200m to -500m -500m to -1000m -1000m to -1500m -1500m to -2000m -2000m to -3000m -3000m to -4500m 			
Probability of adult Antarctic krill occurrence (modelled data)	1	Adult Antarctic krill (<i>Euphausia superba</i>): Categories of different probability of occurrence (low to high) are included by means of a weighting factor	Krillbase: http://www.iced.ac.uk/science/krillbase.htm Atkinson et al. (2004, 2008, 2009); Siegel (1982) Fevolden (1979), Makarov & Sysoeva (1985); Siegel (1982, unpublished data) Siegel (2012, unpublished data), Siegel et al. (2013)	35 % of total area in which adult krill occurs focusing on areas with high probability of occurrence	<u>General objectives:</u> G1, G3 & G6 <u>Specific objectives:</u> S1, S2, S9 & S10
Larval Antarctic krill density (interpolated abundance data)	1	Larval Antarctic krill (<i>Euphausia superba</i>): Categories of different probability of occurrence (low to high) are included by means of a weighting factor	Fevolden (1979, 1980), Hempel & Hempel (1982), Menshenina (1992), Siegel (2005, unpublished data) Siegel (2012)	50 % of total area in which krill larvae occur focusing on areas with high probability of occurrence	<u>General objectives:</u> G1 & G3 <u>Specific objectives:</u> S1, S2, S9 & S10
Potential ice krill habitat	1	Depth (max. 550m) and temperature range ($\leq 0^{\circ}\text{C}$) describing the probability of occurrence north and east of the Filchner Trough	Proxies: <u>Bathymetry:</u> Arndt et al. (2013); www.ibcso.org <u>Seawater temperature range:</u> FESOM model data; Timmermann et al. (2009)	35 % of total area in which a potential Ice krill habitat occur	<u>General objectives:</u> G1, G3 & G6 <u>Specific objectives:</u> S1, S2, S9 & S10
Adult Antarctic silverfish density (interpolated abundance data)	1	Adult silverfish (<i>Pleuragramma antarctica</i>): Categories of different probability of occurrence (low to high) are included by means of a weighting factor	Boysen-Ennen & Piatkowski (1988), Drescher et al. (2012), Ekau et al. (2012a, b), Hureau et al. (2012), Kock et al. (2012), Wöhrmann et al. (2012), Flores et al. (2014) and unpublished data held by R. Knust, AWI	35 % of total area in which adult silverfish occurs focusing on areas with high probability of occurrence	<u>General objectives:</u> G1 & G3 <u>Specific objectives:</u> S1, S2, S9 & S10
Larval Antarctic silverfish density (interpolated)	1	Larval silverfish (<i>Pleuragramma antarctica</i>):	Boysen-Ennen & Piatkowski (1988),	35 % of total area in which larval silverfish occurs focusing on areas	<u>General objectives:</u> G1 & G3

Table 2-1 Description of data sets and conservation objectives for the Marxan scenario.

Parameter	No. features	Description of features	Source (contact person, publication, web site)	Specific regional objective for MARXAN analysis	Relevant conservation objectives
abundance data)		Categories of different probability of occurrence (low to high) are included by means of a weighting factor	Hubold et al. (1988)	with high probability of occurrence	<u>Specific objectives:</u> S1, S2, S9 & S10
Adélie penguins - Potential foraging areas	2	<u>Breeding Adélie penguin (<i>Pygoscelis adeliae</i>):</u> A 50 km buffer and a 50-100 km ring buffer around each colony defining suitable foraging habitats <u>Non-breeding Adélie penguin (<i>P. adeliae</i>):</u> Categories of different habitat suitability (low to high) are included by means of a weighting factor	<u>Breeding and non-breeding Adélie penguins:</u> BAS Inventory (partly unpublished data; contact person: P. Trathan, BAS) US AMLR Program, NOAA (data provider: J. Hinke, W. Trivelpiece) BirdLife International; seabird tracking database, www.seabirdtracking.org <u>Adélie colonies (location, size of colonies):</u> Lynch & LaRue 2014	<u>Breeding Adélie penguin:</u> 100 % of each 50 km buffer around each colony 50 % of each ring buffer (50-100 km) around each colony <u>Non-breeding Adélie :</u> 20 % of total area in which potential foraging areas for non-breeding Adélies during breeding season occurs focusing on areas with high probability of occurrence	<u>General objectives:</u> G1, G3, G5 & G6 <u>Specific objectives:</u> S1, S3, S9 & S10
Emperor penguins - Potential foraging areas (modelled data)	1	Emperor penguin (<i>Aptenodytes forsteri</i>): Categories of different probability of occurrence (low to high) during breeding season are included by means of a weighting factor	<u>Sea ice concentration:</u> Kaleschke et al. (2001), Spreen et al. (2008) Institute of Environmental Physics, University of Bremen: http://www.iup.uni-bremen.de/seaiace/amsr/ <u>Penguin data (location and size of colonies):</u> Fretwell et al. (2012)	40 % of total area in which potential foraging areas for Emperor penguins during breeding season occurs focusing on areas with high probability of occurrence	<u>General objectives:</u> G1, G3, G5 & G6 <u>Specific objectives:</u> S1, S3, S9 & S10
Antarctic petrel - Potential foraging areas (modelled data)	1	Antarctic petrel (<i>Thalassoica antarctica</i>): Sea ice cover (15%-80%), depth (slope and shelf break) and sea surface temperature ($\leq 0.5^{\circ}\text{C}$) describing the probability of occurrence	<u>Proxies:</u> <u>Sea ice concentration:</u> Kaleschke et al. (2001), Spreen et al. (2008) Institute of Environmental Physics, University of Bremen: http://www.iup.uni-bremen.de/seaiace/amsr/ <u>Bathymetry:</u> Arndt et al. (2013); www.ibcso.org <u>Seawater temperature range:</u> FESOM model data; Timmermann et al. (2009)	40 % of total area in which a potential Antarctic petrel foraging habitat occur	<u>General objectives:</u> G1, G3 & G5 <u>Specific objectives:</u> S1, S3, S9 & S10
Seal density (combinations of modelled and interpolated	1	Combined data for crabeater seals (<i>Lobodon carcinophaga</i>) and unspecified taxa:	<u>Crabeater seals:</u> Forcada et al. (2012) <u>Unspecified taxa:</u> Plötz et al. (2011 a-e;	40 % of total area in which seals occur focusing on areas with high probability of occurrence	<u>General objectives:</u> G1, G3, G5 & G6

Table 2-1 Description of data sets and conservation objectives for the Marxan scenario.

Parameter	No. features	Description of features	Source (contact person, publication, web site)	Specific regional objective for MARXAN analysis	Relevant conservation objectives
abundance data)		Categories of different probability of occurrence (low to high) are included by means of a weighting factor	http://www.pangaea.de		<u>Specific objectives:</u> S1, S3, S9 & S10
Sponge presence (interpolated abundance classes)	1	Categories of different probability of sponge presence (i.e. rare, common, very common) are included by means of a weighting factor	Partly unpublished data; Dieter Gerdes (AWI); Ute Mühlenhardt-Siegel (DZMB); e.g. Gerdes et al. (1992) Unpublished data (ANT VII/4, ANT VII/5, ANT IX/1-4, ANT XIII/3, ANT XV/3, ANT XVII/3, ANT XXI/2); contact: Wolf Arntz (AWI, retired)	100 % of total area in which sponges occur focusing on areas with very common sponge presence	<u>General objectives:</u> G1 - G4 <u>Specific objectives:</u> S4, S6, S9 - S11
Potential habitats of cold water shelf echinoderm fauna	1	Temperature range ($\leq -1^{\circ}\text{C}$) describing potential habitats for special communities regarding sea cucumbers and brittle stars	Proxy: <u>Bottom seawater temperature range:</u> FESOM model data; Timmermann et al. (2009)	35 % of total area in which a potential habitat for special echinoderm communities occur	<u>General objectives:</u> G1 – G3 <u>Specific objectives:</u> S4 & S10
Unique shallow water area on the Norsel Bank	1	Feature defining the position of a unique area regarding depth range & benthic diversity	<u>Bathymetry:</u> Arndt et al. (2013); www.ibcso.org Teschke et al. (2016; WG-EMM-16/01, chapter 3.2.3)	100 % of those unique shallow water area	<u>General objectives:</u> G1 - G3 <u>Specific objectives:</u> S4, S6, S7 & S10
Observations of nesting sites	1	Evidence of nest-guarding behaviour of demersal fish, e.g. <i>Chaenodraco wilsoni</i> <i>Neopagetopsis ionah</i>	Unpublished data (ANT XXIX/9, 2014); Dieter Gerdes (AWI) Unpublished data (ANT XXVII/3, 2011); Tomas Lundälv (Swedish Institute for the Marine Environment) Unpublished data (ANT XXXI/2, 2015); Emilio Riginella (University of Padova)	100 % of each observation polygon	<u>General objectives:</u> G2 & G3 <u>Specific objectives:</u> S4, S8 & S10
Probability of demersal fish occurrence (modelled data)	1	Categories of different probability of occurrence (low to high) are included by means of a weighting factor	Unpublished data (ANT XIII/3, ANT XV/3, ANT XVII/3, ANT XIX/5, ANT XXI/2, ANT XXIII/8, ANT XXVII/3, ANT XXIX/9); contact person: Rainer Knust (AWI)	75 % of total area in which demersal fish occurs focusing on areas with high probability of occurrence	<u>General objectives:</u> G1, G3 & G6 <u>Specific objectives:</u> S1, S2, S9 & S10

Table 2-1 Description of data sets and conservation objectives for the Marxan scenario.

Parameter	No. features	Description of features	Source (contact person, publication, web site)	Specific regional objective for MARXAN analysis	Relevant conservation objectives
Potential toothfish habitat	1	Depth range (400 – 3100m) - according to WG-FSA-15/64 - describing a potential habitat of the Antarctic toothfish (<i>Dissostichus</i> spp.)	Proxy: Bathymetry: Arndt et al. (2013); www.ibcso.org	75 % of total area in which a potential toothfish habitat occur	<u>General objectives:</u> G1, G3 & G5 <u>Specific objectives:</u> S4, S5, S9, S10 & S12

Cost layer

The cost layer used for our final Marxan analyses includes (i) accessible areas for fishery vessels, (ii) the potential toothfish habitat and (iii) suitable Antarctic krill habitats as recommended by WG-EMM-15 (see report SC-CAMLR-XXXIV, Annex 6). Such cost layer allows studying whether and how the solution obtained by Marxan will change - in terms of achieving the specific regional conservation objectives - if grid cells identified as e.g. a potential toothfish habitat are loaded with higher costs.

Accessible areas for fishery vessels

The AMSR-E 89 GHz sea ice concentration maps (2002 to 2011) were used to calculate the maximal sequence of ice-free days (for more details see chapter 1.4 in Teschke et al. 2016, WG-EMM-16/02). We defined the “accessibility” with a sea ice concentration $\leq 60\%$ according to Parker et al. (2014), and focused on the austral summer (Dec - Mar). Data on daily sea ice concentration were reclassified, i.e. a value of 1 was assigned to each grid cell with ice cover more than 60 %, whereas grid cells with ice cover $< 60\%$ were set to 0. Then, we counted the sequenced number of days with ice cover $\leq 60\%$ within each grid cell, and recorded the maximal sequence of ice-free days per year. Subsequently, the mean maximal sequence of ice-free days was calculated over 10 years from 2002 to 2011 (see Fig. 2-1).

To incorporate the information about “accessible areas” into the cost layer the mean maximal sequence of ice-free days was grouped (20 classes; see Fig. 2-1), and the values were normalized to a range between 0 and 1 for comparability among the three different cost units.

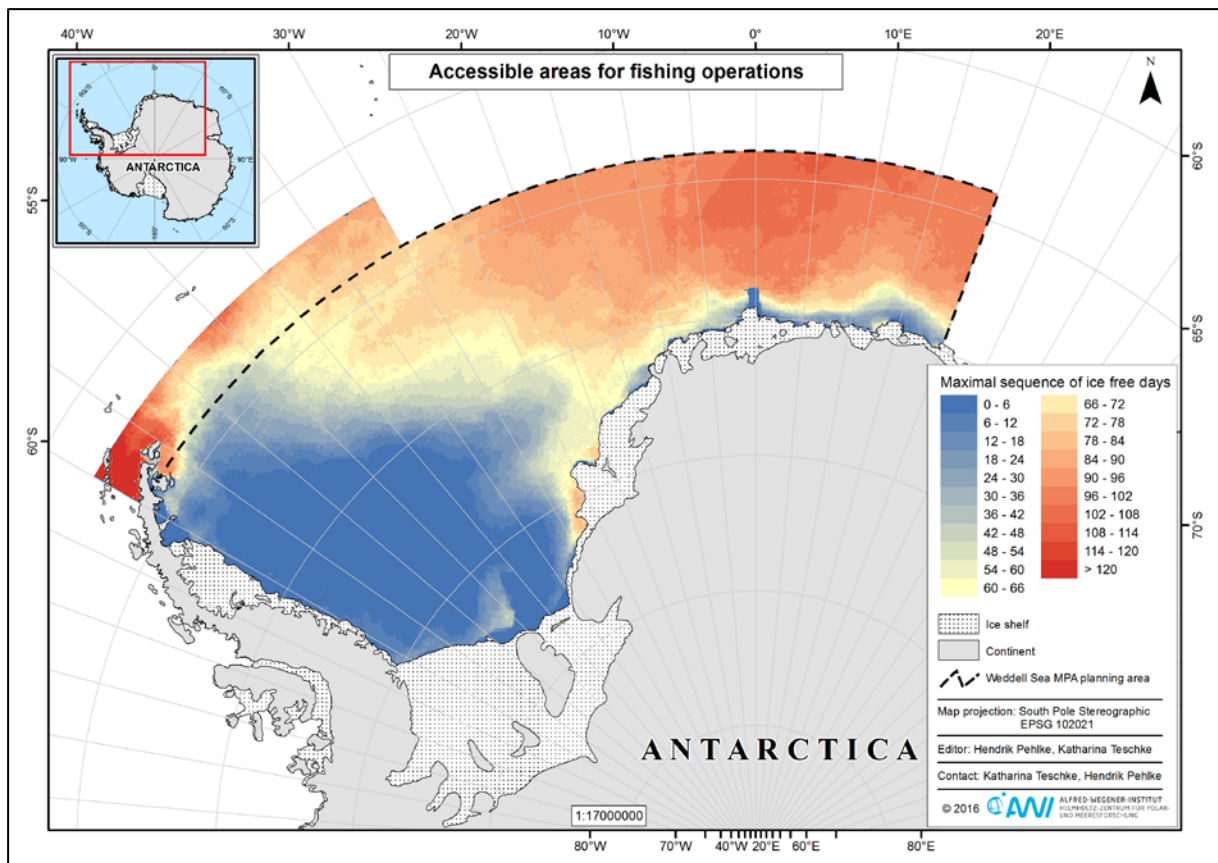


Figure 2-1 Accessible areas for fishing operations defined by the mean maximal sequence of ice-free days over 10 years (2002 – 2011) with focus on austral summer (Dec - Mar). Accessibility is colour-coded with red colours indicating accessible areas and yellow to blue colours indicating less to no accessibility. Black dashed box: Planning area for the evaluation of a WSMMPA. Boundaries of the planning area do not resemble the boundaries of any proposed WSMMPA.

Potential toothfish habitat

The data layer on the potential toothfish habitat is defined by a vertical depth range from 400 m to 3100 m according to WG-FSA-15/64 (see chapter 1.2.3). We reclassified the data layer by assigning a value of 1 to each planning unit grid cell within the potential fishing area and a value of zero to the remaining cells.

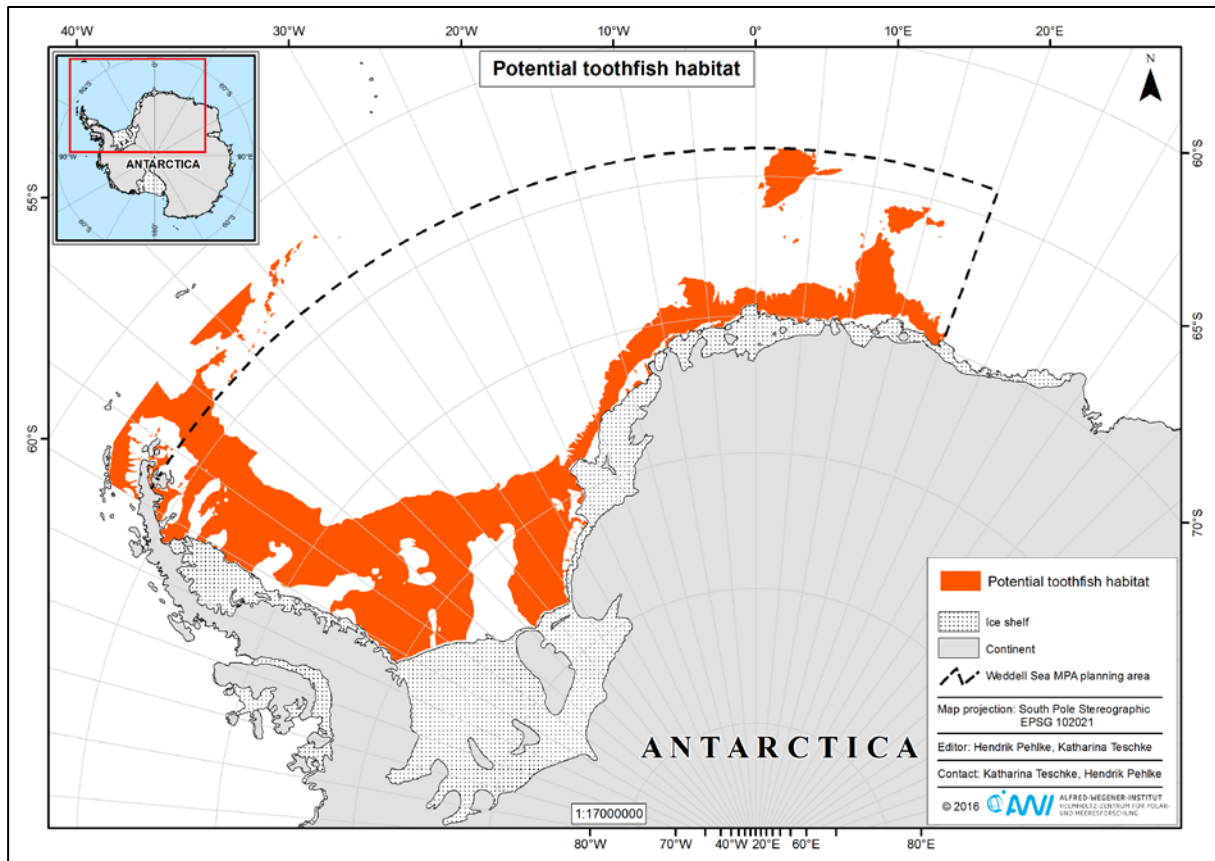


Figure 2-2 Potential toothfish habitat in the Weddell Sea (red coloured area) based on a depth range between 400 m and 3100 m. Black dashed box: Planning area for the evaluation of a WSMPA. Boundaries of the planning area do not resemble the boundaries of any proposed WSMPA.

Suitable Antarctic krill habitats

Here, we used the data layer on Antarctic krill based on habitat suitability model predictions. Please see more information about the model approach, the underlying data base and the comparative analyses between our habitat suitability model and other studies and data on Antarctic krill in chapter 1.2.2.

Four classes in terms of the habitat suitability for the Antarctic krill were defined to incorporate the information about potential krill fishing areas into the cost layer. The values were normalized to a range between 0 and 1, and were divided by two to give minor importance to krill fishery in comparison to toothfish fishery in the WSMPA planning area.

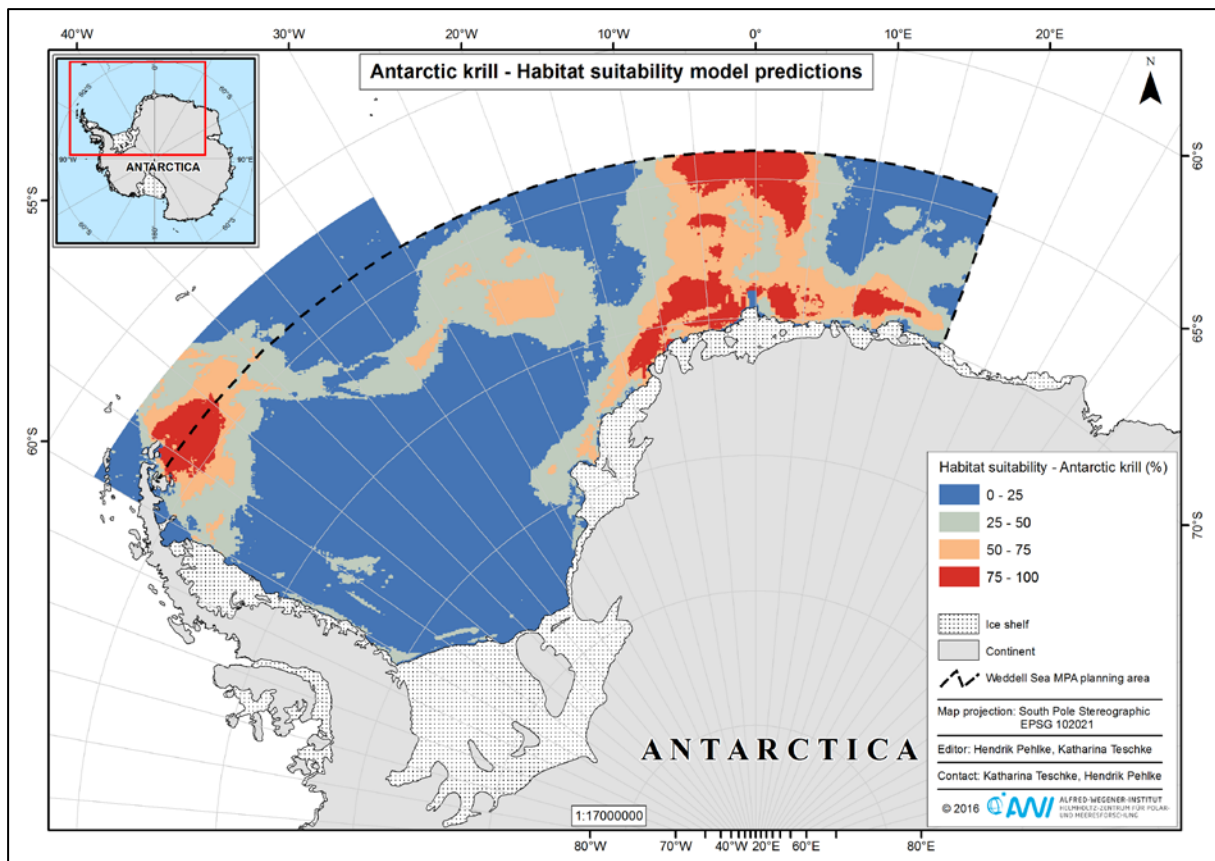


Figure 2-3 Areas suitable for Antarctic krill in the Weddell Sea based on habitat suitability model predictions with the focus on depths deeper than 550 m. Habitat suitability is colour-coded with blue colours indicating suitable habitat conditions and green to yellow colours indicating less suitable to unsuitable habitat. Black dashed box: Planning area for the evaluation of a WSMMPA. Boundaries of the planning area do not resemble the boundaries of any proposed WSMMPA.

For our cost layer approach the cost factor per planning unit grid cell was calculated as the sum of the mean maximal sequence of ice-free days, the potential toothfish habitat and the habitat suitability model predictions for the Antarctic krill. The cost layer was modified by grouping (6 classes) and weighting of the cost factor values (see Fig. 2-4) as the cost layer with continuous values (values from 1.0 to 2.4) had no significant effects on the Marxan solution. It is important to note here, that we assigned the lowest cost factor value of 1 to all planning unit grid cells with depths 550 m and shallower according to CCAMLR research and exploratory fishery and CM 22-08. We refrained from using a cost factor of zero for these grid cells to avoid errors in the Marxan results.

High cost are shown between 15°W and 15°E for the eastern Weddell Sea slope area and for the area around Maud Rise, as well as at the tip of the Antarctic Peninsula in the border area between Planning Domain 1 and Planning Domain 3.

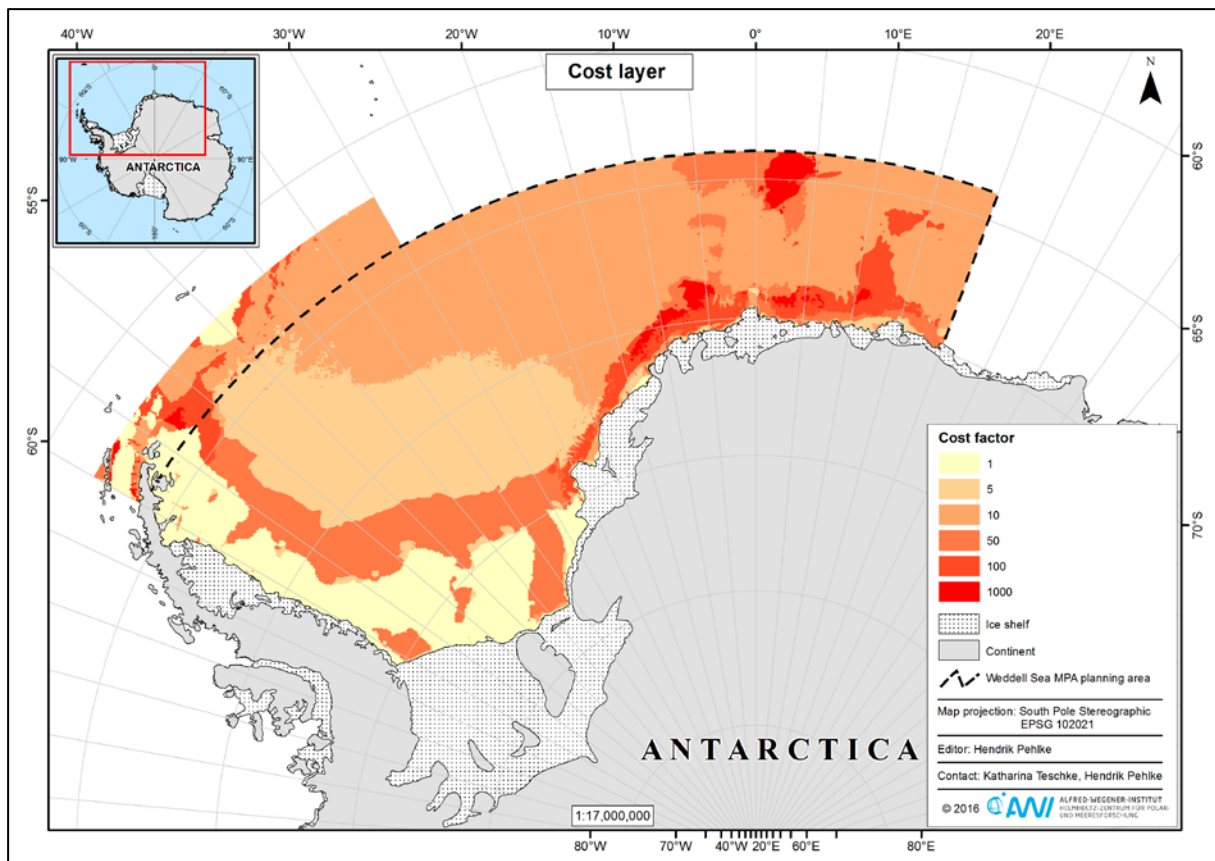


Figure 2-4 Cost layer. Areas in red are relatively easy to access, and represent the location of Antarctic toothfish as well as Antarctic krill fishing areas; possibly a high conflicting use (nature conservation vs. economic interests) exists in these areas. Black dashed box: Planning area for the evaluation of a WSMMPA. Boundaries of the planning area do not resemble the boundaries of any proposed WSMMPA.

2.2 Marxan scenario – recursive approach

Several preparatory steps were performed before the actual Marxan runs.

The Weddell Sea planning area was subdivided into 69,458 grid cells (hexagons) of approx. 50 km² each. This setting represents a reasonable trade-off between computing speed (number of cells to be handled by the Marxan software) and spatial resolution that remains appropriate for finer-scale parameters.

Most of the ecological parameters were scaled in categories of different probability of occurrence such as Antarctic krill (several categories from low to high probability of occurrence). For those parameters we used nesting to create one single shape file that represented all categories by means of assigning higher weighting factors to areas with high probability. A systematic overview of the weighting factor calculations for the different ecological parameters is given in Annex 1.

The planning unit was intersected with each parameter i.e., for each parameter the proportion of occurrence in each hexagon was calculated (planning unit grid values).

The basic Marxan settings were chosen as follows: (i) Boundary Length Modifier (BLM): 0.25, (ii) number of runs (repetitions): 250, (iii) number of iterations per run: 10 000 000.

The BLM were set to 0.25 to represent a reasonable trade-off between proximity effects (i.e. effects on solution clustering) and appearance of hotspots. A brief sensitivity analysis showed that the core area selected by Marxan remained stable across a considerable range of 20 - 500 repetitions. For instance, the scenarios with 20 and with 500 repetitions each elected approx. 7000 identical grid cells with 100 % selection frequency (i.e., in each repetition) and approx. 10 000 identical grid cells with 80 % selection frequency. These cells resemble approximately 70 % and 100 % of the 80-100 % area of the summed solution scenario, respectively. Thus, running the Marxan analysis with 250 repetitions is absolutely sufficient to obtain a robust summed solution scenario, and at the same time a reasonable computing speed is given. Furthermore, the maximum number of iterations per run was constrained to 10 000 000 to keep computing speed acceptable.

1st Marxan recursion

This first recursion targeted all ecological parameters with their specific regional conservation objectives (see Tab. 2-1). All environmental parameters were excluded from the first Marxan recursion by setting the proportion of those parameters to 0 in the spec file. The species penalty factor (spf) of each ecological parameters was defined by the tenfold of the corresponding specific regional conservation objective. The status of all planning unit grid cells was set to 1.

Subsequent to the first Marxan recursion we defined all planning unit grid cells that were selected in all 250 runs (i.e., 100 % selection frequency threshold) of the first recursion, as the "MPA" of this recursion. All those planning unit grid cells were set to status = 3. At this stage of the analysis we chose status = 3 (instead of status = 2) to avoid effects on solution clustering/clumping and let hotspots become more apparent as each planning unit grid cell has the same chance to be chosen irrespective of the position of the planning units to the initial MPA.

Each parameter, whose specific regional objective was achieved completely by this "MPA", was excluded from the second Marxan recursion (i.e. prop`s in spec file were set to 0). For all other parameters we calculated the percentage still missing for meeting the corresponding specific regional objective. These re-calculated values were set as the specific regional objectives for the second Marxan recursion.

2nd Marxan recursion

As mentioned above the 2nd recursion targeted all ecological parameters with their re-calculated specific regional conservation objectives. The environmental parameters were not incorporated yet in the Marxan analysis (i.e. prop`s in spec file were set to 0).

After the 2nd Marxan recursion we selected again all planning unit grid cells with a 100 % selection frequency threshold for inclusion in the "MPA". All those planning unit grid cells were set again to status = 3 for the 3rd recursion.

Each parameter, whose specific regional objective was achieved completely by this expanded "MPA" (i.e. after 1st and 2nd recursion), was excluded from the 3rd Marxan recursion (i.e. prop`s in spec file were set to 0). For all other parameters we calculated the percentage still missing for meeting the corresponding specific regional objective.

3rd Marxan recursion

The 3rd recursion targeted all ecological parameters with their re-calculated specific regional conservation objectives. To give higher weights to those parameters we multiply the original spf's by ten. The environmental parameters were not incorporated yet in the Marxan analysis.

As before, we selected all planning unit grid cells with a 100 % selection frequency for inclusion in the "MPA" (i.e. set status = 3 for the next recursion) and re-calculated for each remaining ecological parameter the area still missing for meeting the specific regional objective.

4th to 6th Marxan recursion

The 4th recursion targeted all remaining ecological parameters with their re-calculated specific regional conservation objectives, and additionally incorporated the environmental parameters in the Marxan analysis by setting their prop's to the corresponding specific regional objectives in the spec file. The spf of each still remaining ecological parameter was reset to the original spf. The spf of the environmental parameters was defined by the tenfold of the corresponding specific regional conservation objective.

Subsequent to the 4th recursion the same procedure as in the previous recursions was applied to the 5th and the 6th recursion. The settings were retained as in the 4th recursion. As no substantial progress was reached regarding the target achievement of the remaining ecological and environmental parameters, we changed the procedure for the 7th recursion.

7th Marxan recursion

All planning unit grid cells that were selected with a 100 % selection frequency in the previous recursions (i.e. 1st to 6th recursion) were set to status = 2 (instead of status = 3) to support that newly selected planning unit grid cells cluster together with previous selected planning units.

The 7th recursion targeted all ecological and environmental parameters with their original specific regional conservation objectives (see Tab. 2-1). The spfs of ecological and environmental parameters were defined by the one millionfold and the tenfold of the corresponding specific regional conservation objective, respectively.

Subsequent to the 7th Marxan recursion we defined all planning unit grid cells that were selected with a 100 % selection frequency threshold for inclusion in the "MPA". All those planning unit grid cells were set to status = 2 for the 8th recursion.

Each parameter, whose specific regional objective was achieved completely by this "MPA", was excluded from the 8th Marxan recursion (i.e. prop's in spec file were set to 0). For all other parameters we calculated the percentage still missing for meeting the corresponding specific regional objective. These re-calculated values were set as the specific regional objectives for the 8th Marxan recursion.

8th Marxan recursion and beyond

As mentioned above the 8th recursion targeted all ecological and environmental parameters with their re-calculated specific regional conservation objectives.

Please note that after the 8th Marxan recursion we selected all planning unit grid cells that were chosen in 200 out of 250 runs (i.e., 80 % selection frequency) for inclusion in the "MPA". All those planning unit grid cells were set to status = 2 for the next recursion.

As before, each parameter, whose specific regional objective was achieved completely by the expanded MPA (i.e., after in total eight recursions) was excluded from the 9th Marxan recursion, i.e. prop`s in spec file were set to 0. For all other parameters we re-calculated the percentage still missing for meeting the corresponding specific regional objective. With this setting the next Marxan recursion was computed. This process was repeated until most of the specific regional objectives were met within $\geq 0.95 * \text{specific regional objective}$. The 95 % threshold means that Marxan tolerated a difference of 5 % to the original specific regional objective.

We completed our Marxan recursive approach after the 12th recursion as no progress was reached regarding the target achievement of the remaining parameters. The specific regional objective (% area) of 17 environmental and two ecological parameters (i.e. areas with high probability of Antarctic krill (larvae) occurrence and potential toothfish habitats) could not completely achieve.

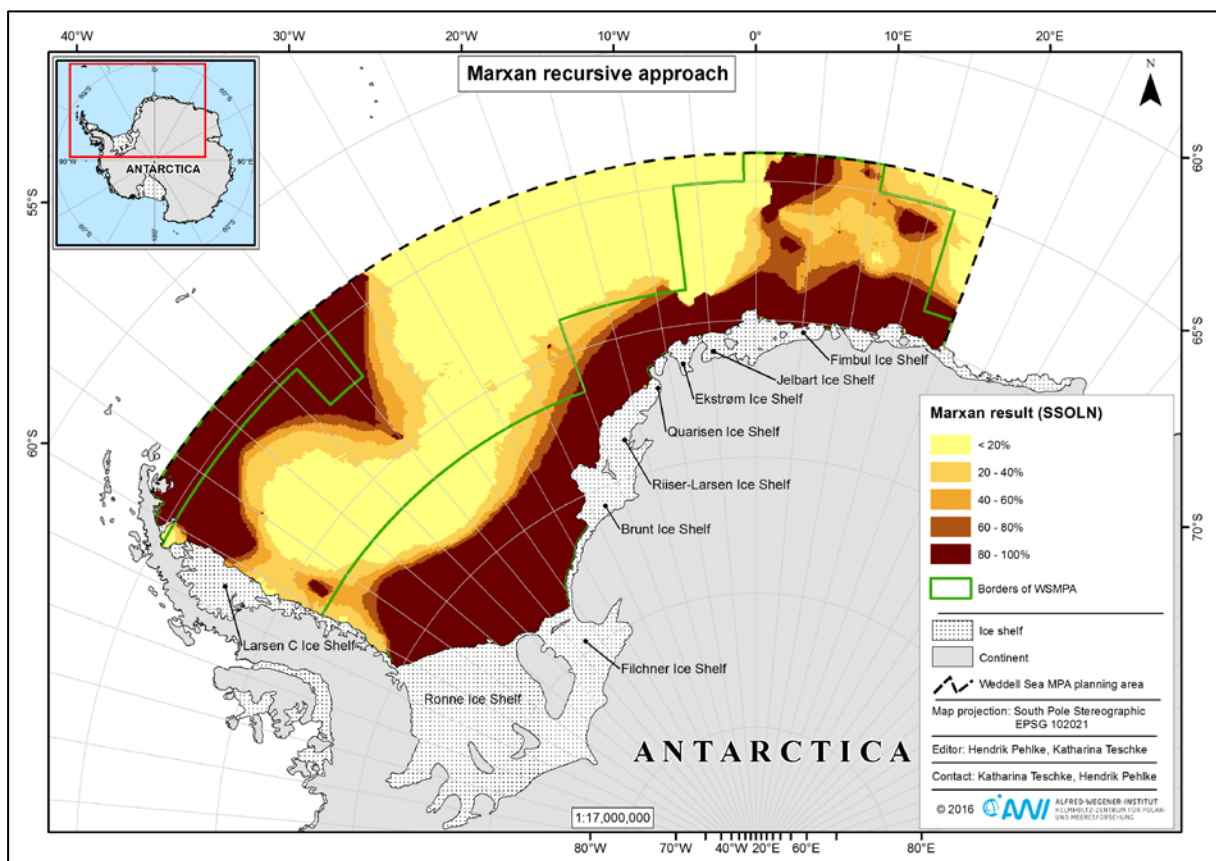


Figure 2-5 Summed solution scenario (SSOLN) of the Marxan recursive approach. Dark brown areas indicate areas of highest MPA importance. Green bordered areas show the WSMPA. The specific regional conservation objectives (% area) of each parameter, that were incorporated in the Marxan approach, and their fulfilment is shown in Tab. 2-2.

2.3 Developing the borders of the WSMPA

It is important to note here that the Marxan result is used to guide decision making and do not constrain the final WSMPA borders. The proposed borders of the WSMPA differ from the areas identified by our Marxan recursive approach (see Fig. 2-5), and are developed based on two principles:

- (i) MPA minimisation, and concurrently achievement of all parameters and their specific regional conservation objectives (% area), and
- (ii) a consistent area with borders those are easy to recognize and to navigate.

Table 2-2 gives a systematic overview of how the WSMPA (see Fig. 2-5, green bordered areas) achieves the specific regional objectives (% area) of each parameter. The threshold was set at 95 % according to Marxan basic settings. All parameters (i.e. 16 ecological and 58 environmental parameters) are met completely (≥ 0.95 * specific regional objective). Table 2-3 shows the spatial overlap between the ecological parameters, and thus indicates which parameters dominate others. Parameters with a strong spatial restriction, such as the fish nests or the potential foraging areas of the Adélie penguins, are often covered by other parameters with high percentage overlap. On the other hand, parameters, such as adult Antarctic krill, Antarctic petrel or demersal fish, which are not spatially restricted, cover most of the other parameters with relatively high percentage. It is important to note here that those parameters often show a widespread occurrence simply because the respective modelling technique gives spatial information for the whole WSMPA planning area. The complete matrix of the spatial overlap between all parameters, including all ecological and environmental parameters, is available at the CCAMLR e-group *Weddell Sea MPA*.

In the following, we describe the WSMPA boundaries based on Marxan recursive approach and adjustment by experts (see Fig. 2-5), and shortly summarise the main characteristics of the WSMPA.

The WSMPA is comprised of two areas and covers approx. 1.8 million km² (Fig. 2-5).

The boundaries of the area easterly of the Antarctic Peninsula are:

- Northern border: 64.0°S (= northern border of the WSMPA planning area)
- Eastern border 1: 39.0°W
- Southern border 1: 67.0°S
- Southern border 2: 62.25°S
- Western border 1: 43.0°W
- Western border 2: Continental margin and shelf ice margin, respectively.

The boundaries of the second area of the WSMPA are:

- Northern border 1: 71.5°S
- Northern border 2: 68.75°S

- Northern border 3: 65.0°S
- Northern border 4: 64.0°S (= northern border of the WSMPA planning area)
- Northern border 5: 65.0°S
- Northern border 6: 68.75°S
- Eastern border 1: 10.5°E
- Eastern border 2: 17.0°E
- Eastern border 3: 20.0°E (= eastern border of the WSMPA planning area)
- Southern border 1: Continental margin and shelf ice margin, respectively
- Western border 1: Continental margin and shelf ice margin, respectively.
- Western border 2: 20.0°W
- Western border 3: 7.0°W
- Western border 3: 1.0°W.

The area easterly of the Antarctic Peninsula is characterized by high primary and secondary production in the water column, and thus constitutes an important feeding ground for seabirds and marine mammals. The main reason for including this area in the WSMPA is the protection of these unique ecosystems. Management approaches of this area will be coordinated with CCAMLR MPA Planning Domain 1 to ensure consistent and gap-free protection.

The second area of the WSMPA spans:

- (i) Shelf areas (from ice shelf edge to 550 m water depth), where high primary production characterise the water column and generally highly diverse and species rich benthic ecosystems occur. The shelf areas within the WSMPA includes locations with rich sponge communities and unique/rare (for the Weddell Sea planning area) fish nesting sites and a small shallow water area, which all are very special and vulnerable key features, thus requiring the highest possible protection. A main reason for including those shelf areas in the WSMPA is protection, integrity and life cycles of ecologically important benthic three-dimensional suspension feeder communities (e.g. sponge associations, which fulfil a similar ecological role like coral reefs in the tropics), thereby maintaining associated benthic diversity. In addition, those shelf areas would protect representative examples of essential pelagic ecosystems, species, habitats and foraging areas for top predators (e.g. marine mammals, penguins, sea birds).
- (ii) Slope areas, where most of the potential fishable area for *Dissostichus* spp. is located. Here, the protection of Antarctic toothfish as a top predator (all life stages and habitats) and the functional integrity and viability of the local ecosystems and ecosystems processes of which Antarctic toothfish is an important part. Furthermore, especially in the south-eastern part of the WSMPA the water column

over the slope is an important feeding ground for marine mammals, penguins and flying seabirds.

- (iii) The Filchner area that is of extraordinary importance and one of the areas with the highest marine scientific research interest world-wide. It is predicted that climate change induced alterations taking place in the area over the next decades could lead to a reduction or even disintegration of the Ronne Filchner Ice Shelf, thereby affecting the global thermohaline ocean circulation and the world climate.
- (iv) The Maud Rise area including Astrid Ridge and seamounts, which represent unique geomorphological features with special living conditions (e.g. due to year round open water and high primary production around Maud Rise). The main reason for including the Maud rise area within the WSMPA is the protection of the pelagic and benthic ecosystems associated with these unique geomorphological and oceanographic features.

Table 2-2 Systematic overview of how the WSMPA, based on Marxan recursive approach plus modification by experts (see Fig. 2-5, green bordered areas), achieves the specific regional conservation objectives (% area) of each parameter. "Area" is expressed as km² for a few ecological parameters and all environmental parameters, whereas for most of the ecological parameters "area" is expressed as km² * corresponding weighting factor. Parameters where a weighting factor has been applied are marked with an asterisk (see Annex 1 for details of different weighting factor calculations).

Parameter	Total "area" in WSMPA planning area	Specific regional objective (% "area")	Minimal achieving "area"	Actual achieving "area"	Actual achieving specific regional objective (% "area")	Fulfilment of specific regional objective (ratio)
<i>Ecological parameters</i>						
*Adult Antarctic krill occurrence	37286052	35	13050118	28120296	75	YES (2.16)
*Larval Antarctic krill density	3289493	50	1644746	3231789	98	YES (1.97)
Potential ice krill habitat	573098	35	200584	437310	76	YES (2.18)
*Adult Antarctic silverfish density	834748	35	292162	800697	96	YES (2.74)
*Larval Antarctic silverfish density	214575	35	75101	198736	93	YES (2.65)
Potential foraging areas for breeding Adélie penguins (50 km buffer)	6585	100	6585	6585	100	YES (1.00)
Potential foraging areas for breeding Adélie penguins (ring buffer 50-100 km)	15272	50	7636	15220	100	YES (1.99)
*Potential foraging areas for non-breeding Adélie penguins	830582	20	166116	352343	42	YES (2.12)
*Potential foraging areas for Emperor penguins	505327	40	202131	500053	99	YES (2.47)
*Potential foraging areas for Antarctic petrel	13396092	40	5358437	8508214	64	YES (1.59)
*Seal density	3091782	40	1236713	1977977	64	YES (1.60)
*Sponges presence	190793	100	190793	190793	100	YES (1.00)
Potential habitats of cold water shelf echinoderm fauna	454648	35	159127	386090	85	YES (2.43)
Observations of nesting sites (demersal fish)	9248	100	9248	9248	100	YES (1.00)
*Demersal fish occurrence	17392505	75	13044379	13373522	77	YES (1.03)
Potential toothfish habitat	972899	75	729675	737848	76	YES (1.01)
<i>Environmental parameters</i>						
Unique shallow water area	18	100	18	18	100	YES (1.00)
Abyssal Plain: > -3000m	1346077	20	269215	342572	25	YES (1.23)

Table 2-2 Systematic overview of how the WSMPA, based on Marxan recursive approach plus modification by experts (see Fig. 2-5, green bordered areas), achieves the specific regional conservation objectives (% area) of each parameter. "Area" is expressed as km² for a few ecological parameters and all environmental parameters, whereas for most of the ecological parameters "area" is expressed as km² * corresponding weighting factor. Parameters where a weighting factor has been applied are marked with an asterisk (see Annex 1 for details of different weighting factor calculations).

Parameter	Total "area" in WSMPA planning area	Specific regional objective (% "area")	Minimal achieving "area"	Actual achieving "area"	Actual achieving specific regional objective (% "area")	Fulfilment of specific regional objective (ratio)
Bank: 0m to -100m	4440	20	888	3287	74	YES (3.70)
Bank: -100m to -200m	9111	20	1822	7531	83	YES (4.13)
Bank: -200m to -500m	243189	20	48638	207052	85	YES (4.26)
Bank: -500m to -1000m	53748	20	10750	32640	61	YES (3.04)
Canyon Shelf Commencing	16682	60	10009	15002	90	YES (1.50)
Canyon Slope Commencing	57761	60	34656	35064	61	YES (1.01)
Coastal Terrane	10127	20	2025	10043	99	YES (4.96)
Cross Shelf Valley: 0m to -100m	1778	20	356	421	24	YES (1.18)
Cross Shelf Valley: -100m to -200m	2105	20	421	590	28	YES (1.40)
Cross Shelf Valley: -200m to -500m	85562	20	17112	69716	81	YES (4.07)
Cross Shelf Valley: -500m to -1000m	130243	20	26049	86189	66	YES (3.31)
Cross Shelf Valley: -1000m to -1500m	6959	20	1392	6947	100	YES (4.99)
Cross Shelf Valley: Filchner Trough	80797	60	48478	80797	100	YES (1.67)
Lower Slope: -2000m to -3000m	106360	20	21272	69216	65	YES (3.25)
Lower Slope: > -3000m	650854	20	130171	311338	48	YES (2.40)
Margin Ridge: -500m to -1000m	1372	60	823	1372	100	YES (1.67)
Margin Ridge: -1000m to -1500m	3248	60	1949	3248	100	YES (1.67)
Margin Ridge: -1500m to -2000m	9760	60	5856	9760	100	YES (1.67)
Margin Ridge: -2000m to -3000m	23064	60	13839	23064	100	YES (1.67)
Margin Ridge: -3000m to -4500m	6523	60	3914	6523	100	YES (1.67)

Table 2-2 Systematic overview of how the WSMPA, based on Marxan recursive approach plus modification by experts (see Fig. 2-5, green bordered areas), achieves the specific regional conservation objectives (% area) of each parameter. "Area" is expressed as km² for a few ecological parameters and all environmental parameters, whereas for most of the ecological parameters "area" is expressed as km² * corresponding weighting factor. Parameters where a weighting factor has been applied are marked with an asterisk (see Annex 1 for details of different weighting factor calculations).

Parameter	Total "area" in WSMPA planning area	Specific regional objective (% "area")	Minimal achieving "area"	Actual achieving "area"	Actual achieving specific regional objective (% "area")	Fulfilment of specific regional objective (ratio)
Marginal Plateau: -2000m to -3000m	5502	60	3301	5502	100	YES (1.67)
Marginal Plateau: -3000m to -4500m	9695	60	5817	9695	100	YES (1.67)
Plateau Slope: -2000m to -3000m	2207	60	1324	2207	100	YES (1.67)
Plateau Slope: -3000m to -4500m	100018	60	60011	97576	98	YES (1.63)
Plateau: -2000m to -3000m	28307	60	16984	28306	100	YES (1.67)
Plateau: -3000m to -4500m	4635	60	2781	4635	100	YES (1.67)
Ridge: -1500m to -2000m	1116	20	223	1116	100	YES (5.00)
Ridge: -2000m to -3000m	9986	20	1997	9978	100	YES (5.00)
Ridge: -3000m to -4500m	3515	20	703	2380	68	YES (3.39)
Rugose Ocean Floor: > -3000m	277671	20	55534	101220	36	YES (1.39)
Seamount Ridge: -1000m to -1500m	871	60	522	871	100	YES (1.67)
Seamount Ridge: -2000m to -3000m	3100	60	1860	3100	100	YES (1.67)
Seamount Ridge: -3000m to -4500m	2297	60	1378	1418	62	YES (1.03)
Seamount: -1000m to -1500m	1612	60	967	1612	100	YES (1.67)
Seamount: -1500m to -2000m	2945	60	1767	2945	100	YES (1.67)
Seamount: > -3000m	1672	60	1003	1610	96	YES (1.61)
Shelf Deep: 0m to -100m	133	60	80	133	100	YES (1.66)
Shelf Deep: -200m to -500m	35245	60	21147	31661	90	YES (1.50)
Shelf Deep: -500m to -1000m	35389	60	21234	32705	92	YES (1.54)
Shelf	1008	60	605	1008	100	YES (1.67)

Table 2-2 Systematic overview of how the WSMPA, based on Marxan recursive approach plus modification by experts (see Fig. 2-5, green bordered areas), achieves the specific regional conservation objectives (% area) of each parameter. "Area" is expressed as km² for a few ecological parameters and all environmental parameters, whereas for most of the ecological parameters "area" is expressed as km² * corresponding weighting factor. Parameters where a weighting factor has been applied are marked with an asterisk (see Annex 1 for details of different weighting factor calculations).

Parameter	Total "area" in WSMPA planning area	Specific regional objective (% "area")	Minimal achieving "area"	Actual achieving "area"	Actual achieving specific regional objective (% "area")	Fulfilment of specific regional objective (ratio)
Upper Slope: 0m to -100m	1624	60	974	1624	100	YES (1.67)
Upper Slope: -100m to -200m	1196	60	717	1196	100	YES (1.67)
Upper Slope: -200m to -500m	8435	60	5061	8251	98	YES (1.63)
Upper Slope: -500m to -1000m	34418	60	20651	23954	70	YES (1.16)
Upper Slope: -1000m to -1500m	52570	60	31542	34306	65	YES (1.09)
Upper Slope: -1500m to -2000m	70634	60	42380	51254	73	YES (1.21)
Upper Slope: -2000m to -3000m	121874	60	73124	82860	68	YES (1.13)
Upper Slope: -3000m to -4500m	162	60	97	162	100	YES (1.67)
Pelagic region - Coastal polynya I	7547	100	7547	7547	100	YES (1.00)
Pelagic region - Coastal polynya II	258863	100	258863	258863	100	YES (1.00)
Pelagic region - Coastal polynya III	87979	100	87979	86773	99	NO (0.99)
Pelagic region – Transition zone	1330	20	266	1298	98	YES (4.88)
Pelagic region - Deepwater I	637920	20	127584	318421	50	YES (2.50)
Pelagic region - Deepwater II	1098799	20	219760	315787	29	YES (1.44)
Pelagic region - Deepwater III	868117	20	173623	490362	56	YES (2.82)
Pelagic region - Ice covered area	651469	20	130294	347000	53	YES (2.66)

Table 2-3 Spatial overlap between the ecological parameters. Each cell shows the spatial overlap (in %) between the certain parameters. In general, parameters in columns are overlapped by parameters in rows. For example, 59 % of the potential adult Antarctic silverfish habitat (in column) is overlapped by the potential seal habitat (in row), whereas only 16 % of the potential seal habitat (in column) is covered by the potential adult Antarctic silverfish habitat (in row).

	Adult Antarctic krill	Antarctic krill larvae	Ice krill	Adult Antarctic silverfish	Antarctic silverfish larvae	Breeding Adélie (50km)	Breeding Adélie (50 -100km)	Non-breeding Adélie	Emperor penguins	Antarctic petrel	Seals	Sponges	Echinoderms	Fish nests	Demersal fish	Toothfish
Adult Antarctic krill	100	98	94	96	98	87	95	100	96	98	99	99	100	92	99	99
Antarctic krill larvae	21	100	20	61	34	0	0	16	38	21	20	32	20	44	21	19
Ice krill	25	24	100	31	49	98	91	8	48	27	37	16	79	89	26	38
Adult Antarctic silverfish	17	48	20	100	82	0	0	1	50	17	16	40	14	74	17	19
Antarctic silverfish larvae	6	9	11	28	100	0	0	1	32	6	6	25	11	37	6	8
Breeding Adélie (50 km)	0	0	2	0	0	100	12	3	4	1	1	0	0	0	0	0
Breeding Adélie (50 -100 km)	1	0	4	0	0	24	100	4	3	1	1	0	0	0	1	1
Non-breeding Adélie	7	5	2	1	2	46	30	100	2	7	2	0	0	0	7	1
Emperor penguins	13	24	24	39	74	93	35	4	100	13	15	59	18	70	13	21
Antarctic petrel	100	100	100	100	100	100	100	100	100	100	100	100	100	100	100	100
Seals	62	59	87	59	62	71	71	22	70	62	100	72	93	46	62	83
Sponges	9	13	6	22	39	0	0	0	41	9	11	100	6	42	9	16
Echinoderms	22	21	65	18	42	0	0	0	29	22	33	15	100	49	22	38
Fish nests	1	2	3	3	5	0	0	0	4	1	1	4	2	100	1	1
Demersal fish	100	98	96	98	98	93	98	100	96	99	99	100	100	98	100	100
Toothfish	45	40	63	50	64	13	57	6	71	44	60	78	76	66	45	100

References

- Ainley DG, Jacobs SS (1981) Seabird affinities for ocean and ice boundaries in the Antarctic. *Deep-Sea Research*, 28a (10), 1173-1185.
- Ainley DG, O'Connor EF, Boekelheide RJ (1984) The marine ecology of birds in the Ross Sea, Antarctica. *Ornithological Monographs*, 32, 1-97.
- Ainley DG, Ribic CA, Fraser WR (1994) Ecological structure among migrant and resident seabirds of the Scotia-Weddell Confluence region. *Journal of Animal Ecology*, 63, 347-364.
- Allouche O, Tsoar A & Kadmon R (2006) Assessing the accuracy of species distribution models: prevalence, kappa and the true skill statistic (TSS). *Journal of Applied Ecology*, 43, 1223-1232.
- Arndt JE, Schenke HW, Jakobsson M, Nitsche F, Buys G, Goleby B, Rebesco M, Bohoyo F, Hong JK, Black J, Greku R, Udintsev G, Barrios F, Reynoso-Peralta W, Morishita T, Wigley R (2013) The International Bathymetric Chart of the Southern Ocean (IBCSO) Version 1.0 - A new bathymetric compilation covering circum-Antarctic waters. *Geophysical Research Letters*, doi: 10.1002/grl.50413.
- Arrigo KR, van Dijken GL (2003) Phytoplankton dynamics within 37 Antarctic coastal polynya systems. *Journal of Geophysical Research* 108, No. 3271, doi:10.1029/2002JC001739.
- Atkinson A, Siegel V, Pakhomov EA, Rothery P (2004) Longterm decline in krill stock and increase in salps within the Southern Ocean. *Nature*, 432, 100-103.
- Atkinson A, Siegel V, Pakhomov EA, Rothery P, Loeb V, Ross RM, Quetin LB, Schmidt K, Fretwell P, Murphy EJ, Tarling GA, Fleming AH (2008) Oceanic circumpolar habitats of Antarctic krill. *Marine Ecology Progress Series*, 362, 1-23.
- Atkinson A, Siegel V, Pakhomov EA, Jessopp MJ, Loeb V (2009) A re-appraisal of the total biomass and production of Antarctic krill. *Deep-Sea Research I*, 56, 727-740.
- Ball IR, Possingham HP, Watts M. (2009) Marxan and relatives: Software for spatial conservation prioritisation. In: *Spatial conservation prioritisation: Quantitative methods and computational tools* (eds. Moilanen A, Wilson KA, Possingham HP). Oxford University Press, Oxford, UK, 185-195.
- Bester MN, Erickson AW, Ferguson JWH (1995) Seasonal change in the distribution and density of seals in the pack ice off Princess Martha Coast, Antarctica. *Antarctic Science*, 7, 357-364.
- Bester MN, Odendaal PN (2000) Abundance and distribution of Antarctic pack ice seals in the Weddell Sea. In: Davison W, Howard-Williams C, Broady P (eds). *Antarctic Ecosystems: Models for Wider Ecological Understanding*. Caxton Press, Christchurch, 51-55.
- Bester MN, Ferguson JWH, Jonker FC (2002) Population densities of pack ice seals in the Lasarev Sea, Antarctica. *Antarctic Science*, 14, 123-127.
- Bombosch A (2013) Modelling habitat suitability of humpback and Antarctic minke whale feeding grounds in the southern ocean. PhD thesis, University of Bremen, Germany, 173 pp.
- Bombosch A, Zitterbart DP, van Opzeeland I, Frickenhaus S, Burkhardt E, Wisz MS, Boebel O (2014) Predictive habitat modelling of humpback (*Megaptera novaeangliae*) and Antarctic minke (*Balaenoptera bonaerensis*) whales in the Southern. *Deep-Sea Research I*, 91, 101-114.
- Boysen-Ennen E, Piatkowski U (1988) Meso- and macrozooplankton communities in the Weddell Sea, Antarctica. *Polar Biology*, 9, 17-35.
- Branch TA (2011) Humpback whale abundance south of 60°S from three complete circumpolar sets of surveys. *Journal of Cetacean Research and Management*, 3, 53-69.
- Brandt A, Brix S, Brökeland W, Choudhury M, Kaiser S, Malyutina M (2007) Deep-sea isopod biodiversity, abundance and endemism in the Atlantic sector of the Southern Ocean – results from the ANDEEP I - III expeditions. *Deep-Sea Research II*, 54, 1760-1775.
- Breiman L (2001) Random forests. *Machine Learning* 45(1), 5-32.
- Brodeur JC, Calvo J, Clarke A, Johnston IA (2003) Myogenic cell cycle duration in *Harpagifer* species with sub-Antarctic and Antarctic distributions: evidence for cold compensation. *The Journal of Experimental Biology*, 206, 1011-1016.
- Burrough PA, McDonnell RA (1988) *Principals of geographical information systems*. Oxford University Press, 333 pp.
- Clapham PJ (2002) Humpback whale *Megaptera novaeangliae*. In: Perrin WF, Würsig B, Thewissen JGM (eds), *Encyclopedia of Marine Mammals*, Academic Press, London, 589-592.

- Cuzin-Roudy J, Irisson J-O, Penot F, Kawaguchi S, Vallet C (2014) Chapter 6.9. Southern Ocean Euphausiids. In: De Broyer C, Koubbi P, Griffiths HJ, Raymond B, Udekem d'Acoz C d' et al. (eds.). Biogeographic Atlas of the Southern Ocean. Scientific Committee on Antarctic Research, Cambridge, pp. 309-320.
- Daniels RA (1978) Nesting Behaviour of *Harpagifer bispinis* in Arthur Harbour, Antarctic Peninsula. *Journal of Fish Biology*, 12, 465-474.
- Daniels RA (1979) Nest guard replacement in the Antarctic fish *Harpagifer bispinis*: Possible altruistic behaviour. *Science*, 205 (4408), 831-833.
- Diekmann B, Kuhn G (1999) Provenance and dispersal of glacial-marine surface sediments in the Weddell Sea and adjoining areas, Antarctica: ice-rafting versus current transport. *Marine Geology*, 158(1-4), 209-231.
- Douglass LL, Turner J, Grantham HS, Kaiser S, Constable A, et al. (2014) A Hierarchical Classification of Benthic Biodiversity and Assessment of Protected Areas in the Southern Ocean. *PLoS ONE*, 9(7), e100551, doi:10.1371/journal.pone.0100551.
- Drescher H-E, Hubold G, Piatkowski U, Plötz J, Voß J, Kock K-H, Gutt J (2012) Counts of fish species from trawl and dredge samples in the eastern Weddell Sea and at the Antarctic Peninsula during POLARSTERN cruise ANT-I/2. doi:10.1594/PANGAEA.786877.
- Duhamel G, Hulley P-A, Causse R, Koubbi P, Vacchi M, Pruvost P, Vignetta S, Irisson J-O, Mormède S, Belchier M, Dettai A, Detrich HW, Gutt J, Jones CD, Kock K-H, Lopez Abellan LJ, Van de Putte AP (2014) Chapter 7. Biogeographic patterns of fish. In: De Broyer C, Koubbi P, Griffiths HJ, Raymond B, Udekem d'Acoz C d' et al. (eds.). Biogeographic Atlas of the Southern Ocean. Scientific Committee on Antarctic Research, Cambridge, pp. 328-362.
- Ekau W, Hubold G, Kock K-H, Gutt J (2012a) Counts of fish species from trawl and dredge samples in the eastern Weddell Sea and at the Antarctic Peninsula during POLARSTERN cruise ANT-III/3. doi:10.1594/PANGAEA.786883.
- Ekau W, Hubold G, Wöhrmann A, Kock K-H, Gutt J (2012b) Counts of fish species from trawl and dredge samples in the eastern Weddell Sea and at the Antarctic Peninsula during POLARSTERN cruise ANT-V/3. doi:10.1594/PANGAEA.786884.
- Elith J & Graham CH (2009). Do they? How do they? WHY do they differ? On finding reasons for differing performances of species distribution models. *Ecography*, 32 (1), 66-77.
- Erdey-Heydorn MD (2008) An ArcGIS Seabed Characterization Toolbox Developed for Investigating Benthic Habitats. *Marine Geodesy*, 31, 318-358.
- ESRI (2011) ArcGIS Desktop: Release 10. Redlands, CA: Environmental Systems Research Institute.
- Fevolden SE (1979) Investigations on krill (Euphausiacea) sampled during the Norwegian Antarctic Research Expedition 1976/77. *Sarsia*, 64, 189-198.
- Fevolden SE (1980) Krill off Bouvetoya and in the southern Weddell Sea with a description of larval stages of *Euphausia crystallorophias*. *Sarsia*, 65, 149-162.
- Flemming BW (2000) A revised textural classification of gravel - free muddy sediments on the basis of ternary diagrams. *Continental Shelf Research*, 20 (10-11), 1125-1137.
- Flores H, Haas C, van Franeker JA, Meesters E (2008) Density of pack-ice seals and penguins in the western Weddell Sea in relation to ice thickness and ocean depth. *Deep Sea Research II*, 55 (8), 1068-1074; doi: 10.1016/j.dsr2.2007.12.024.
- Flores H, Hunt BPV, Kruse S, Pakhomov EA, Siegel V, van Franeker JA, Strass V, Van de Putte AP, Meesters EHWG, Bathmann U (2014) Seasonal changes in the vertical distribution and community structure of Antarctic macrozooplankton and micronekton. *Deep-Sea Research I*, 84, 127-141.
- Folk RL (1954) The distinction between grain size and mineral composition in sedimentary rock nomenclature. *Journal of Geology*, 62(4), 344-359.
- Forcada J, Trathan PN, Boveng PL, Boyd IL, Burns JM, Costa DP, Fedak M, Rogers TL, Southwell CJ (2012). Responses of Antarctic pack-ice seals to environmental change and increasing krill fishing. *Biological Conservation*, 149, 40-50.
- Fretwell PT, LaRue MA, Morin P, Kooyman GL, Wienecke B, Ratcliffe N, Fox AJ, Fleming AH, Porter C, Trathan PN (2012) An Emperor Penguin Population Estimate: The First Global, Synoptic Survey of a Species from Space. *PLoS ONE*, 7(4), e33751, doi:10.1371/journal.pone.0033751.

- Fretwell PT, Trathan PN, Wienecke B, Kooyman GL (2014) Emperor Penguins Breeding on Iceshelves. *PLoS ONE* 9(1), e85285, doi:10.1371/journal.pone.0085285.
- Garcia HE, Locarnini RA, Boyer TP, Antonov JI, Baranova OK, Zweng MM, Reagan JR, Johnson DR (2014a) World Ocean Atlas 2013, Volume 3: Dissolved Oxygen, Apparent Oxygen Utilization, and Oxygen Saturation. In: Levitus S & Mishonov A (ed.), NOAA Atlas NESDIS, 75, 27 pp.
- Garcia HE, Locarnini RA, Boyer TP, Antonov JI, Baranova OK, Zweng MM, Reagan JR, Johnson DR (2014b) World Ocean Atlas 2013, Volume 4: Dissolved Inorganic Nutrients (phosphate, nitrate, silicate). In: Levitus S (ed.) & Mishonov A (technical ed.), NOAA Atlas NESDIS, 76, 25 pp.
- Geibert et al. (2005) Accumulation rates of bulk sediment and opal in surface sediments of the South Atlantic. doi: 10.1594/PANGAEA.230042; *Supplement to: Geibert W, Rutgers van der Loeff MM, Usbeck R, Gersonde R, Kuhn G, Seeberg-Elverfeldt J* (2005) Quantifying the opal belt in the Atlantic and southeast Pacific sector of the Southern Ocean by means of 230Th normalization. *Global Biogeochemical Cycles* 19(4), GB4001, doi: 10.1029/2005GB002465.
- Gerdes D, Klages M, Arntz WE, Herman RL, Galéron J, Hain S (1992) Quantitative investigations on macrobenthos communities of the southeastern Weddell Sea shelf based on multibox corer samples. *Polar Biology*, 12, 291-301.
- Gill A, Evans PGH (2002) Marine mammals of the Antarctic in relation to hydro-acoustic activities. Report for the German Federal Agency for Nature Conservation, Oxford, 226 pp.
- Gill PC, Thiele D (1997) A winter sighting of killer whales (*Orcinus orca*) in Antarctic sea ice. *Polar Biology*, 17, 401-404.
- Gutt J (2007) Antarctic macro-zoobenthic communities: a review and an ecological classification. *Antarctic Science*, 19, 165-182.
- Gutt J, Barratt I, Domack E, d'Udekem d'Acoz C, Dimmler W, Grémare A, Heilmayer O, Isla E, Janussen D, Jorgensen E, Kock K-H, Lehnert LS, López-González P, Langner S, Linse K, Manjón-Cabeza ME, Meißner M, Montiel A, Raes M, Robert H, Rose A, Sañé Schepisi E, Saucède T, Scheidat M, Schenke H-W, Seiler J, Smith C (2011) Biodiversity change after climate-induced ice-shelf collapse in the Antarctic. *Deep Sea Research II*, 58, 74-83.
- Gutt J, Griffiths HJ, Jones CD (2013) Circum-polar overview and spatial heterogeneity of Antarctic macrobenthic communities. *Marine Biodiversity*, 43, 481-487.
- Haid V (2013) Coastal polynyas in the southwestern Weddell Sea: Surface fluxes, sea ice production and water mass modification, Dissertation, Universität Bremen, 160 pp, <http://elib.suub.uni-bremen.de/edocs/00103445-1.pdf>
- Haid V, Timmermann R (2013) Simulated heat flux and sea ice production at coastal polynyas in the southwestern Weddell Sea, *Journal of Geophysical Research*, 118(5), 2640-2652, doi:10.1002/jgrc.20133.
- Harris U, Orsi AH (2001, updated 2008) Locations of the various fronts in the Southern Ocean Australian Antarctic Data Centre - CAASM Metadata (https://data.aad.gov.au/aadc/metadata/metadata_redirect.cfm?md=/AMD/AU/southern_ocean_fronts).
- Hartigan JA, Wong MA (1979) A K-means clustering algorithm. *Applied Statistics*, 28, 100-108.
- Hastie TJ, Tibshirani RJ (1990) Generalized Additive Models. Monographs on Statistics and Applied Probability 43. Chapman & Hall/CRC, 352 pp.
- Hedley SL, Buckland ST (2004) Spatial models for line transect sampling. *Journal of Agricultural, Biological, and Environmental Statistics*, 9, 181-199.
- Hempel I, Hempel G (1982) Distribution of euphausiid larvae in the southern Weddell Sea. *Meeresforschung*, 29, 253-266.
- Hubold G, Hempel I, Meyer M (1988) Zooplankton communities in the southern Weddell Sea (Antarctica). *Polar Biology*, 8, 225-233.
- Hureau J-C, Balguerias E, Duhamel G, Kock K-H, Ozouf-Costaz C, White M, Gutt J (2012) Counts and mass of fish species from trawl and dredge samples in the eastern Weddell Sea during POLARSTERN cruise ANT-VII/4, doi:10.1594/PANGAEA.786886.
- International Whaling Commission (2011) Report of the workshop on the comprehensive assessment of Southern Hemisphere humpback whales. *Journal of Cetacean Research and Management - Special Issue*, 3, 1-50.
- UCN (2014) The IUCN Red List of Threatened Species. Version 2014.2, retrieved from www.iucnredlist.org.

- Jerosch K, Krajnik I, Martinez R, Dorschel B, Kuhn G (in preparation) Geostatistical sediment texture analysis of the Weddell Sea and the adjacent Southern Ocean on the basis of ternary grain size diagrams.
- Jerosch K, Scharf FK, Deregibus D, Campana GI, Zacher K, Pehlke P, Hass C, Quartino ML, Abele D (submitted) Habitat modeling as a predictive tool for analyzing spatial shifts in Antarctic benthic communities due to global climate change. *Global Change Biology*.
- Jerosch K, Kuhn G, Krajnik I, Scharf FK, Dorschel B (2015) A geomorphological seabed classification for the Weddell Sea, Antarctica. *Marine Geophysical Research*, doi: 10.1007/s11001-015-9256-x.
- Jerosch K (2013) Geostatistical mapping and spatial variability of surficial sediment types on the Beaufort Shelf based on grain size data. *Journal of Marine Systems*, 127, 5-13. doi:10.1016/j.jmarsys.2012.02.013
- Johnson DS (2011) *crawl*: Fit continuous-time correlated random walk models for animal movement data. R package version 1.3-1. <http://CRAN.R-project.org/package=crawl>.
- Johnson DS, London JM, Lea M-A, Durban JW (2008) Continuous-time correlated random walk model for animal telemetry data. *Ecology*, 89, 1208–1215.
- Jones CD, Near TJ (2012) The reproductive behaviour of *Pogonophryne scotti* confirms widespread egg-guarding parental care among Antarctic notothenioids. *Journal of Fish Biology*, 80, 2629-2635.
- Kaleschke L, Lupkes C, Vihma T, Haarpaintner J, Bochert A, Hartmann J, Heygster G (2001) SSM/I sea ice remote sensing for mesoscale ocean-atmosphere interaction analysis. *Canadian Journal of Remote Sensing*, 27, 526-537.
- Kasamatsu F, Joyce G, Ensor P, Memorez J (1996) Current occurrence of Baleen whales in Antarctic waters. Report of the International Whaling Commission, 46, 293-304.
- Kock K-H, Busch M, Holst M, Klimpel S, Pietschok D, Pshenichnov L, Riehl R, Schöling S, Gutt J (2012) Counts and mass of fish species from trawl samples in the western Weddell Sea during POLARSTERN cruise ANT-XXIII/8. doi:10.1594/PANGAEA.786888.
- Kroese DP, Brereton T, Taimre T, Botev ZI (2014) Why the Monte Carlo method is so important today? *WIREs Computational Statistics* 6(6), 386-392, doi: 10.1002/wics.1314.
- La Mesa M, De Felice A, Jones CD, Kock K-H (2009) Age and growth of spiny icefish (*Chaenodraco wilsoni* Regan 1914) off Joinville-D'Urville Islands (Antarctic Peninsula). *CCAMLR Science*, 16, 115-130.
- Liu C, White M, Newell G (2009) Measuring the accuracy of species distribution models: a review. Modelling and Simulation Society of Australia and New Zealand and International Association for Mathematics and Computers in Simulation (eds. Anderssen RS, Braddock RD, Newham LTH), 4241-4247. In: 18th World IMACS Congress and MODSIM09 International Congress on Modelling and Simulation, Cairns, Australia.
- Lu GY, Wong DW (2008) An adaptive inverse-distance weighting spatial interpolation technique. *Computers & Geosciences* 34 (9), 1044-1055.
- Lynch HJ, LaRue MA (2014) First global census of the Adélie Penguin. *The Auk: Ornithological advances* 131, 457–466.
- Maechler M, Rousseeuw P, Struyf A, Hubert M, Hornik K (2014) *Cluster: cluster analysis basics and extensions*. R package version 1.15.2.
- Makarov RR, Sysoyeva MV (1985) Biology and distribution of *Euphausia superba* in the Lazarev Sea and adjacent Waters. *Hydrobiological Journal*, 23, 95-99.
- Margules CR, Pressey RL (2000) Systematic conservation planning. *Nature* 405, 243–253.
- McCullagh P & Nelder JA (1989) *Generalized linear models*. Monographs on Statistics and Applied Probability 37. Chapman & Hall/CRC, 532 pp.
- Menshenina L (1992) Distribution of euphausiid larvae in the Weddell Gyre in September-October 1989. Proceedings of the National Institute of Polar Research Symposium on Polar Biology (Tokyo), 5, 44-54.
- Moore JK, Abbott MR, Richman JG (1999) Location and dynamics of the Antarctic Polar Front from satellite sea surface temperature data. *Journal of Geophysical Research*, 104, 3059-3073.
- Moore JK, Abbott MR (2000) Phytoplankton chlorophyll distributions and primary production in the Southern Ocean. *Journal of Geophysical Research*, 105, 709-722.

- O'Brien PE, Post AL, Romeyn R (2009) Antarctic-wide geomorphology as an aid to habitat mapping and locating vulnerable marine ecosystems. CCAMLR document: WS-VME-09/10, 22 pp.
- Ohsumi S, Masaki Y, Kawamura A (1970) Stock of the Antarctic minke whale. Scientific Reports of the Whales Research Institute, Tokyo, 22, 75-125.
- Orsi AH, Whitworth T, Nowlin WD (1995) On the meridional extent and fronts of the Antarctic Circumpolar Current. Deep-Sea Research I, 42, 641-673.
- Parker SJ, Hoyle SD, Fenaughty JM, Kohout A (2014) Methodology for automated spatial sea ice summaries in the Southern Ocean. CCAMLR WG-FSA-14, 20 pp.
- Pearce J & Ferrier S (2000) Evaluating the predictive performance of habitat models developed using logistic regression. Ecological Modelling, 133, 225-245.
- Penhale P, Grant S (2007) Commission of the Conservation of Antarctic Marine Living Resources (CCAMLR) Workshop on Bioregionalisation of the Southern Ocean (Brussels, Belgium, 13 - 17 Aug. 2007), Annex 9: Report of the Workshop Executive Summary.
- Petschick R, Kuhn G, Gingele F (1996) Clay mineral distribution in surface sediments of the South Atlantic: sources, transport, and relation to oceanography. Marine Geology, 130(3-4), 203-229.
- Plötz J, Steinhage D, Bornemann H (2011a-e) Seal census raw data during campaign EMAGE-I to EMAGE-V, doi:10.1594/PANGAEA.760097; doi:10.1594/PANGAEA.760098; doi:10.1594/PANGAEA.760099; doi:10.1594/PANGAEA.760100; doi:10.1594/PANGAEA.760101.
- Post A (2012, updated 2014) Antarctic wide seafloor geomorphology *Australian Antarctic Data Centre-CAASM-Metadata*; https://data.aad.gov.au/aadc/metadata/metadata_redirect.cfm?md=/AMD/AU/ant_seafloor_geomorph.
- R Core Team (2014) R: A language and environment for statistical computing. R Foundation for Statistical Computing, Vienna, Austria. <http://www.R-project.org/>.
- Risch D, Gales NJ, Gedamke J, Kindermann L, Nowacek DP, Read AJ, Siebert U, Van Opzeeland IC, Van Parijs SM, Friedlaender AS (2014). Mysterious bioduck sound attributed to the Antarctic minke whale (*Balaenoptera bonaerensis*). Biology Letters 10(4), 1-8.
- Ropert-Coudert Y, Hindell MA, Phillips R, Charrassin JB, Trudelle L, Raymond B (2014) Biogeographic patterns of birds and mammals. In: De Broyer C & Koubbi P (eds) The Biogeographic Atlas of the Southern Ocean. Scientific Committee on Antarctic Research, <http://atlas.biodiversity.aq>, pp 364 – 387.
- SC-CAMLR-XXXIII (2014) Report of the thirty-third meeting of the Scientific Committee. Hobart, Australia, 20-24 October, 397 pp.
- SC-CAMLR-XXXIII/BG/02 (2014) Scientific background document in support of the development of a CCAMLR MPA in the Weddell Sea (Antarctica) – Version 2014. Delegation of Germany, 110 pp.
- SC-CAMLR-XXXIV (2015) Report of the thirty-fourth meeting of the Scientific Committee. Hobart, Australia, 19-23 October, 423 pp.
- SC-CAMLR-XXXIV/BG/16 (2015) Scientific background document in support of the development of a CCAMLR MPA in the Weddell Sea (Antarctica) – Version 2015; Part B: Description of available data. Delegation of Germany, 19 pp.
- Scheidat M, Friedlaender A, Kock K-H, Lehnert L, Boebel O, Roberts J, Williams R (2011) Cetacean surveys in the Southern Ocean using icebreaker-supported helicopters. Polar Biology, 34, 1513-1522.
- Seiter K et al. (2004a) Global compilation of benthic data sets I. doi:10.1594/PANGAEA.733692; *Supplement to*: Seiter K, Hensen C, Schröter J, Zabel M (2004) Organic carbon content in surface sediments-defining regional provinces. Deep Sea Research Part I: Oceanographic Research Papers 51(12), 2001-2026.
- Seiter K et al. (2004b) Total organic carbon content in surface sediments, a compilation from different sources. doi:10.1594/PANGAEA.199835; *In Supplement to*: Seiter K, Hensen C, Schröter J, Zabel M (2004) Organic carbon content in surface sediments-defining regional provinces. Deep Sea Research Part I: Oceanographic Research Papers 51(12), 2001-2026.
- Shepard FP (1954) Nomenclature based on sand-silt-clay ratios. Journal of Sedimentary Petrology, 24, 151–158.
- Siegel V (1982) Investigations on krill (*Euphausia superba*) in the southern Weddell Sea. Meeresforschung, 29, 244-252.

- Siegel V (2005) Distribution and population dynamics of *Euphausia superba*: summary of recent findings. *Polar Biology*, 29(1), 1-22.
- Siegel V (2012) Krill stocks in high latitudes of the Antarctic Lazarev Sea: seasonal and interannual variation in distribution, abundance and demography. *Polar Biology*, 35(8), 1151-1177.
- Siegel V, Reiß CS, Dietrich KS, Haraldsson M, Rohardt G (2013) Distribution and abundance of Antarctic krill (*Euphausia superba*) along the Antarctic Peninsula. *Deep-Sea Research I*, 177, 63-74.
- Širović A, Hildebrand JA (2011) Using passive acoustics to model blue whale habitat off the Western Antarctic Peninsula. *Deep Sea Research Part II: Topical Studies in Oceanography*, 58, 1719-1728.
- Soimasuo J, Neteler M, Blazek R, Landa M, Metz M (1994) GRASS GIS package 'v.distance', <http://grass.osgeo.org/grass70/manuals/v.distance.html>.
- Spreen G, Kaleschke L, Heygster G (2008) Sea ice remote sensing using AMSR-E 89-GHz channels. *Journal of Geophysical Research-Oceans*, 113: C02S03, doi:10.1029/2005JC003384.
- Stewart BS, Leatherwood S (1985) Minke whale *Balaenoptera acutorostrata* Lacépède, 1804. In: Ridgeway SH, Harrison R (eds), *Handbook of Marine Mammals*. Academic Press, London. 91-136.
- Thiele D, Gill P (1999) Cetacean observations during a winter voyage into Antarctic sea ice south of Australia. *Antarctic Science*, 11(1), 48-53.
- Thiele D, Chester ET, Gill PC (2000) Cetacean distribution off Eastern Antarctica (80-150 degrees E) during the Austral summer of 1995/1996. *Deep-Sea Research II*, 47, 2543-2572.
- Thuiller W, Lafourcade B, Engler R, Araujo MB (2009) BIOMOD – A platform for ensemble forecasting of species distributions. *Ecography*, 32, 369-373.
- Thuiller W, Lafourcade B, Araujo M (2010) Presentation Manual for BIOMOD; https://r-forge.r-project.org/scm/viewvc.php/*checkout*/pkg/inst/doc/Biomod_Presentation_Manual.pdf?revision=218&root=biomod&pathrev=218
- Thuiller W, Georges D, Engler R, Lafourcade B (2012) BIOMOD: Tutorial; <http://www.will.chez-alice.fr/pdf/BiomodTutorial.pdf>
- Thuiller W, Georges D & Engler R (2014) biomod2: Ensemble platform for species distribution modelling; <https://cran.r-project.org/web/packages/biomod2/index.html>.
- Timmermann R, Danilov S, Schröter J, Böning C, Sidorenko D, Rollenhagen K (2009) Ocean circulation and sea ice distribution in a finite element global sea ice-ocean model. *Ocean Modelling*, 27, 114–129; doi:10.1016/j.ocemod.2008.10.009.
- Turner J, Bindshadler R, Convey P, di Prisco G, Fahrbach E, Gutt J, Hodgson D, Mayewsky P, Summerhayes C (2009) Antarctic climate change and the environment. SCAR, Scott Polar Research Institute, Cambridge.
- Ugland KI, Gray JS, Ellingsen KE (2003) The species accumulation curve and estimation of species richness. *Journal of Animal Ecology*, 72, 888-897.
- Van Franeker JA (1996) Pelagic distribution and numbers of the Antarctic Petrel *Thalassoica antarctica* in the Weddell Sea during spring. *Polar Biology*, 16, 565-572.
- Van Franeker JA, Gavrilov M, Mehlum F, Veit RR, Woehler EJ (1999) Distribution and abundance of the Antarctic Petrel. *Waterbirds*, 22, 14-28.
- Van Opzeeland I, Van Parijs SM, Kindermann L, Burkhardt E, Boebel O (2013) Calling in the cold: pervasive acoustic presence of humpback whales (*Megaptera novaeangliae*) in Antarctic coastal waters. *PLoS ONE*, 8(9), e73007. doi:10.1371/journal.pone.0073007.
- WG-EMM-14/19 (2014) Progress report on the scientific data compilation and analyses in support of the development of a CCAMLR MPA in the Weddell Sea (Antarctica). Teschke K, Jerosch K, Pehlke, H, Brey T (authors), 62 pp.
- WG-EMM-15 (2015) Report of the Working Group on Ecosystem Monitoring and Management; preliminary version. Warsaw, Poland, 6 - 17 July 2015, 99 pp.
- WG-EMM-15/42 (2015) Report of the Second International Workshop for identifying Marine Protected Areas (MPAs) in Domain 1 of CCAMLR (Palacio San Martín, Buenos Aires, Argentina, 25 to 29 May 2015), 42 pp.
- WG-EMM-15/64 (2015) Modelling the circumpolar distribution of Antarctic toothfish (*Dissostichus mawsoni*) habitat suitability using correlative species distribution modelling methods. CCAMLR Secretariat, 30 pp.

- WG-EMM-16/01 (2016) Scientific background document in support of the development of a CCAMLR MPA in the Weddell Sea (Antarctica) - Version 2016; Part A: General context of the establishment of MPAs and background information on the Weddell Sea MPA planning area. Teschke K et al. on behalf of the Weddell Sea MPA (WSMPA) project team, 112 pp.
- WG-EMM-15/02 (2016) Scientific background document in support of the development of a CCAMLR MPA in the Weddell Sea (Antarctica) - Version 2016; Part B: Description of available spatial data. Teschke K, Pehlke H & Brey T on behalf of the German Weddell Sea MPA (WSMPA) project team, with contributions from the participants at the International Expert Workshop on the WSMPA project (7-9 April 2014, Bremerhaven), 20 pp.
- WG-FSA-15/64 (2015) Modelling the circumpolar distribution of Antarctic toothfish (*Dissostichus mawsoni*) habitat suitability using correlative species distribution modelling methods. CCAMLR Secretariat, 29 pp.
- Wienberg C, Wintersteller P, Beuck L, Hebbeln D (2013) Coral Patch seamount (NE Atlantic) – a sedimentological and megafaunal reconnaissance based on video and hydroacoustic surveys. *Biogeosciences*, 10, 3421-3443.
- Williams GD, Nicol S, Aoki S, Meijers AJS, Bindoff NL, Iijima Y, Marsland SJ, Klocker A (2010) Surface oceanography of BROKE-West, along the Antarctic margin of the south-west Indian Ocean (30-80°E). *Deep-Sea Research II*, 57, 738-757.
- Wöhrmann A, Zimmermann C, Kock K-H, Gutt J (2012) Counts of fish species from trawl and dredge samples in the eastern Weddell and Lazarev Seas during POLARSTERN cruise ANT-IX/3. doi:10.1594/PANGAEA.786887.
- Wright DJ, Lundblad ER, Larkin EM, Rinehart RW, Murphy J, Cary-Kothera L, Draganov K (2005) ArcGIS Benthic Terrain Modeler. Corvallis, Oregon, Oregon State University, Davey Jones Locker Seafloor Mapping/Marine GIS Laboratory and NOAA Coastal Services Center. Accessible online at: <https://coast.noaa.gov/digitalcoast/tools/btm>.
- WS-MPA-11/6 (2011) A circumpolar pelagic regionalisation of the Southern Ocean. Raymond B (author), 11 pp.
- Zimmer I, Wilson RP, Gilbert C, Beaulieu M, Ancel A, Plötz J (2008) Foraging movements of emperor penguins at Pointe Géologie, Antarctica. *Polar Biology*, 31, 229-243.

Calculation of weighting factors for Marxan analysis

Adult Antarctic krill occurrence

For the Marxan scenario the modelled values were classified into four classes representing the habitat suitability (in %) of adult Antarctic krill per planning grid cell:

- Class 1 : 0 - 25
- Class 2: 25 - 50
- Class 3: 50 - 75
- Class 4: 75 - 100.

Subsequently, all values from 1 to 100 were listed, and the arithmetic mean for each class was calculated (e.g. class 2: sum of numbers from 25 to 50 divided by 26 = 38; see Tab. A1-1). To calculate the weighting factors for each class following exponential function was used:

$$\text{Weighting factor} = \text{EXP}(0.05*x) - (\text{EXP}(0.05*a)) + 1$$

where x is the mean of the corresponding class and a is the mean of class 1.

Table A1-1: Calculated mean and corresponding weighting factor of the four classes representing the habitat suitability of adult Antarctic krill.

Class	Habitat suitability (%)	Mean	Weighting factor
1	0 - 25	13	1
2	25 - 50	38	6
3	50 - 75	63	22
4	75 - 100	88	80

Please note that the four classes representing the habitat suitability of adult Antarctic krill were differently weighted for the cost layer analysis (i.e. potential krill fishing areas). The values of the weighting factor in Tab. 1-1 were scaled between 0 and 0.5, i.e. following weighting factors were used for the data layer of potential krill fishing areas: 0 (class 1), 0.03 (class 2), 0.13 (class 3) and 0.5 (class 4).

Larval Antarctic krill density

For the Marxan scenario the interpolated values (non-transformed) were classified into four classes representing the density of Antarctic krill larvae (individuals/m²) for a 30 km radius around each record (see Tab. A1-2). Subsequently, all values from 1 to 6457 were listed, and the arithmetic mean for each class was calculated (e.g. class 1: sum of numbers from 0 to 10 divided by 11 = 5). To calculate the weighting factors the mean of each class was divided by five; the weighting factors were finally rounded down to integers.

Table A1-2: Calculated mean and corresponding weighting factor of the four classes representing the density of Antarctic krill larvae.

Class	Density (individuals/m ²)	Mean	Weighting factor
1	0 - 10	5	1
2	10 - 100	55	11
3	100 - 1000	550	110
4	1000 - 6457	3729	745

Adult Antarctic silverfish density

For the Marxan scenario the interpolated values (non-transformed) were classified into four classes representing the density of adult Antarctic silverfish (individuals/1000 m²) for a 30 km radius around each record (Tab. A1-3). The weighting factor was simply defined by the maximum value of each class.

Table A1-3: Weighting factor of the four classes representing the density of adult Antarctic silverfish.

Class	Density (individuals/1000 m ²)	Weighting factor
1	100 - 650	650
2	10 - 100	100
3	1 - 10	10
4	0 - 1	1

Larval Antarctic silverfish density

For the Marxan scenario the interpolated values (log-transformed) were classified into three classes (see Tab. A1-4) representing the mean density (mean = 1.4) +/- n-fold of standard deviation (SD) of Antarctic silverfish larvae (log₁₀ (individuals/1000 m³) +1) for a 30 km radius around each record. The weighting factor was simply defined according to the density class, i.e. the higher the densities the higher the weighting factor.

Table A1-4: Weighting factor of the three classes representing the density of Antarctic silverfish larvae.

Class	Mean density +/- n-fold SD log ₁₀ (individuals/1000 m ³)+1	Weighting factor
1	> 3.42	5
2	1.56 - 3.42	2
3	-0.3 - 1.56	1

Potential foraging areas for non-breeding Adélie penguins

For the Marxan scenario the modelled and subsequently log-transformed values were classified into four classes (defined by rounded quantiles) representing the habitat utilization for non-breeding Adélie_penguins (see Tab. A1-5). Subsequently, the arithmetic mean for each class was calculated, and the weighting factor was determined by following formula:

$$\text{Weighting factor} = (10/\max) * \text{mean (class } i) / ((10/\max) * \text{mean (class } 1))$$

where *max* (maximum value) is 4.4.

Table A1-5: Calculated mean and corresponding weighting factor of the four classes representing the habitat utilization for non-breeding Adélie penguins.

Class	Habitat utilization (log ₁₀ values)	Mean	Weighting factor
1	0 - 1.7	0.9	1
2	1.7 - 2.5	2.1	2.3
3	2.5 - 3.2	2.8	3.1
4	3.2 - 4.4	3.8	4.2

Potential foraging areas for Emperor penguins

For the Marxan scenario the modelled values were classified into four classes representing the probability of Emperor penguin occurrence during foraging (see Tab. A1-6). The weighting factor was defined by the maximum value of each class multiply by 20 (i.e., 20 equates to the maximum value of class 1 divided by maximum value of class 4).

Table A1-6: Weighting factor of the four classes representing the probability of Emperor penguin occurrence during foraging.

Class	Probability of occurrence (%)	Weighting factor
1	0.5 - 1.0	20
2	0.1 - 0.5	10
3	0.05 - 0.1	2
4	0 - 0.05	1

Potential foraging areas for Antarctic petrel

For the Marxan scenario the modelled values were classified into five classes (see Tab. A1-7) representing the probability of occurrence (%) of Antarctic petrel per planning grid cell. Subsequently, all values from 1 to 100 were listed, and the arithmetic mean for each class was calculated. To calculate the weighting factors for each class following exponential function was used:

$$\text{Weighting factor} = \text{EXP}(0.05*x) - (\text{EXP}(0.05*a)) + 1$$

where x is the mean of the corresponding class and a is the mean of class 1.

Table A1-7: Calculated mean and corresponding weighting factor of the five classes representing the probability of occurrence of Antarctic petrel.

Class	Probability of occurrence (in %)	Mean	Weighting factor
1	1 - 20	10.5	1
2	21 - 40	30.5	4
3	41 - 60	50.5	12
4	61 - 80	70.5	33
5	81 - 100	90.5	92

Seal density

For the Marxan scenario the interpolated and modelled values, respectively, were classified into four classes representing the probability of occurrence of pinnipeds (see Tab. A1-8). The weighting factor for class 4 was simply defined by 1. The weighting factor for all other classes was calculated by following formula:

$$\text{Weighting factor} = (x_{\min} * 10) / 5$$

where x_{\min} is the minimum value of the corresponding class.

Additionally, the weighting factor of class 1 was divided by 2 to provide for a relative adjustment of this class to the other classes.

Table A1-8: Calculated mean and corresponding weighting factor of the four classes representing the probability of occurrence of pinnipeds.

Class	Probability of occurrence (individuals/km ²)	Weighting factor
1	> 15	15
2	2 - 15	4
3	1 - 2	2
4	0 - 1	1

Sponge presence

For the Marxan scenario the interpolated values of the sponges abundance classes were classified into three classes (see Tab. A1-9). The weighting factor was defined by rounding down the maximum value of each class. Interpolated values up to 0.7 were defined as sponge absence, and were excluded from the spatial planning analysis.

Table A1-9: Weighting factor of the three classes representing the presence of sponges.

Class	Interpolated value (abundance class)	Weighting factor
1	2.2 - 3.0	3
2	1.5 - 2.2	2
3	0.7 - 1.5	1

Occurrence of demersal fish fauna

For the Marxan scenario the modelled values of the probability raster map were classified into five classes representing the probability of occurrence (in %) of demersal fish per planning grid cell (see Tab. A1-10). Subsequently, all values from 1 to 100 were listed, and the arithmetic mean for each class was calculated. To calculate the weighting factors for each class following exponential function was used:

$$\text{Weighting factor} = \text{EXP}(0.05*x) - (\text{EXP}(0.05*a)) + 1$$

where x is the mean of the corresponding class and a is the mean of class 1.

Table A1-10: Calculated mean and corresponding weighting factor for the five classes representing the probability of demersal fish occurrence.

Class	Probability of occurrence (in %)	Mean	Weighting factor
1	0 - 20	10.5	1
2	21 - 40	30.5	4
3	41 - 60	50.5	12
4	61 - 80	70.5	33
5	81 - 100	90.5	92